


12-2013

Development and Evaluation of Chitosan Particle Based Antigen Delivery Systems for Enhanced Antigen Specific Immune Response

Bhanuprasanth Koppolu
University of Arkansas, Fayetteville

Follow this and additional works at: <http://scholarworks.uark.edu/etd>

 Part of the [Biomedical Commons](#), and the [Other Public Health Commons](#)

Recommended Citation

Koppolu, Bhanuprasanth, "Development and Evaluation of Chitosan Particle Based Antigen Delivery Systems for Enhanced Antigen Specific Immune Response" (2013). *Theses and Dissertations*. 1000.
<http://scholarworks.uark.edu/etd/1000>

This Dissertation is brought to you for free and open access by ScholarWorks@UARK. It has been accepted for inclusion in Theses and Dissertations by an authorized administrator of ScholarWorks@UARK. For more information, please contact scholar@uark.edu, ccmiddle@uark.edu.

Development and Evaluation of Chitosan Particle Based Antigen Delivery Systems for Enhanced
Antigen Specific Immune Response

Development and Evaluation of Chitosan Particle Based Antigen Delivery Systems for Enhanced
Antigen Specific Immune Response

A dissertation submitted in partial fulfillment
of the requirements for the degree of
Doctor of Philosophy in Biomedical Engineering

by

Bhanuprasanth Koppolu
Jawaharlal Nehru Technological University
Bachelor of Technology in Biomedical Engineering, 2006
University of Texas Arlington
Master of Science in Biomedical Engineering, 2008

December 2013
University of Arkansas

This dissertation is approved for recommendation to the Graduate Council.

Dr. David A. Zaharoff
Dissertation Director

Dr. Gisela Erf
Committee Member

Dr. Robert Beitle
Committee Member

Dr. Jeffrey Wolchok
Committee Member

ABSTRACT

Particle-based vaccine delivery systems are under exploration to enhance antigen-specific immunity against safe but poorly immunogenic polypeptide antigens. Chitosan is a promising biomaterial for antigen encapsulation and delivery due to its ability to form nano- and microparticles in mild aqueous conditions thus preserving the antigenicity of loaded polypeptides. The objective of this work is to develop a chitosan particle based antigen delivery system for enhanced vaccine response. Chitosan particle sizes, which ranged from 300 nm to 3 μm , were influenced by chitosan concentration, chitosan molecular weight and addition rate of precipitant salt. The composition of precipitant salt played a significant role in particle formation with upper Hofmeister series salts containing strongly hydrated anions yielding particles with a low polydispersity index (PDI) while weaker anions resulted in aggregated particles with high PDIs. Sonication power had minimal effect on mean particle size, however, it significantly reduced polydispersity. Protein loading efficiencies in chitosan nano/microparticles, which ranged from 14.3% to 99.2%, was inversely related to the hydration strength of precipitant salts, and protein molecular weight and directly related to the concentration and molecular weight of chitosan. Protein release rates increased with particle size and were generally inversely related to protein molecular weight. In vitro studies showed that the uptake of antigen loaded chitosan particles (AgCPs) by dendritic cells and macrophages was found to be dependent on particle size, antigen concentration and exposure time. Flow cytometry analysis revealed that compared to soluble antigen, uptake of AgCPs enhanced upregulation of surface activation markers on APCs and increased the release of pro-inflammatory cytokines. Lastly, antigen-specific T cells exhibited higher proliferative responses when stimulated with APCs activated with AgCPs versus soluble antigen. These data suggest that encapsulation of antigens in chitosan particles

enhances uptake, activation and presentation by APCs with 1 μm mean particle size being optimal. Similarly, in vivo studies showed that immunizing mice with AgCPs enhanced both humoral and cell mediated immune response. Compared to PLGA nanoparticle and standard alum adjuvants, AgCPs induced more potent humoral immune responses as evidenced by the high total antigen specific IgG titer.

©2013 by Bhanuprasanth Koppolu
All Rights Reserved

ACKNOWLEDGEMENTS

First, I would like to express my sincere appreciation and gratitude to my major advisor Dr. David A. Zaharoff for his continuous support, encouragement, guidance, and advice throughout my journey in achieving the PhD degree. I am very thankful and grateful to him for giving me this opportunity and for his support both in my academic and personal life. I would also like to thank him for the time he spent on reading and editing the draft of this dissertation.

I would like to thank my committee members, Dr. Gisela F. Erf, Dr. Robert Beitle, and Dr. Jeff Wolchok for their valuable advice, and technical inputs throughout my PhD program. I would also like to thank them for their time and agreeing to serve on my doctoral dissertation committee. I would also like to thank our collaborators Dr. T.K.S Kumar and Dr. Srinivas Jayanti for their constant support and help throughout my PhD program.

It would not have been possible for me to earn my degree without the unfailing support of my family, my mother Dhana lakshmi Koppolu and my father Bhupathi naidu Koppolu. I would like to offer my most sincere appreciation to both of them, who have dealt with many hardships to provide better education for their children. I would like to thank my fiancé and dearest friend Weiwei, for the care and support she provided from day one of my Ph.D program. I would also like to thank my brother Mouli and all my friends at Fayetteville for their support throughout this journey.

I would also like to thank all my colleagues at LVID lab who shared my burdens without expectations. Specifically I want to thank Sean Smith, Sruthi Ravindranathan, Samantha Kurtz, and Haitao Chen for their continuous support.

TABLE OF CONTENTS

1. BACKGROUND	1
1.1. Vaccines	1
1.1.1. Whole pathogen vaccines	1
1.1.2. Subunit vaccines	3
1.1.3. Adjuvants	4
1.2. Immunopotentiators	5
1.2.1. Monophosphoryl lipid A (MPL)	5
1.2.2. Unmethylated CpG dinucleotides motifs	6
1.2.3. Saponins	6
1.2.4. Cytokines	7
1.3. Antigen delivery systems	8
1.3.1. Viral vectors	10
1.3.2. Virus like particles	10
1.3.3. Liposomes	11
1.3.4. Immunostimulating complexes	12
1.3.5. Non-degradable particulate carriers	13
1.3.6. Biodegradable polymeric particles	14
1.4. Chitosan based antigen delivery systems	17
Hypothesis	19
Approach	20

TABLE OF CONTENTS (CONTINUED)

2. SPECIFIC AIM 1: Synthesis and Characterization of Chitosan Particles of Varying Sizes- Effect of Formulation Factors on Particle Size	21
2.1. Rationale	21
2.2. Methodology	23
2.2.1. Reagents	23
2.2.2. Preparation and characterization of chitosan particles	23
2.2.3. Effect of formulation factors on particle properties	24
2.2.4. Protein loading and release studies	24
2.2.5. Statistical analysis	25
2.3. Results	26
2.3.1. Effect of precipitant salt type on chitosan particle properties	26
2.3.2. Effect of chitosan molecular weight and concentration on chitosan particle properties	27
2.3.3. Effect of sonication on chitosan particle properties	28
2.3.4. Effect of salt addition rate on chitosan particle properties	28
2.3.5. Effect of protein molecular weight on chitosan particle properties	29
2.3.6. Effect of solvent salinity on protein release	29
2.3.7. Effect of chitosan particle size on protein release	30
2.3.8. Effect of precipitant salt on protein release	31
2.3.9. Effect of encapsulated protein on protein release	31
2.4. Discussion	32
2.5. Conclusion	35

TABLE OF CONTENTS (CONTINUED)

3. SPECIFIC AIM 2: Access <i>In Vitro</i> Particulate Antigen Uptake and Presentation by Antigen Presenting Cells	37
3.1. Rationale	37
3.2. Methodology	39
3.2.1. Reagents	39
3.2.2. Mice	40
3.2.3. Cell culture	40
3.2.4. Preparation of AgCPs	40
3.2.5. Characterization of AgCPs	41
3.2.6. Uptake of AgCPs by APCs	41
3.2.7. APC activation	42
3.2.8. Antigen presentation	43
3.2.9. Statistical Analysis	43
3.3. Results	44
3.3.1. Characterization of AgCPs	44
3.3.2. Uptake of AgCPs by APCs	45
3.3.3. Macrophage activation	45
3.3.4. BMDC activation	46
3.3.5. Antigen presentation by BMDCs	47
3.4. Discussion	48
3.5. Conclusion	51

TABLE OF CONTENTS (CONTINUED)

4. SPECIFIC AIM 3: Access In Vivo Immunological Activity of Chitosan Particulate	
Antigen Delivery System	53
4.1. Rationale	53
4.2. Methodology	53
4.2.1. Reagents	53
4.2.2. Mice	54
4.2.3. Preparation of OVA loaded chitosan particles	54
4.2.4. Preparation of OVA loaded PLGA nanoparticle	54
4.2.5. Characterization of OVA loaded PLGA nanoparticles	55
4.2.6. Immunization	55
4.2.7. OVA-specific antibody response	56
4.2.8. Lymphocyte proliferation assay	56
4.3. Results	57
4.3.1. AgCPs generated higher antigen specific humoral response	57
4.3.2. AgCPs generated higher antigen specific lymphocyte proliferation	58
4.4. Discussion	58
4.5. Conclusion	60
5. CONCLUSIONS AND FUTURE DIRECTIONS	61
6. REFERENCES	93

LIST OF TABLES

Table 1. Effect of formulation factors on particle size, size distribution and protein loading efficiency; *Data are presented as mean \pm standard deviation for three independent experiments. ** No particle formation. ^a Viscosity range of chitosan was indicated by manufacture as obtained at a concentration of 1 mg/ml (w/v) in 1% acetic acid **Page 67**

Table 2: Experimental design for protein release studies: Effect of particle size. Data are presented as mean \pm standard deviation for three independent experiments. **Page 68**

Table 3: Experimental design for protein release studies: Effect of precipitant salt composition. Data are presented as mean \pm standard deviation for three independent experiments. **Page 69**

Table 4: Experimental design for protein release studies: Effect of protein molecular weight. Data are presented as mean \pm standard deviation for three independent experiments. **Page 70**

LIST OF FIGURES

- Figure. 1.** Schematic representation of viral vector particle constituting carrier viral protein envelop and antigen genetic material. **Page 71**
- Figure. 2.** Schematic representation of virus like particle delivery system. **Page 72**
- Figure. 3.** Schematic representation of multi-layered liposomal particle encompassing both antigen and immunopotentiators. **Page 73**
- Figure. 4.** Schematic representation of ISCOM with hydrophobic antigen loaded into the phospholipid/cholesterol cage. **Page 74**
- Figure. 5.** Schematic representation of non-degradable nano/micoparticle vaccine delivery system; Particle can be designed to carry antigens while particle itself acts as an adjuvant or have adjuvant conjugated along with antigen. **Page 75**
- Figure. 6.** Schematic representation of degradable polymeric particle; Particle can be designed to carry antigens while particle itself acts as an adjuvant or have adjuvant conjugated along with antigen. **Page 76**
- Figure. 7.** Chemical structure of chitosan. Chitosan is an unbranched copolymer of N-acetylglucosamine (x) and glucosamine (y) units linked by $\beta(1-4)$ glycosidic bonds where the ratio of y to x is greater than 1.5. **Page 77**
- Figure. 8.** Effect of precipitation-coacervation parameters on chitosan-FITC-BSA particle size and PDI. Parameters including: chitosan concentration, molecular weight/viscosity, precipitant salt addition rate, and sonication power were varied following the experimental design described in Table 1. Resultant particle size and PDI of the resultant particles were determined by DLS. Data are presented as mean \pm standard deviation of three independent experiments. **Page 78**
- Figure. 9.** Effect of ionic strength of release medium on protein release; Particles prepared using precipitant salt Na_2SO_4 encapsulating model protein FITC-BSA are incubated with 0.1X, 0.5X, 1 X PBS. Particles incubated in deionized water (DI water) served as negative control. Samples were collected at each time point and protein release was quantified by measuring fluorescence of protein via fluorescence spectroscopy. Cumulative protein release was calculated by adding the protein released at each individual time point. **Page 79**

LIST OF FIGURES (CONTINUED)

Figure. 10. Morphology and size distribution of AgCPs. Representative SEM images and DLS data show that 300 nm AgCPs, 1 μm AgCPs, and 3 μm AgCPs, are unimodally distributed and spherical to elliptical with porous non-uniform structures. **Page 80**

Figure. 11. Effect of chitosan particle size on protein release; 300nm, 1 μm , and 3 μm CPs encapsulating model protein FITC-BSA were incubated with PBS. Samples were collected at each time point and protein release was quantified by measuring fluorescence via fluorescence spectroscopy. Cumulative protein release was calculated by adding the protein release at each individual time point. **Page 81**

Figure. 12. Effect of ionic strength of precipitating salt on protein release; Particles prepared using Hofmeister series ionic precipitant salts Na_2SO_4 , $(\text{NH}_4)_2\text{SO}_4$, MgSO_4 , $\text{Na}_3\text{C}_6\text{H}_5\text{O}_7$, and Na_3PO_4 encapsulating model protein FITC-BSA were incubated with PBS. Samples were collected at each time point and protein release was quantified by measuring fluorescence via fluorescence spectroscopy. Cumulative protein release was calculated by adding the protein release at each individual time point. **Page 82**

Figure.13. Effect of encapsulated protein size on protein release by particles; Particles encapsulating model proteins FITC-Insulin, FITC-OVA, FITC-BSA, and FITC-Con A were incubated with PBS. Samples were collected at each time point and protein release was quantified by measuring fluorescence via fluorescence spectroscopy. Cumulative protein release was calculated by adding the protein release at each individual time point. **Page 83**

Figure. 14. Effect of size, concentration, and incubation time on uptake of AgCPs by APCs. (a) RAW 264.7 macrophages or (c) BMDCs were co-incubated with 1 μm AgCPs at an effective antigen/FITC-BSA concentration of 30 $\mu\text{g}/\text{ml}$ for 12, 24, or 48 h. (b) RAW 264.7 macrophages or (d) BMDCs were co-incubated with 300nm, 1 μm , or 3 μm AgCPs at effective antigen concentrations of 1, 5, 10, 20, or 30 $\mu\text{g}/\text{ml}$ for 24 h. After each co-incubation, cells were rinsed three times with PBS and lysed with 1% triton solution. The amount of FITC-BSA released was quantified via fluorescence spectroscopy. Data are presented as mean \pm standard deviation from three independent experiments. * $p \leq 0.05$ vs. 12 h incubation; ** $p \leq 0.05$ comparing AgCP sizes for a particular antigen concentration. **Page 84**

LIST OF FIGURES (CONTINUED)

Figure. 15. Surface marker expression by RAW 264.7 macrophages following exposure to soluble antigen, CPs without antigen or AgCPs. Macrophages were co-incubated with soluble or particulate antigens at a final antigen concentration of 30 µg/ml. After 24 h, cells were rinsed three times, harvested, blocked with purified anti-mouse CD16/CD32 and stained with fluorescence-labeled antibodies to MHC molecules and activation markers (solid lines). Filled histograms represent cells treated with medium alone. Dotted line histograms are treated cells stained with appropriate isotype controls. All histograms are from one representative experiment of three independent experiments producing similar results. Panel numbers indicate the mean percentages of positive cells (top number) and mean fluorescence intensities (bottom number) of respective samples. **Page 85**

Figure. 16. Cytokine release by RAW 264.7 macrophages. Cells were co-incubated with soluble or particulate antigens at a final antigen concentration of 30 µg/ml. After 24 h, supernatants of all groups were collected and analyzed for cytokine production using a customized CBA flex set. Data are presented as mean ± standard deviation from three independent experiments. * $p \leq 0.05$ vs. soluble antigen (FITC-BSA); ** $p \leq 0.05$ vs. other sizes of AgCPs. **Page 86**

Figure. 17. Surface marker expression by BMDCs following exposure to soluble antigen, CPs without antigen or AgCPs. Macrophages were co-incubated with soluble or particulate antigens at a final antigen concentration of 30 µg/ml. After 24 h, cells were rinsed three times, blocked with purified anti-mouse CD16/CD32 and stained with fluorescence-labeled antibodies to MHC molecules and activation markers (solid lines). Filled histograms represent cells treated with medium alone. Dotted line histograms are treated cells stained with appropriate isotype controls. All histograms are from one representative experiment of three independent experiments producing similar results. Panel numbers indicate the mean percentages of positive cells (top number) and mean fluorescence intensities (bottom number) of respective samples. **Page 87**

Figure. 18. Cytokine release by BMDCs. Cells were co-incubated with soluble or particulate antigens at a final antigen concentration of 30 µg/ml. After 24 h, supernatants of all groups were collected and analyzed for cytokine production using a customized CBA flex set. Data are presented as mean ± standard deviation from three independent experiments. * $p \leq 0.05$ vs. soluble antigen (FITC-BSA); ** $p \leq 0.05$ vs. other sizes of AgCPs. **Page 88**

LIST OF FIGURES (CONTINUED)

Figure. 19. Proliferation of (a) OVA-specific CD4⁺ T-cells, and (b) OVA-specific CD8⁺ T-cells in response to presentation of antigen by BMDCs. BMDCs were pulsed with CPs, AgCPs, soluble full length OVA or the MHC I-restricted OVA₂₅₇₋₂₆₄ peptide for 24 h and then co-incubated with CD4⁺ or CD8⁺ T-cells from OT-II or OT-I mice, respectively. After 72 h, T cell proliferation was determined via a non-radioactive proliferation assay (CellTiter Glo; Promega, Madison, WI). Data are presented as mean relative light unit (RLU) ± standard deviation from one of two independent experiments with similar results. *p ≤ 0.05 vs. OVA or OVA peptide; **p ≤ 0.05 vs other AgCP sizes. **Page 89**

Figure. 20. Serum anti-OVA IgG antibodies. Adult C57BL/6J mice were immunized two weeks apart with one of six vaccines: OVA alone, OVA formulated with alum, PLGA-OVA, 300 nm, 1 μm, and 3 μm OvaCPs. Sera were collected five days after booster injection and analyzed using ELISA. Mouse anti-OVA antibodies were used as positive controls with PBS acting as negative control. The data represent the mean ± standard deviation of two independent immunization experiments (n = 10, 5 mice per vaccine x 2). **Page 90**

Figure. 21. Serum anti-OVA IgG1 antibodies. Adult C57BL/6J Mice were immunized two weeks apart with one of six vaccines: OVA alone, OVA formulated with alum, PLGA-OVA, 300 nm, 1 μm, and 3 μm OvaCPs. Sera were collected five days after booster injection and analyzed using ELISA. Mouse anti-OVA antibodies were used as positive controls with PBS acting as negative control. The data represent the mean ± standard deviation of two independent immunization experiments (n = 10, 5 mice per vaccine x 2). **Page 91**

Figure. 22. (a) Proliferation of CD4⁺ T-cells isolated from immunized mice. Adult C57BL/6J Mice were immunized two weeks apart with one of six vaccines: OVA alone, OVA formulated with alum, PLGA-OVA, 300 nm, 1 μm, and 3 μm OvaCPs. Five days post-booster injection. CD4⁺ T-cells from individual mice were isolated from immunized mice spleens and co-cultured with irradiated splenocytes isolated from naïve mice pulsed with OVA. (b) Cells stimulated with Con A served as the positive controls. The data represent the mean ± standard deviation of two independent immunization experiments (n = 10, 5 mice per vaccine x 2). **Page 92**

LIST OF ABBREVIATIONS

APCs – Antigen presenting cells

BMDCs – Bone marrow dendritic cells

BSA – Bovine serum albumin

CMI – Cell mediated immunity

Con A – Concanavalin A

CTL – Cytotoxic T lymphocytes

DCM - Dichloromethane

DCs – Dendritic cells

DD – Degree of deacetylation

DNA – Deoxyribonucleic acid

FBS – Fetal bovine serum

FITC – Fluorescein isothiocyanate

GM-CSF – Granulocyte macrophage colony – stimulating factor

HBV – Hepatitis B virus

HCV – Hepatitis C virus

Hep B – Human papillomavirus bivalent

HIV – Human immunodeficiency virus

LIST OF ABBREVIATIONS (CONTINUED)

HPV – Human papillomavirus

HSV – Human simplex virus

IFN – Interferon

IL – Interleukin

ISCOM – Immunomodulatory complexes

ITC – Isothermal titration calorimetry

LPS – Lipopolysaccharides

MHC – Major histocompatibility complex

MPL – Monophosphoryl lipid A

MVA – Modified vaccinia virus *Ankara*

OVA – Ovalbumin

PBS – Phosphate buffer saline

PCL – Poly(caprolactone)

PGA – Poly(glutamic acid)

PLA – Poly(lactic acid)

PLGA – Poly(lactic – co – glycolic acids)

PMMA – Poly(methyl methacrylate)

LIST OF ABBREVIATIONS (CONTINUED)

RNA – Ribonucleic acid

TLR – Toll like receptor

TNF – Tumor necrotic factor

VLP – Virus like particles

1. BACKGROUND

1.1. Vaccines

A vaccine is a biological or chemical preparation used to develop immunity towards disease causing organisms including bacteria, viruses, or autologous carcinogenic cells/tissue. Vaccines mainly capitalize the immune system's ability to respond rapidly to microorganisms after a second encounter. As such, the goal of vaccination is to stimulate a strong, protective and long-lasting immune response to the administered antigen. Based on the components of pathogen used, vaccines are generally divided into three categories namely live whole pathogen vaccines, subunit or inactivated vaccines, and deoxyribonucleic acid (DNA) vaccines. Live vaccine uses active or partially inactivated microorganisms that can replicate in the host and can infect cells, thereby functioning as an immunogen. A subunit vaccine includes only the specific parts of pathogen that best stimulate the immune system but do not replicate in the host. In some cases, these vaccines use epitopes—the very specific parts of the antigen that antibodies or T cells recognize and bind to. A DNA vaccine gets transfected into human cells and directs the synthesis of vaccine antigen *in vivo*.

1.1.1. Whole pathogen vaccines

The use of whole pathogen vaccines has led to some of the most spectacular achievements in medical history. Some of the most deadly of diseases like small pox, measles, mumps, rubella etc., have been nearly eradicated world-wide thanks to inexpensive live attenuated vaccines. In the early days of vaccination live attenuated or inactivated pathogens were used to generate a long-lasting immunity. These approaches in general, have been

successful in inducing an immunogenic response including, antibodies, which neutralize viruses or bacterial toxins, inhibit the binding of microorganisms to cells, or promote their uptake by phagocytes [1]. Advantages of live bacterial vaccines include their mimicry of a natural infection, intrinsic adjuvant properties and easy manufacturing and administration. Derivatives of pathogenic and non-pathogenic bacteria or virus including influenza, smallpox, rotavirus etc., are some of the routinely used live vaccines. However, pathogenic bacteria or viruses demands for attenuation to weaken their virulence [2].

Increased immunological understanding and the development of molecular biology made possible the development of new generation of live attenuated or inactivated pathogen vaccines that can avoid the downsides of live vaccines [3]. These vaccines can be delivered orally or nasally mimicking the route of entry of many pathogens and stimulate mucosal immune response. Furthermore they can be designed to act as adjuvants to subunit antigens from a more virulent or dangerous pathogen.

Even with latest advancements, attenuated or inactivated vaccines have been unsuccessful against persistent pathogens inducing chronic infections including, Human immunodeficiency virus (HIV) and hepatitis C virus (HCV) [4]. In such cases, induction of potent and focused cell mediated immunity (CMI) will be necessary and may require the induction of cytotoxic T lymphocytes (CTL), which kill host cells infected with intracellular organisms. Unfortunately, non-living vaccines generally have proven ineffective at inducing potent CMI responses. Although attenuated vaccines can induce CTL, they may still cause disease in immune-suppressed individuals. Also, some pathogens are difficult or impossible to grow in culture (e.g., HCV), making the development of live attenuated vaccines impossible. In

addition, many traditional live attenuated or inactivated vaccines based on whole bacterial cells often contain components like endotoxins that can cause side effects and safety problems [5, 6].

1.1.2. Subunit vaccines

Subunit vaccines use a portion of the pathogen such as an individual protein as the antigen. These vaccines are attractive because of their increased safety since they cannot revert to a virulent form. The past decade, vaccine development has been shifting towards subunit antigens including, recombinant protein subunits, synthetic peptides, protein polysaccharide conjugates, and microbial DNA. Recent efforts have focused on developing conjugate vaccines in which a weak antigen is linked to a stronger immunogen such as a protein or membrane complex. The vaccine responsible for nearly eliminating HIB meningitis from infants and young children is an example of a conjugate vaccine [7, 8]. DNA encoding pathogenic antigens have been used as vaccines for veterinary use. They have also shown promise as vaccines in preclinical studies against a wide variety of diseases including tuberculosis and HIV [9, 10].

In addition to being safer, subunit antigens are easier to manufacture and characterize. However, subunit antigens are rapidly degraded by proteases and lack the immune stimulus, i.e. co-stimulation and/or danger signals, often required for the generation of robust antigen-specific immunity. As a result, a great deal of effort has been spent in evaluating delivery systems and/or adjuvants capable of enhancing antigen delivery and providing the appropriate stimulus to generate antigen-specific immunity [11, 12]. This is especially important when developing vaccines for cancer using protein or peptide antigens that lack immune stimulus and degrade rapidly *in vivo* [10, 13]. In contrast, a more immunogenic antigen may benefit from a specific

delivery vehicle that can influence the direction of the immune response. As such, adjuvants play a major role in the development of modern vaccines.

1.1.3. Adjuvants

Adjuvants have traditionally been defined as agents added to vaccine formulations that enhance the immunogenicity of antigens *in vivo*. An updated version of this definition divides adjuvants into two classes: delivery systems and immunopotentiators, based on their dominant mechanism of action [14]. Adjuvants can enhance the duration of immune response and reduce the dose of antigen thus reducing the costs and toxicity. Also, adjuvants can be designed to elicit required immune response including the modulation of antibody avidity, specificity, isotype or subclass distribution, promoting antigen uptake by APCs, and stimulating CTLs [15]. Many of the immunopotentiating adjuvants are sensed by various members of the Toll-like receptor (TLR) family, a subclass of pathogen-recognition receptors [16]. Adjuvant delivery systems can be used to protect subunit antigens and improve persistency. Along with protecting antigens, delivery systems can be used for controlled and targeted delivery of antigen. Also, combinations of delivery systems and immunopotentiating substances are being developed as multi-component adjuvants with the potential to act synergistically to enhance the antigen-specific immune response *in vivo*.

Until recently, the aluminum salt/gel-based (alum) adjuvants are the only ones contained in vaccines licensed for human use in the United States with squalene-oil-water emulsion based MF59TM being approved in European union [17]. Although alum has an excellent safety record, comparative studies pitting alum to particulate adjuvants including virus like particles,

polymeric, and liposomal particles have shown that it is a poor adjuvant for humoral response inducing comparatively lower antigen specific IgG antibodies. Also, alum has been shown to induce Th2 rather than Th1 cytokine response resulting in weakened cell mediated response to antigens [18]. As such, focus has shifted in the last decade towards the development of more effective adjuvants constituting both immunopotentiating and delivery systems.

1.2. Immunopotentiators

1.2.1. Monophosphoryl lipid A (MPL)

MPL is a non-toxic component derived from lipopolysaccharide (LPS) of gram negative *Salmonella Minnesota* bacterial cell wall. MPL is obtained by exposing the LPS to acid and base hydrolysis sufficient to cause the loss of certain chemical groups. MPL retains immunopotentiating properties of LPS but can be used safely in humans [19]. It is believed to interact with TLR-2 and TLR-4 on APCs inducing a Th1-skewed response. MPL is thought to directly activate macrophages resulting in the induction of IFN- γ and IL-2 [20]. However, it is not as potent at inducing antibody responses compared to other adjuvants like QS21TM [20, 21]. As such, MPL has often been used in complex formulations, including liposomes, MF59TM, Alum, and QS21TM [15]. MPL is being looked into for use in cancer immunotherapy, infectious disease vaccine, and treatment for allergies. MPL has been approved in Europe for use in combination with allergy vaccines [22]. Also, MPL is among the few adjuvants approved by Food & Drug administration (FDA) in recent history for use in HPV and H1N1 vaccines [23-25].

1.2.2. Unmethylated CpG dinucleotide motifs

CpG are small stands of DNA motifs consisting of an unmethylated CpG dinucleotide flanked by two 5' purines (optimally GpA) and two 3' pyrimidines (optimally TpC or TpT). CpG motifs are considered pathogen-associated molecular patterns (PAMPs) due to their abundance in microbial genomes but are rare in mammalian genomes. Unmethylated CpG's can stimulate innate immune responses characterized by the production of antigen specific IgM, IFN γ , IL-6, IL-12, IL-18 and TNF α [26]. The immune response to unmethylated CpG has been linked in humans to the activation of TLR-9. Interactions with CpG results in the maturation of dendritic cells, upregulation of MHC class II to produce professional antigen presenting cells, induction of Th1 cytokines and triggering B-cell proliferation [27]. Studies have shown that CpG motifs in the bacterial plasmid backbone of DNA vaccines contributed to vaccine immunogenicity [28]. CpGs motifs are also being looked into as immunopotentiators for antibody and cytokine production against protein based antigens including tumor antigens [29, 30].

1.2.3. Saponins

Saponins are steroid or triterpenoid glycosides found in wild or cultivated plants, lower marine animals and some bacteria. Adjuvant activity of saponins is associated with branched sugar chains or aldehyde groups or with an acyl residue bearing the aglycone [31]. Saponins work by forming pores in cell membranes that allow antigens to gain access to the endogenous presentation pathway resulting in antigen presentation by MHC class I and hence CTL activation [32]. Saponin-based adjuvants have the ability to modulate the cell mediated immune system as

well as to enhance antibody production [33, 34]. They induce strong cytotoxic CD8+ lymphocyte responses and potentiate the response to mucosal antigens. Also, saponins have been shown to induce cytokines such as, IL-2, and INF- γ that can induce a strong Th1 response [31].

Saponins extracted from the bark of *Quillaja saponaria* tree bark have shown great promise and are the most studied for use as adjuvants. A highly purified fraction called QS21TM is a potent adjuvant for the induction of a Th1- response, including CTLs and IgG2a antibody secretion [32, 34]. A number of clinical trials are underway using QS21 as adjuvant for cancer vaccines (melanoma, breast, and prostate) and infectious diseases (HIV, malaria, and hepatitis B) [35, 36].

1.2.4. Cytokines

All immunopotentiating adjuvants induce cytokine production. Cytokines are key immunomodulators during the development of an adaptive immune response. Therefore, it makes sense to incorporate recombinant cytokines directly into vaccine formulations. As such, cytokines are being evaluated as adjuvants instead of cytokine inducing adjuvants. The cytokines that have been evaluated most extensively as adjuvants include IL-1, IL-2, IFN- γ , IL-12 and granulocyte-macrophage colony-stimulating factor (GM-CSF) [37]. IL-6, IL-1, and IL-12 which promote both humoral and cell mediated responses are being used in mucosal or nasal vaccines for viral and bacterial infections including HIV [38, 39]. However, cytokines are dangerous at high levels in circulation. Systemic exposure to pro-inflammatory cytokines can induce systemic toxicity, chronic inflammation, and infections in immune compromised patients [37]. Also, cytokines have low *in vivo* half-life and are relatively expensive. Nevertheless, considerable

progress has been made in the use of cytokines for the immunotherapy of cancer. Cytokines like GM-CSF IL-2 and IL-12 in combination with other adjuvants or particulate carriers are being used in cancer immunotherapy and viral vaccines [40, 41].

Other classes of immunopotentiating adjuvants include viral vectors, virus like particles, and immunostimulatory complexes. However these adjuvants are also classified as antigen delivery systems and are covered in the following sections.

1.3. Antigen delivery systems

Antigen presenting cells (APCs) like dendritic cells (DCs) play a crucial role in initiating T-cell-mediated immunity. They can control a substantial part of the adaptive immune response by internalizing and processing antigens through major histocompatibility complex (MHC) class I and class II pathways, presenting antigenic peptide complexes with MHC I and MHC II to CD4⁺ and CD8⁺ T lymphocytes, and producing cytokines. Therefore, targeting APCs with an antigen delivery system provides tremendous potential in developing new vaccines. Particles with size similar to that of pathogens the immune system has evolved to combat can be efficiently internalized by APCs. The uptake of particles of sizes <5µm by phagocytic cells has been well documented and uptake into APC is likely to be important in the ability of particles to perform as vaccine adjuvants. It has been reported that macrophages carry antigens within the microparticles to lymph nodes and differentiate into dendritic cells (DC) [42]. In addition, uptake of nano/micro particles encapsulating antigens by APC's including DC's, macrophages, and B-cells has been demonstrated. The appropriate size for particulate carriers appears to be in the

range of 1–3 μ m [43, 44], and it appears that cationic particles are particularly effective for uptake into macrophages and DC [45].

Particulate carriers can be modulated to present multiple copies of antigens on their surface, which has been shown to be optimal for B cell activation. It has been demonstrated that organized arrays of antigens on surfaces are able to efficiently cross-link B cell receptors and constitute a strong activation signal [46, 47]. In addition, particulate carriers can enhance the persistence of antigens by protecting them from degradation. Recent studies showed that, together with the activation of innate immunity, the duration of antigen persistence is important in triggering protective T cell responses [48]. Finally, immunopotentiators may be included in particulate delivery systems to enhance immune responses by focusing effects on the APC and to limit the potential for adverse events by restricting their systemic distribution to the injection site. Given the advantages of particulate carriers, a myriad of particulate platforms including viral carriers, liposomes, immunostimulatory complexes (ISCOM), proteasomes, polysaccharide, and polymeric particles are being developed for vaccine delivery. However, only the Recombinant Human Papillomavirus bivalent (Hep B) vaccine that employs virus like particles (VLP) for antigen delivery has been approved by the FDA for use in humans [49-51]. Particulate antigen carrier's lack of success can be attributed to the complexity of particulate systems that requires extensive studies for approval. As such, there is a need to develop a simple particulate system that can be customized to deliver antigens/immunopotentiators to various immune modalities. We will further review the different types of particle antigen delivery/adjuvant systems below.

1.3.1. Viral vectors

Viral vectors make use of this natural immunogenicity of viruses to develop vaccine response towards the embedded antigens making them ideal for antigen delivery. Viral vector vaccines consist of replicating or non-replicating viruses that carry defined genetic material from the pathogen (Figure 1). Viral vector vaccine is essentially a combination of DNA and live attenuated vaccines. Viral vector vaccines transfect DNA into host cell for production of antigenic proteins that can be tailored to stimulate a range of immune responses, humoral or cell mediated response (CD4, CTL, and CD8) [52].

Viral vector vaccines, unlike DNA vaccines, can be tailored to actively invade host cells and replicate, much like a live attenuated vaccine, further activating the immune system like an adjuvant. Adenovirus is the most frequently used vector platform being evaluated for vaccines against Alzheimer's disease, Malaria, Influenza, Tetanus, and HIV [53, 54]. Other vectors that have shown success include modified vaccinia virus Ankara (MVA) and canarypox vector [54].

1.3.2. Virus like particles

Virus like particles (VLP) are self-assembling non-infective viral protein envelopes without any viral genetic materials (Figure 2). The protein envelopes are used as platforms to deliver components of pathogenic virus or bacteria that are attached or inserted into the particle depots [55]. VLPs like viral vectors can be designed to elicit strong humoral and cell mediated immune responses.

Several recombinant VLP vaccines are at different stages of clinical trials including Recombivax™ (Merck) and Engerix-B™ (GSK), which are composed of the viral small envelope protein, which upon expression in yeast formed VLPs [56]. While these were effective at delivering the antigens, they suffered from a lack of immunogenicity. However, an updated version consisting of Pre-S1, Pre-S2, and HBV surface antigens elicited a strong antibody response [57]. The most recently approved VLP vaccine is Gardasil™ for immunization against HPV and subsequent prevention of cervical cancer and genital warts. This vaccine is composed primarily of self-assembled particles of L1 protein from HPV encompassing alum and has been shown to reduce infection by up to 90% [58]. Additionally, a malaria vaccine composed of a VLP of HBV core antigen containing proteins from the circumsporozoite stage of the Plasmodium parasite was shown to produce significant humoral and cellular immune responses when formulated with Alhydrogel™ [59]. Other VLP based vaccines in preclinical studies include vaccines for influenza, hepatitis C virus (HCV), Ebola virus, rotavirus and SARS [56].

1.3.3. Liposomes

Liposomes are self-assembling particles constituting phospholipid bilayer shell with an aqueous core [60]. They can be generated as either vesicles with single phospholipid bilayer shell, or multilayered vesicles, that are made of several concentric phospholipid shells separated by aqueous layers (Figure3) [61]. Multilayered liposomes can be used to delivery both antigens and adjuvants. Antigens can either be encapsulated in the core of the liposome, buried within the lipid bilayer or adsorbed on the surface for presentation to antigen presenting cells. Liposomes are generally considered non-toxic given that the phospholipids are extracted from mammalian

sources. However, they are relatively non-immunogenic and are most useful as delivery agents that can carry encapsulated antigen/adjuvant complexes for recognition and uptake by APCs [62].

Liposomes can be made immunogenic by modifying the surface of the particle by adding an immunopotentiating compound to the formulation [63]. Also, cationic liposomes have been shown to aid in the development of cell mediated immune responses by facilitating uptake of antigens by APCs [64]. Guan et al., showed that liposome-associated MUC1 peptide (BP25) produced a strong specific CTL response and antibody response [65]. A lyophilized liposomal formulation of BP25 lipopeptide, MPL and three lipids called L-BLP25 (StimuvaxTM, Merck) had been shown to elicit a cancer antigen specific cellular immune response in patients with non-small-cell lung cancer [66]. Apart from StimuvaxTM which is in later stage 3 clinical trials for lung and breast cancer, no major liposomal formulations are being evaluated for vaccine delivery. This may be attributed to the use of organic solvents in liposome preparations that can denature protein antigens, and instability of liposomes during storage resulting in limited shelf life [67].

1.3.4. Immunostimulating complexes

Another vaccine delivery vehicle with potent adjuvant activity being studied in the clinic is the immunostimulating complex (ISCOM). The cage-like particles encapsulating antigens were produced by combining a protein antigen (preferable hydrophobic), cholesterol, phospholipid and the saponin adjuvant Quil A (Figure 4) [68]. A similar vaccine delivery vehicle and adjuvant has also been developed that uses the same material minus the antigen and is

referred to as ISCOMATRIX. The antigen can be added later to the ISCOMATRIX during formulation of the vaccine. This material seems to work similarly to ISCOMs, but provides for more general applications by removing the requirement for hydrophobic antigens [68]. ISCOMs carrying multiple copies of antigens are shown to be effectively internalized by APCs resulting in cross presentation of antigens with both MHC-I and MHC-II [69].

A clinical study that compared a classical trivalent flu vaccine with an ISCOM adjuvant version composed of the same three virus strains revealed a stronger immune response with the ISCOM vaccine eliciting rapid antibody responses as well as CD4⁺ and CD8⁺ T-cell response [70]. A separate study of an ISCOM based flu vaccine showed that virus-specific CTL memory was achieved in 50–60% of the patients, compared to only 5% who received the standard flu vaccine [71]. Additional ISCOM vaccines have been in clinical studies for HIV, herpes simplex virus (HSV), HPV, HCV, and cancer [68, 72, 73]. Despite these successes, the actual use of ISCOMs in human vaccines has been deterred by concerns regarding safety since some saponins used in ISCOMs were shown to be toxic at elevated levels [74]. Nevertheless, certain saponins, such as QuilA and QS-21TM have not shown major signs of toxicity in humans at the doses administered [74].

1.3.5. Non-degradable particulate carriers

Non-degradable particles can vary from non-degradable polymeric particles (polystyrene, latex, etc.) to metallic/ceramic particles (gold, silica, magnetic oxide particles, etc.) [75]. The ability of non-degradable particles to remain in tissues for extended periods of time is meant to help improve antigen persistence [55]. Gold and iron oxide particles have been frequently

described for vaccine delivery usually to enhance the potency of DNA vaccines by improving delivery into cellular interiors [76]. However, these results are obtained using electroporation. In the absence of electroporation, the immunological effects of gold particle antigen carriers are weak [77]. Also, recent studies show that the use of gold nanoparticles along with alum can enhance the immune response against HBV, influenza, and malaria antigens [78]. Additionally, vaccines using iron oxide particle delivery systems have been in clinical studies for blood stage malaria [79].

Compared to metallic particles, polymeric particles have several technological advantages including the ability to functionalize the particles surface to achieve effective conjugation of antigens. Furthermore, when the antigen is covalently coupled to the particle, it induced higher cellular and humoral responses when the antigen is absorbed [80]. Latex particles, for example have been shown to increase the co-presentation of antigens with MHC-I and MHC-II molecules by 1000-10,000 fold [81]. However, in general, non-degradable particles are much less effective at cross-presenting antigens than degradable particles like chitosan based antigen delivery systems [82]. Other disadvantages of non-degradable delivery systems include, chronic inflammation, induration, pruritis, and cyst formation at the injection site [83].

1.3.6. Biodegradable polymeric particles

Biodegradable polymers provide sustained release of the encapsulated antigen and degrade in the body to nontoxic, low molecular weight products that are easily eliminated [84-86]. Polymeric biodegradable particles have considerable advantages over more traditional antigen delivery systems including the controlled delivery of antigens and adjuvants to the

desired location at predetermined rates and durations to generate an optimal immune response. The carrier may also protect subunit antigens from degradation until they are released either outside or inside the APCs [84]. Other potential advantages of the controlled delivery approach include reduced systemic side effects and the possibility of co-encapsulating multiple antigenic epitopes or both antigen and adjuvant in a single carrier.

Biodegradable polymeric nanoparticles or microparticles can be prepared from natural polymers like proteins, polysaccharides or using synthetic biodegradable polymers. The selection of the base material is based on various factors including but not restricted to size and antigen properties (solubility, stability, size, etc.) [75]. Synthetic polymers such as poly (lactic acid) (PLA), poly (lactide-co-glycolic acids) (PLGA), poly (methyl methacrylate) (PMMA), and poly (ϵ -caprolactone) (PCL) have been developed for traditional drug delivery applications. Synthetic polymer based particles enable better drug release kinetics compared to polysaccharide particles as the former can provide drug release over a period of days to several weeks compared to the quick release of the latter [87].

Polyesters including PLA, PLG, and PLGA are the most popular materials for the preparation of polymer nanoparticle based antigen delivery systems [70]. These polymers have been approved for use in humans (e.g., as sutures, bone implants and screws as well as implants for sustained drug delivery) and have been extensively studied for subunit antigen delivery) [88, 89]. Studies have shown that PLGA particles can be loaded or functionalized with immunogenic moieties that can target antigen presenting cells (APCs), eliciting the cellular and humoral immune response that is several times superior to soluble antigen [90, 91]. Fredriksen et al. have shown that PLGA and PLA microparticles delivering Atlantic salmon antigens induced an elevated humoral response compared to soluble antigen alone [92]. Preclinical studies have

shown that PLG nanoparticles can induce systemic antigen specific antibody titers comparable to those of aluminum salts [88]. Additionally, a study using tetanus toxoid (TT) found that a synergistic immune response could be achieved by injecting TT bound to an aluminum salt along with TT-loaded nanoparticles [93]. Another study showed that PLG nanoparticles loaded with MPL and a cancer-associated antigen (MUC1) were efficiently taken up by dendritic cells [94]. PCL nanoparticles together with mucoadhesive polysaccharide chitosan were used for delivering *Streptococcus equi* surface proteins significantly increased the antigen specific serum IgG antibody levels of vaccinated mice [95]. Studies showed that particles prepared from Poly(γ -glutamic acid) (γ -PGA) can activate human monocyte-derived dendritic cells and strongly stimulate the production of chemokines and inflammatory cytokines as well as upregulation of costimulatory molecules and immunomodulatory mediators involved in efficient T cell priming. Furthermore, *in vitro* studies with DCs pulsed with allergen *Phleum pratense* loaded γ -PGA nanoparticles showed an increase allergen-specific IL-10 production and proliferation of autologous CD4⁺ memory T cells [96].

Despite obvious interest in nanoparticulate adjuvants and delivery systems, the use of these polymers as peptide or protein delivery systems may negatively affect the stability of the loaded compound due to the use of solvents in particle preparation and the acidic degradation byproducts [94, 97, 98]. As such none of the polymer based vaccine delivery systems discussed here have progressed beyond preclinical trials.

1.4. Chitosan based antigen delivery systems

Chitosan is a natural polysaccharide obtained by alkaline deacetylation of chitin, a principle component of shellfish exoskeleton [99, 100]. It is an unbranched copolymer of glucosamine and N-acetylglucosamine units linked by α -glycosidic bonds (Figure 7). In solution, chitosan's primary amine groups become protonated and the polycationic charge facilitates cell adhesion, uptake and interaction with various anionic proteins and peptides. The biological properties of chitosan including biocompatibility, bioactivity, wound healing, and immune system stimulation makes it suitable for biomedical applications including drug delivery, gene delivery, wound healing, tissue engineering and vaccine delivery [101-106]. Finally, chitosan has an excellent safety record in humans as a pharmaceutical excipient, a weight loss supplement, an experimental mucosal adjuvant and in an FDA-approved hemostatic dressing [107, 108].

Chitosan in different forms including solution, hydrogels, conjugates, and particles are being used for various applications. Chitosan based delivery systems are being used for molecular imaging, delivery of DNA, RNA, low molecular drugs, and protein therapeutics. Chitosan's mucoadhesive and absorption-enhancing properties have been extensively studied for delivery of therapeutic proteins and antigens particularly via mucosal routes [109]. Chitosan can interact with mucus and epithelial cells and induce a redistribution of cytoskeletal F-actin and the tight junction protein ZO-1 resulting in opening of cellular tight junctions and increasing the paracellular permeability of the epithelium [110, 111]. Also, chitosan charge and other structural elements likely contribute to penetration-enhancing activity, since cationic polysaccharides, such as quaternized diethyl aminoethyl (DEAE)-dextran were ineffective as an enhancer [112]. In many studies, it has been demonstrated that chitosan-based formulations were superior in

enhancing absorption of therapeutic proteins as well as induction of antibodies after mucosal vaccination [113, 114]. While chitosan in different forms was used for vaccination, very few studies involved the use of chitosan particles for vaccine and immunotherapy applications.

Chitosan micro/nanoparticulate systems are under intense investigation for drug, gene, and protein delivery [115-119]. Chitosan particles have been manufactured via a variety of chemistries including cross-linking, ionotropic gelation and precipitation-coacervation [120-123]. The last two methods are particularly attractive for the delivery of labile peptides and proteins because encapsulation is accomplished under mild, aqueous conditions. This is in contrast to commonly used synthetic biomaterials that require organic solvents capable of denaturing polypeptides and destroying bioactivity. Also, chitosan particles can be surface functionalized with immunopotentiating compounds like LPS to mimic pathogens that elicits an enhanced humoral and cell mediated immune response.

HYPOTHESIS

The future of vaccine development has been clearly shifting towards particulate based antigen delivery systems. The properties of chitosan along with its ability to actively encapsulate labile polypeptides and peptides makes it ideal for delivery of antigens. Our laboratory's previous studies have shown that mixtures of recombinant cytokines or full-length protein antigens in chitosan solution can enhance local retention and bioactivity following injection [41, 117, 124]. However, particles are naturally more immunogenic and may provide more robust adaptive immunity than solution based formulations. Also, particle size can be optimized to improve uptake by APCs, enhance APC activation, and antigen presentation. In this project we explore the feasibility of chitosan particle based antigen delivery systems for enhanced antigen specific immunity.

We hypothesize that protein antigens can be effectively encapsulated by chitosan particles. The encapsulated antigens can then be taken by APCs resulting in APC activation. Activated APCs would then present peptide antigen with both MHC-I and MHC-II to T-cells resulting in robust antigen specific immunity. Also, the size of chitosan particles can be optimized to attain enhanced immune response.

APPROACH

Our research plan was to develop and evaluate chitosan particle based antigen delivery platforms based on the direct encapsulation of antigens in chitosan particles. This strategy was expected to hinder the *in vivo* dissemination of antigens through electrostatic immobilization on and in chitosan molecules. In addition, highly cationic chitosan particles would adhere to negatively charged extracellular matrix and cell membranes upon injection. This electrostatic interaction would effectively anchor antigens at the injection site and allow their uptake by APCs.

In this project, antigen-encapsulated chitosan particles (AgCPs) were developed and evaluated as a novel antigen delivery system. In the first aim, AgCPs of mean sizes ranging from 300nm to 3µm were developed and characterized. The effect of formulation factors on particle properties was evaluated. In the second aim, AgCPs of various sizes were evaluated *in vitro* for their ability to enhance antigen presentation. Specifically, the effect of particle size on antigen uptake by APCs was explored. Also, the ability of particulate antigens to induce APC activation/maturation compared to that of soluble antigen was evaluated. The third and final aim evaluated the ability of AgCPs to enhance antigen specific immune response *in vivo*.

2. SPECIFIC AIM 1: Synthesis and Characterization of Chitosan Particles of Varying Sizes- Effect of Formulation Factors on Particle Properties

2.1. Rationale

Chitosan is under investigation for a wide variety of biomedical applications including drug delivery, gene delivery, wound healing, antimicrobial applications, tissue engineering and vaccine delivery [101, 102, 104-106, 125]. The use of chitosan in these diverse applications is supported by its exceptional versatility. Chitosan can be used in solutions, hydrogels and/or nano/microparticles, while an endless array of chitosan derivatives with customized biochemical properties can be prepared through facile conjugation of side chain moieties to solvent-accessible amine and hydroxyl groups. As a result, chitosan is currently among the well-studied biomaterials with more than 1800 publications in 2013 using chitosan as a keyword. For reference, other ubiquitous biomaterials, polylactic-co-glycolic acid (PLGA) and polycaprolactone (PCL) are keywords in only about 700 and 340 publications, respectively.

Chitosan nano/microparticulate systems, in particular, are intensively studied for the delivery of genes, protein biologics and antigens [116-119, 126, 127]. When developing nano/microparticulate systems for drug/protein delivery applications it is important to be able to control characteristics, such as particle size, size distribution, and surface charge, as these can significantly influence release kinetics. For example, increasing particle size has been shown to increase drug release rates of encapsulated drugs/proteins [128, 129]. In addition, particle size has been shown to influence uptake by immune cells in vaccine applications. Particles with sizes similar to pathogens, such as viruses (5-300 nm) and bacteria (1-5 μm), are readily taken up and processed by antigen presenting cells (APCs) which leads to enhanced vaccine responses. Our

recent studies demonstrated that 1 μm chitosan particles were optimal for uptake by both dendritic cells and macrophages, however, APC activation was highest with 300 nm chitosan particles [127].

It is clear that different biomedical applications will require unique chitosan particles with well-defined dimensions and release characteristics. Thus, there exists a need to develop a methodology for effective control of chitosan particle size, protein loading efficiency and protein release. Chitosan particles have been manufactured via a variety of chemistries including cross-linking, ionotropic gelation and precipitation-coacervation [120-123]. These last two methods are particularly attractive for the delivery of labile polypeptides as encapsulation is accomplished under mild aqueous conditions.

In this study, we utilized the precipitation-coacervation technique to comprehensively characterize the effects of various formulation factors, such as chitosan concentration, precipitant salt concentration, chitosan molecular weight, rate of precipitant addition, protein size and sonication power on chitosan particle size, polydispersity, and protein loading efficiency. A range of precipitant salts with varying strengths of hydration in the Hofmeister series were explored. In vitro release studies were performed to determine the effect of particle size, precipitant salt, and encapsulated protein on protein release from chitosan nano/microparticles. An analysis of the binding between proteins and chitosan explains the impact of protein-chitosan interactions during encapsulation and release. The results obtained in this study will be useful in the standardization of protocols for the preparation of antigen encapsulating chitosan particles (AgCPs).

2.2. Methodology

2.2.1. Reagents

Chitosans with viscosities of 20, 20-200, 200-600, 600-1200, and 1200-2000 cPs, were purchased from Primex (Siglufjordur, Iceland) and purified via filtration in hydrochloric acid and precipitation in sodium hydroxide. Pluronic F-68, acetic acid, sodium chloride (NaCl), potassium chloride (KCl), sodium sulfate (Na_2SO_4), ammonium sulfate ($(\text{NH}_4)_2\text{SO}_4$), magnesium sulfate (MgSO_4), potassium sulfate (K_2SO_4), sodium citrate ($\text{Na}_3\text{C}_6\text{H}_5\text{O}_7$), trisodium phosphate (Na_3PO_4), fluorescein isothiocyanate-labeled bovine serum albumin (FITC-BSA), unlabeled BSA and ovalbumin (OVA) were purchased from Sigma (St. Louis, MO). FITC- OVA, FITC-insulin and FITC-concanavalin A (FITC-ConA) were purchased from Life Technologies (Green Island, NY).

2.2.2. Preparation and characterization of chitosan particles

Chitosan particles were prepared using the precipitation-coacervation method developed by Berthold et al., with slight modifications [130, 131]. In brief, chitosan was dissolved in a 2% (v/v) acetic acid solution. Chitosan particles were formed by adding 50 mM precipitant salt solution drop wise to the chitosan solution using an infusion pump (Pump 11 Elite, Harvard Apparatus, Holliston, MA). Nonionic stabilizer Pluronic F-68 was added and particles were allowed to stabilize for 2 hours under constant stirring and intermittent sonication using a sonicator (S4000; Misonix Inc., Farmingdale, New York). Chitosan particles were collected after centrifugation at 25,000 xg for 10 min at 4°C and freeze dried (FreeZone, Labconco, Kansas City, MO) before further use. Chitosan particles loaded with various proteins including FITC-

BSA, FITC-Insulin, FITC-OVA, and FITC-ConA, were prepared in a similar manner except that proteins were dissolved in chitosan solution before adding the precipitant salt solution. Size and polydispersity index (PDI) of the resultant particles were determined by dynamic light scattering (DLS) (Zetasizer, NanoZS90, Malvern). PDI was calculated as a value between 0 and 1 with the value closer to 1 indicating highly poly dispersed particles and value closer to 0 indicating mono dispersed sample.

2.2.3. Effect of formulation factors on particle properties

The influence of formulation factors, including chitosan concentration, molecular weight, rate of precipitant addition, protein size, and sonication power, on chitosan particle size and size distribution was determined. Preliminary experiments indicated that precipitant concentration, stabilizer concentration, pH, and chitosan:protein ratio had negligible effect on chitosan particle size (data not shown). Therefore, an experimental design using 6 factors including chitosan concentration (0.5 to 5 mg/ml), chitosan viscosity (< 20 to 1200 cPs), precipitant salt composition, infusion rate of precipitant (0.2 to 8 ml/min), sonication power (0 to 40 W), and proteins of different sizes (insulin – (6 kDa), ovalbumin – (45 kDa), BSA – (66.5 kDa), and ConA – (105 kDa)) was utilized. A constant chitosan-to-protein mass ratio of 10:1 was maintained for all experiments. The experimental design is shown in Table 1.

2.2.4. Protein loading and release studies

Protein loading efficiency was calculated indirectly. Briefly, the amount of FITC-conjugated protein remaining in the supernatant after removing the protein-loaded chitosan

particles was determined via fluorescence spectroscopy. The difference between the initial and the unencapsulated protein concentrations was divided by the initial concentration (equation 1).

$$\text{Percentage loading efficiency} = \frac{(\text{Initial conc} - \text{Unencapsulated conc})}{\text{Initial conc}} \times 100 \quad (1)$$

For protein release studies, FITC-BSA loaded chitosan particles with discrete sizes (300 nm, 1 μm , and 3 μm) (see Table 2) and salt groups (Na_2SO_4 , $(\text{NH}_4)_2\text{SO}_4$, MgSO_4 , K_2SO_4 , and $\text{Na}_3\text{C}_6\text{H}_5\text{O}_7$) (see Table 3) were prepared using data gathered from previous experiments. FITC-BSA loaded chitosan particles were suspended in deionized water or phosphate buffered saline (PBS) and incubated in total darkness at 37°C. To determine the effect of protein size on release profile, chitosan particles loaded with different proteins, i.e. FITC-labeled insulin, OVA, BSA, and ConA (see Table 4), were suspended in PBS and incubated at 37°C. Supernatants were collected and replaced by fresh deionized water or PBS at regular intervals for 2 weeks. Samples were stored in the dark at -20°C until batch analysis via fluorescence spectroscopy (excitation wavelength: 490 nm, emission wavelength: 540 nm). Percent protein released was determined by dividing the amount of released protein by total encapsulated protein.

2.2.5. Statistical analysis

All experiments were carried out in triplicate or quadruplicate. Where appropriate, data are presented as means \pm standard deviation. Where indicated, analysis of variance (ANOVA) was performed using JMP software (SAS, Cary, NC). Statistical significance was accepted at the $p \leq 0.05$ level.

2.3. Results

2.3.1. Effect of precipitant salt type on chitosan particle properties

Preliminary studies indicated that salt concentration (above 100 mM), surfactant (Pluronic F-68) concentration, and chitosan:protein ratio had negligible effect on chitosan particle size, polydispersity and encapsulation efficiency. Therefore, subsequent experiments focused on other factors such as chitosan concentration, chitosan molecular weight, precipitant salt composition, precipitant salt addition rate, sonication power, and protein size. The viscosity of chitosan was used as a surrogate for molecular weight as the two properties are related [132] and molecular weight of polydisperse chitosan is not often reported.

To isolate the effect of precipitant salt composition, all other formulation parameters were fixed. Chitosan concentration was kept at 1 mg/ml, chitosan viscosity was 200-600 cPs, precipitant salt concentration was 100 mM, precipitant salt addition rate was 8 ml/min, sonication power was maintained at 10 W, and FITC-BSA was used as a model protein.

Salts with anions and cations of varying hydration strength, according to the Hofmeister series, were utilized. Sodium was used as a cationic constant while the effect of anion type was explored. Likewise, sulfate was used as anionic constant while the effect of cation type was investigated. As seen in Table 1, decreasing the hydrating strength of anionic component of precipitant salt affected particle size. Specifically, sulfate and citrate anions with high degrees of hydration induced the formation of 427 ± 5.5 nm to 490 ± 18.3 nm particles, respectively. As the degree of hydration was reduced, through the phosphates, particle size increased from 427 ± 5.5 to 1621 ± 188 nm. A further reduction in hydration strength to chloride anions was not able to form particles. Changing the cationic component of the salt had less of an effect on particle size

with sulfate salts of magnesium, sodium, and ammonium producing 445 ± 7.7 nm, 427 ± 7.6 nm, and 550 ± 3.5 nm particles, respectively. In general, the PDI for all particles formed was between 0.11 to 0.15 except when Na_3PO_4 was used and PDI increased to 0.66 indicating a fairly poly dispersed sample.

Increasing the hydration strength of the anionic component from phosphate to sulfate to citrate resulted in marked increases in protein loading efficiencies from $14.68 \pm 1.7\%$ to $54 \pm 2.6\%$ to $83.7 \pm 3.5\%$, respectively. Once again, changing the cationic component of the salt did not significantly influence the protein loading efficiency. In fact, sulfate salts of sodium, ammonium, and magnesium produced chitosan particles with protein loading efficiencies of $54 \pm 2.6\%$, $62.5 \pm 6.1\%$, and $47.5 \pm 2.0\%$, respectively.

2.3.2. Effect of chitosan molecular weight and concentration on chitosan particle properties

To isolate the effect of the chitosan molecular weight, Na_2SO_4 was used as the precipitant salt and all other formulation parameters were fixed as described above. Chitosan particle size was found to be directly related to chitosan molecular weight, i.e. viscosity (Figure 8). Particle sizes more than doubled, from 418 ± 16.2 nm to 854 ± 26.2 nm, by increasing the intrinsic viscosity of chitosan from <20 cPs to 1200 – 2000 cPs (Table 1). In contrast, chitosan molecular weight did not significantly influence protein loading efficiencies which were between $50.4 \pm 2.3\%$ to $58.5 \pm 4.2\%$ (Table 1).

To isolate the effect of the chitosan concentration, chitosan with viscosity of 20-200 cPs was used, and all other formulation parameters were fixed as described above. Increasing chitosan concentration from 0.5 mg/ml to 5 mg/ml resulted in particle size increasing from $334 \pm$

27.5 nm to 656 ± 10.6 nm (Figure 8, Table 1). Protein loading efficiencies were similar for 0.5, 1.0 and 2.0 mg/ml. However, when chitosan concentration was increased to 3 and 5 mg/ml, the protein loading efficiency jumped to $73.6 \pm 2.2\%$ and $92 \pm 0.8\%$ respectively.

2.3.3. Effect of sonication on chitosan particle properties

To isolate the effect of sonication, Na_2SO_4 was used as the precipitant salt and all other formulation parameters were fixed as describe above. Chitosan particles prepared using 10 W sonication decreased in size to 438 ± 3.9 nm from 922 ± 79.2 nm without sonication (Figure 8). PDI also decreased from 0.657 without sonication to 0.182 at 10 W (Table 1). Further increasing sonication power to 40 W did not significantly affect particle size. However, PDI was further reduced to 0.098 at 40 W (Table 1).

While increasing sonication power was effective in increasing particle uniformity, protein loading efficiency was reduced. Loading efficiencies decreased from $92.3 \pm 1.8\%$ without sonication, to $88.3 \pm 5.3\%$ at 10 W, to $74.2 \pm 6.3\%$ at 20 W, and $56.5 \pm 2.6\%$ at 40 W (Table 1).

2.3.4. Effect of salt addition rate on chitosan particle properties

To isolate the effect of salt addition rate, Na_2SO_4 was used as the precipitant salt and all other formulation parameters were fixed as described above. Precipitant salt addition rate was inversely related to chitosan particle size. Increasing the salt addition rate from 0.2 ml/min to 8 ml/min resulted in a decrease in particle size from 774 ± 33.23 nm to 424 ± 2.1 nm (Figure 8, Table 1). Most of the size reduction was observed in the lower range of salt addition rates. In

addition to becoming smaller, particles also became more uniform as PDI was reduced from 0.580 to 0.121.

Protein loading efficiency was also inversely related to precipitant salt addition rate. Loading efficiencies decreased steadily from $71.9 \pm 7.0\%$ at 0.2 ml/min, to $67.3 \pm 3.2\%$ at 1 ml/min, $65.3 \pm 3.6\%$ at 3 ml/min, $62 \pm 2.8\%$ at 5 ml/min and $58.1 \pm 2.2\%$ at 8 ml/min.

2.3.5. Effect of protein molecular weight on chitosan particle properties

A range of proteins, FITC-Insulin (6 kDa), FITC-OVA (45 kDa), FITC-BSA (66.5 kDa), and FITC-ConA (105 kDa) were selected to study the effect of protein size on chitosan particle properties. Na_2SO_4 was used as the precipitant salt while all other formulation parameters were fixed as described above. The size of the encapsulated protein had no significant effect on chitosan particle size ($p > 0.05$). However, loading efficiencies decreased with increasing protein molecular weight. Chitosan particles were loaded with FITC-Insulin, FITC-OVA, FITC-BSA, and FITC-ConA at $98.3 \pm 0.5\%$, $96.5 \pm 1.1\%$, $58.1 \pm 2.5\%$, and $53.5 \pm 3.6\%$ efficiency, respectively (Table 1). Interestingly, even though the molecular weight of OVA is similar to BSA, OVA was encapsulated by chitosan at a much higher efficiency than BSA.

2.3.6. Effect of release medium ionic strength on protein release

Chitosan and protein molecules are expected to bind electrostatically before and after particle formation. As a result, exposure of particles to solutions with high concentrations of ions is expected to disrupt electrostatic bonds and affect protein release. To explore the effect of

release medium ionic strength on protein release, FITC-BSA encapsulated chitosan particles formulated with Na_2SO_4 with mean size of 448 ± 12 nm and protein loading of $56.4 \pm 6.3\%$ were exposed to increasing concentrations of PBS. Indeed, FITC-BSA release increased with ionic strength of the releasing medium (Figure 9). Particles incubated in 0.1X, 0.5X, and 1X PBS released 34.2%, 39.7%, and 45.2% of encapsulated FITC-BSA over a 1 week period. In contrast, particles incubated with deionized water released only 2.6% of encapsulated protein.

2.3.7. Effect of chitosan particle size on protein release

To study the influence of particle size on protein release, FITC-BSA encapsulated chitosan particles with nominal sizes of 300 nm, 1 μm , and 3 μm were generated based on the results of Table 1. As seen in Figure 10, SEM pictures showed that the chitosan particles obtained have spherical to elliptical morphology with good size distribution. The actual particle sizes were 318.2 ± 11 nm, 1133 ± 54.1 nm, and 2871 ± 216 nm (Table 2). FITC-BSA loading efficiencies were $58.1 \pm 3.7\%$, $83.5 \pm 8.3\%$, and $96.6 \pm 0.6\%$, respectively.

As seen in Figure 11, FITC-BSA release profiles from all particle sizes were characterized by an initial burst of about 5-10% of the encapsulated protein followed by a slow, sustained release in which a total of 30-50% of the protein was released in PBS over 1 week. The amount of FITC-BSA released increased with increasing particle size. The “300 nm,” “1 μm ,” and “3 μm ” groups released 31.4%, 42.6%, and 46.9% of their encapsulated FITC-BSA within one week.

2.3.8. Effect of precipitant salt on protein release

FITC-BSA encapsulated chitosan particles formulated with Na_2SO_4 , $(\text{NH}_4)_2\text{SO}_4$, MgSO_4 , $\text{Na}_3\text{C}_6\text{H}_5\text{O}_7$, and Na_3PO_4 yielded particles of sizes 448 ± 12 nm, 561 ± 3.4 nm, 462 ± 6.3 nm, 478 ± 64.3 nm, and 1423 ± 156 nm respectively, with protein loading efficiency of $56.4 \pm 6.3\%$, $62 \pm 5.3\%$, $54.3 \pm 3.4\%$, $86 \pm 2.1\%$, and $14.3 \pm 6.6\%$, respectively.

Protein release profiles of particles were dependent on the cationic component of precipitant salt with total amount protein release decreasing with decreasing hydrating strength of cations. MgSO_4 , Na_2SO_4 , and $(\text{NH}_4)_2\text{SO}_4$ particles released 50.87%, 45.2%, and 31.7% respectively over one week. However, changing the anion of the salt caused significant change in protein release profile of the particles with $\text{Na}_3\text{C}_6\text{H}_5\text{O}_7$, Na_2SO_4 , and Na_3PO_4 particles releasing 51.4%, 45.2%, and 98.1% of encapsulated protein over one week.

2.3.9. Effect of encapsulated protein on protein release

Chitosan particles precipitated with Na_2SO_4 and loaded with FITC-insulin, FITC-OVA, FITC-BSA, and FITC-ConA were similarly sized at 421 ± 10.1 nm, 429 ± 3.6 nm, 448 ± 22.4 nm, and 452 ± 5 nm, respectively (Table 4). Protein loading efficiencies varied as before (Table 1) at $99.2 \pm 0.1\%$, $98 \pm 0.4\%$, $56.4 \pm 3.2\%$, and $53.4 \pm 1.8\%$, respectively.

As shown in Figure 12, the nature of encapsulated protein had a significant effect on release kinetics. The two largest proteins, FITC-BSA and FITC-ConA, exhibited the highest levels of burst and cumulative release, 48.2% and 48.9%, respectively, over a one week period. The smallest protein, FITC-insulin, exhibited very little burst release but reached 40.42% release

over one week. Interestingly, the vast majority of FITC-OVA remained in chitosan particles after one week with only 2.4% released.

2.4. Discussion

There are several published methods for manufacturing drug or protein-loaded chitosan particles [120-123]. Methods include the use of crosslinking agents [122, 133, 134], emulsion-precipitation [135], ionotropic gelation and precipitation-coacervation. The use of crosslinkers or organic solvents during emulsion-precipitation can be detrimental when encapsulating labile proteins. While both precipitation-coacervation and ionotropic gelation can form chitosan particles in mild aqueous conditions, precipitation-coacervation was preferred for two reasons. First, based on our own experiences, as well as published data, the size of chitosan particles on any subsequent exploration of the effects of particle size in biomedical applications. Second, ionotropic gelation generally results in lower drug/protein loading efficiencies with 38-72% of BSA loading efficiencies observed with ionotropic gelation compared to 74-98% obtained with precipitation coacervation method [40, 115].

In this study, we comprehensively explored the effects of 10 precipitation-coacervation parameters on chitosan particle size, polydispersity, protein loading efficiency and protein release. Four of the 10 parameters were eliminated in preliminary studies as having no impact. The remaining 6 factors were studied individually by isolating a single parameter while fixing the other 5 parameters.

Chitosan particle size was found to increase with chitosan concentration and molecular weight/viscosity and decreased with precipitant salt addition rate and sonication power. The

effect of chitosan concentration and molecular weight can be explained by the fact that addition of increased amounts of the chitosan starting material to the precipitation-coacervation reaction increases the probability of interaction of chitosan polymers to form larger particles. Conversely, a higher salt addition rate reduced chitosan-chitosan and chitosan-protein interactions and led to the formation of smaller sized particles. The effect of sonication was consistent with published studies demonstrating that chitosan particles prepared through ionotropic gelation were reduced in both size and PDI after sonication [114, 133, 134, 136]. Our data indicate that a threshold level of sonication is preferred to produce a more uniform size distribution of chitosan particles, but that further increases in sonication power adversely affected loading efficiency.

Protein loading efficiencies increased with chitosan concentration and molecular weight/viscosity. These findings were consistent with previous studies demonstrating that drug loading and release from chitosan particles was directly related to chitosan molecular weight/viscosity [137]. Higher chitosan molecular weight and/or concentration increases the likelihood of anionic proteins interacting with cationic chitosan molecules prior to precipitation.

In general, protein loading efficiencies decreased as protein molecular weight increased. However, we also identified protein charge as a major factor in loading efficiency. Our findings that protein release increased with ionic strength of the releasing medium (Figure 9) and that NaCl disrupts protein-chitosan binding indicate that protein-chitosan binding is mediated via electrostatic interactions. Therefore, a highly negatively charged protein, such as OVA, will be loaded in cationic chitosan particles more efficiently and released more slowly than a similarly sized protein with a more neutral or positive net charge.

Among the strongest effects on chitosan-protein particle formation was the hydration strength of precipitant salt anions. Strong Hofmeister series anions with high degrees of hydration, such as citrate and sulfate, induced formation of smaller and more uniform particles. Decreasing the degree of hydration by using phosphate anions resulted in an increase in both particle size and polydispersity likely due to particle aggregation of weakly formed particles. A further decrease down the Hofmeister classification to chloride anions abrogated particle formation. These results were expected as salts with strongly hydrated ions can strip away water molecules from proteins or biopolymers resulting in salting out or precipitation [138, 139]. Weaker ions such as Cl^- are unable to remove a sufficient amount of water to induce precipitation.

Interestingly, strong Hofmeister anions also induced higher loading efficiencies. It was originally predicted that strong anions would independently disrupt chitosan-protein binding and precipitate chitosan and protein. However, it appears that mixing chitosan and protein prior to addition of precipitant salt allows sufficient electrostatic binding for the chitosan-protein complexes to salt out together. Taken together with our particle size analysis, in general, strong Hofmeister anions were better at forming highly loaded, chitosan-protein particles.

Release studies demonstrated that protein release from chitosan particles, regardless of the sample group was characterized by an initial burst followed by sustained release. The release was found to be strongly dependent on the releasing medium with 34.1-45.2% protein release observed in PBS compared to that of 2.6% observed in deionized water. While previous studies showed that the release of drug from chitosan particles was dependent on solution pH [40, 140], our studies show that the release is also dependent on the ionic strength of the medium. ITC studies showed that chitosan-protein binding was dependent on the salinity of solution.

Specifically, chitosan-protein interaction was significant at 0mM NaCl, but was eliminated at 25 mM NaCl. In mildly acidic aqueous solutions, chitosan's primary amines are protonated. Thus, polycationic chitosan molecules interact electrostatically with co-formulated proteins. These positive charges are likely to be responsible for electrostatic interactions with proteins. However, when high levels of free anions, such as chlorides and phosphates, are present, they can interact with the protonated chitosan and disrupt protein binding resulting in lower loading efficiencies and/or faster release rates [130, 141].

Overall, smaller proteins were released from chitosan particles much more quickly. However, OVA, despite being similar in size to BSA, was a notable exception. Only 2.4% of OVA was released compared to 48.1% of BSA. This discrepancy can be explained by the higher binding constant and free energy change of OVA versus BSA (Data not shown). In general, proteins with higher densities of negative surface charges are likely to be loaded in chitosan particles more efficiently and released more slowly. We are currently investigating the effects of a protein's charge density on its interactions with chitosan and other polysaccharides.

Finally, protein release rate was found to increase with particle size. Whether this effect is driven by pore size, which we believe increases with particle size, is the subject of future studies. Nevertheless, these data imply that one can customize protein release profiles through manipulation of chitosan particle size

2.5. Conclusion

Different biomedical applications will require chitosan particles with specific dimensions and release characteristics. The results of this study demonstrate that the properties of chitosan

particles including size, size distribution, and protein loading can be effectively modulated by controlling precipitation-coacervation formulation parameters. Understanding the influence of these parameters will help standardize chitosan particle based delivery of proteins for continued preclinical and clinical development. Furthermore, these data are valuable in engineering controllable chitosan nano/microparticles for customized delivery of protein biologics and vaccines. As such, the parameters were optimized to prepare chitosan particles of varying sizes and were used in further studies.

3. SPECIFIC AIM 2: Assess *In Vitro* Particulate Antigen Uptake and Presentation by Antigen Presenting Cells

3.1. Rationale

Over the last several decades, vaccine development has shifted away from using attenuated or inactivated whole pathogens in favor of recombinant subunit antigens [142-144]. This shift is partly due to safety concerns over potentially harmful pathogens and partly due to an increasing interest in inducing immunity towards non-pathogenic self or self-like antigens such as tumor-associated antigens or overexpressed proteins implicated in disease (e.g. amyloid beta) [145-147]. While subunit antigens are much safer, they are also much less immunogenic than whole pathogens. Subunit antigens are rapidly degraded by proteases and lack the requisite secondary immune stimulus, i.e. co-stimulation and/or danger signals, required for the generation of antigen-specific immunity [12]. As a result, a great deal of effort has been spent developing delivery systems and/or adjuvants capable of enhancing vaccine responses to subunit and polypeptide antigens [11, 12, 148].

The encapsulation of polypeptide antigens in nano- and/or microparticles has been explored extensively as a strategy to enhance immunogenicity. The advantage of this strategy is three-fold: First, encapsulation of antigens in particles can prevent antigen degradation and enhance antigen persistence. Second, antigen presenting cells (APCs), such as macrophages and dendritic cells, have been shown to readily phagocytose and process particles ranging in size from 150 nm to 4.5 μm [149, 150]. Third, most particle-based platforms can be engineered to contain additional adjuvants and/or targeting moieties to further influence immunogenicity [142, 143]. In general, antigens in particulate form have been shown to be more immunogenic than their soluble counterparts [151, 152]. A myriad of particle-based antigen delivery approaches

including liposomes, Immune stimulating complexes (ISCOMs), and polymeric particles are under development and have been reviewed elsewhere [72, 142, 153].

Chitosan-based vaccine delivery systems have received increasing attention due to chitosan's remarkable versatility and unique characteristics [41, 51, 117, 124, 154-157]. Chitosan is a natural polysaccharide derived primarily from the exoskeletons of crustaceans. Chitosan nano- and microparticles can be manufactured via either precipitation-coacervation [158] or ionotropic gelation [153]. Polypeptides can be encapsulated either during particle formation [40] or adsorbed to particle surfaces after formation [131]. Chitosan's mucoadhesiveness and ability to loosen epithelial gap junctions justifies its use in mucosal vaccines. Several studies have shown that chitosan nano- and microparticles loaded with antigens can generate mucosal immunity following intranasal vaccination [116, 159]. However, chitosan particles are also expected to elicit robust immune responses via non-mucosal routes. Yet, in the only s.c. vaccination study to date, no significant immunity was generated with a vaccine comprised of ovalbumin (OVA) adsorbed to chitosan nanoparticles [131].

While the above study may have failed to induce immune activation due to a documented change in antigen conformation, it is important to note that vaccine responses are highly complex, involve multiple cell types and require successful completion of many interdependent processes including antigen uptake, cytokine release, immune cell trafficking, antigen presentation, co-stimulation, etc. To simplify the contributions of chitosan-based particles, in this study, we focused solely on APC function. In particular, we evaluated the ability of antigen-encapsulated chitosan particles (AgCPs) to enhance antigen uptake, APC activation and antigen presentation. The effect of particle size on antigen uptake by both bone marrow-derived dendritic cells and RAW 264.7 macrophages was quantified via spectrophotometry and flow cytometry.

The ability of AgCPs to induce APC activation was determined by measuring upregulation of surface activation markers as well as cytokine release. Finally, APCs exposed to AgCPs or soluble antigens were compared for their ability to present antigen and induce proliferation of antigen-specific T cells.

3.2. Methodology

3.2.1. Reagents

Chitosan (viscosity 20-200, 200-600, and 600-1200 cPs degree of deacetylation 90%) was purchased from Primex (Siglufjordur, Iceland) and purified via filtration in hydrochloric acid and precipitation in sodium hydroxide. Pluronic F-68, acetic acid, sodium sulfate (Na₂SO₄), FITC-BSA, OVA, L-glutamine, HEPES buffer, trypsin-EDTA, and lipopolysaccharide (LPS) were purchased from Sigma (St.Louis, MO). Ammonium-Chloride-Potassium (ACK) lysing buffer, Cell culture medium components including, fetal bovine serum (FBS), antibiotics, Dulbecco's Modified Eagle Medium (DMEM), and RPMI-1640 medium were purchased from Thermo Scientific (Rockford, IL). Recombinant murine granulocyte-macrophage colony-stimulating factor (GM-CSF) was purchased from Peprotech (Rocky Hill, NJ) and OVA₂₅₇₋₂₆₄ peptide were purchased from Thermo Scientific (Rockford, IL). All antibodies used for flow cytometry along with cytometric bead array kits were purchased from BD Biosciences (San Jose, CA).

3.2.2. Mice

Female C57BL/6J, OT-1 and OT-II mice with respective CD4⁺ and CD8⁺ T-cells expressing T-cell receptors specific to OVA protein peptides were purchased from The Jackson Laboratory (Bar Harbor, ME). Mice were housed in a pathogen-free animal facility and used at 8 to 12 weeks of age. All experimental procedures were approved by the Institutional Animal Care and Use Committee at the University of Arkansas and animal care was in compliance with The Guide for Care and Use of Laboratory Animals (National Research Council).

3.2.3. Cell culture

RAW 264.7 mouse macrophage cells obtained from American Type Culture Collection (Manassas, VA) were cultured in complete medium consisting of DMEM supplemented with 20% FBS and 1% penicillin/streptomycin. Bone marrow-derived dendritic cells (BMDCs) were cultured from mouse bone marrow cells using an established protocol [160].

3.2.4. Preparation of AgCPs

Antigen encapsulating chitosan particles (AgCPs) were prepared via precipitation-coacervation as described previously with slight modifications [40, 131]. Briefly, chitosan was dissolved in 2% acetic acid and passed through a 0.2 μm filter. AgCPs were formed by adding a 10% w/v sodium sulfate solution containing either FITC-BSA or OVA as model protein antigens, henceforth referred to as BsaCPs or OvaCPs, respectively. Chitosan particles containing no antigen (CPs) were formed in the same manner but without BSA or OVA. Pluronic F-68 was added as a nonionic stabilizer and particles were stirred for 2 h with

intermittent sonication (S4000, Misonix, Farmingdale, NY). Chitosan particles were separated through centrifugation at 25,000 xg for 10 min and freeze dried before further use. Particles of various sizes were obtained by varying formulation factors as seen in Table 2.

3.2.5. Characterization of AgCPs

Particle size and surface charge was measured via dynamic light scattering (DLS) (Nano ZS90, Malvern Instruments, Malvern, UK). Morphological characteristics were documented using scanning electron microscopy (SEM) (Nanolab 200, FEI, Hillsboro, OR). Briefly, AgCPs dispersed in DI water were vacuum dried onto a glass slide. The sample slides are then sputter coated with gold before examining under SEM. The encapsulation efficiency of FITC-BSA in AgCPs was quantified via fluorescence spectroscopy (Synergy2, Biotek, Winooski, VT), measuring the supernatant fluid after centrifugation. Antigen encapsulation efficiency was calculated as seen in equation 2.

$$\text{Antigen encapsulation efficiency} = \frac{(\text{Initial antigen conc} - \text{Unencapsulated antigen conc})}{\text{Initial antigen conc}} \times 100 \quad (2)$$

3.2.6. Uptake of AgCPs by APCs

RAW 264.7 macrophages or BMDCs were collected and seeded at a density of 50,000 cells/well in 24 well plates. To determine the effect of particle size on uptake, cells were co-incubated with 300 nm, 1 μm , or 3 μm BsaCPs. To determine the effect of antigen concentration on uptake, cells were co-incubated with BsaCPs at an effective antigen concentration of 1, 5, 10, 20, or 30 $\mu\text{g/ml}$. To determine the effect of incubation time on uptake, cells were co-incubated with 1 μm BsaCPs at an effective antigen concentration of 30 $\mu\text{g/ml}$ for 12, 24, or 48 h. After each co-incubation, cells were rinsed three times with PBS to remove

particles not uptaken by cells. Cells were then lysed with 1% triton solution. The amount of FITC-BSA released was quantified via fluorescence spectroscopy. To assess the percentage of cells taking up BsaCPs, cells were rinsed three times with PBS and briefly trypsinized to form a single cell suspension prior to analyzing on a FACSCantoII (BD Biosciences, San Jose, CA).

3.2.7. APC activation

Activation markers on macrophages and BMDCs co-cultured with AgCPs were analyzed via flow cytometry. Briefly, RAW 264.7 macrophages and BMDCs were seeded onto 6 well plates at a density of 1×10^6 cells/well and cultured in their respective growth medium for 24 h. Medium containing BsaCPs was then added at a final antigen concentration of 30 $\mu\text{g/ml}$. Unloaded 300nm CPs that contained no antigen were used at the same dry weight as 300nm AgCPs. Medium alone was used as a negative control. After 24 h, cells were rinsed three times with PBS and briefly trypsinized to form a single cell suspension. FcII and FcIII receptors were blocked via incubation with 1 μg purified anti-mouse CD16/CD32 (clone: 2.4G2) per 1×10^6 cells for 15 min on ice. Cells were stained for 30 min on ice with fluorescence-labeled mouse monoclonal antibodies (1 $\mu\text{g}/1 \times 10^6$ cells) to the following markers: MHC I (clone: AF6-88.5), MHC II (clone: 2G9), CD11b (clone: M1/70), CD11c (clone: HL3), CD80 (clone: 16-10A1), CD86 (clone: GL1), CD40 (clone: HM40-3) and CD53 (clone: 3E2). Cells were then washed twice with cold PBS and analyzed on a six-color FACS CantoII. Data analysis was performed using BD FACSDiva software (BD Biosciences, San Jose, CA).

Cytokines released from macrophages and BMDCs were quantified via cytometric bead array (CBA) analysis. In brief, RAW 264.7 macrophages and BMDCs were seeded at 5×10^5 cells/well in 96 well plates. Cells were co-incubated with FITC-BSA alone or BsaCPs with

approximate mean diameters of 300 nm, 1 μm or 3 μm . Once again, unloaded CPs and medium alone were used as controls. After 72 h, culture supernatants were harvested to quantify concentrations of inflammatory cytokines including, IL-1 β , IL-6, TNF- α , MCP-1 α , and MIP-1 with a customized CBA flex set (BD Biosciences, San Jose, CA). The multiplex beads were read on a FACSCantoII and analyzed using FACP Array software (Soft Flow, Burnsville, MN).

3.2.8. Antigen presentation

The antigen presenting ability of BMDCs co-incubated with AgCPs was evaluated by quantifying proliferation of Ag-specific T-cells. Briefly, BMDCs were seeded onto 6 well plates at a density of 1×10^6 cells/well and cultured with OvaCPs with approximate mean diameters of 300 nm, 1 μm , or 3 μm at final antigen concentration of 10 $\mu\text{g/ml}$. BMDCs pulsed with peptide OVA₂₅₇₋₂₆₄ (SIINFEKL) or whole OVA protein, and unloaded CPs were used as positive and negative controls, respectively. After 24 h, BMDCs were collected and co-cultured with CD8⁺ or CD4⁺ T-cells isolated via negative selection using magnetic beads (Invitrogen, Grand Island, NY) from the spleens of OT-I and OT-II mice, respectively. After 72 h of co-culture, T-cell proliferation was assessed by the CellTiter-Glo (Promega, Madison, WI) cell proliferation assay.

3.2.9. Statistical Analysis

All particle characterization measurements, i.e. mean diameter, polydispersity index, encapsulation efficiency and surface charge, are presented as mean \pm standard deviation for 3 independent chitosan particle preparations. Antigen uptake, APC activation and cytokine release experiments were carried out in triplicate. Antigen presentation experiments, which evaluated the proliferation of antigen-specific T cells, were performed in duplicate. Student's t-test was

used to compare data from two groups of interest as indicated. For example, cytokine release and T cell proliferation data in response to the soluble antigen treatment group and an AgCP treatment group were compared. Analysis of variance was used to identify treatment-related differences among the three different AgCP sizes. All statistical analyses were performed using JMP software (SAS, Cary, NC). Significance was accepted at the $p \leq 0.05$ level.

3.3. Results

3.3.1. Characterization of AgCPs

SEM images revealed that AgCPs were spherical to elliptical in shape with porous non-uniform structures (Figure 10). Formulation factors including chitosan concentration, sodium sulfate addition rate, and sonication power were varied to generate AgCPs with nominal sizes of 300nm, 1 μ m, or 3 μ m. The measured mean diameters of these particles as determined by DLS were 318 ± 11 nm, 1133 ± 54.1 nm, and 2871 ± 216 nm (Table 2). All preparations displayed a unimodal size distribution (Figure 10) with modest polydispersity (Table 2). Antigen encapsulation efficiencies were very reproducible and increased with particle size from 58.1 ± 3.7 % to 96.6 ± 0.6 %. To determine the effect of antigen on particle size and charge, unloaded CPs were prepared using the same conditions as the “300 nm” AgCPs except without antigen. The mean diameter of CPs was slightly smaller than similarly prepared AgCPs – 289 ± 9 nm vs. 318.2 ± 11 nm. Also, the surface charge of CPs, +36.8 mV, was higher than the surface charge of similarly sized AgCPs, +16.8 mV.

3.3.2. Uptake of AgCPs by APCs

Uptake of AgCPs by APCs was found to depend on particle size, total antigen concentration, and incubation time. Regarding incubation time, uptake of AgCPs by both macrophages and BMDCs increased from 12 h to 24 h (Figure 14a, c). After 24 h, no significant increase in antigen uptake was observed. Flow cytometry analysis revealed that 100% of macrophages and BMDCs exposed to AgCPs produced a strong FITC signal indicating that every cell had internalized some amount of AgCPs.

Regarding antigen concentration, antigen uptake by both macrophages and BMDCs increased steadily up to the maximum total antigen concentration of 30 $\mu\text{g/ml}$ (Figure 14b, d). At lower concentrations, nearly all of the AgCPs co-incubated with macrophages were internalized. As antigen concentration increased, uptake efficiency decreased for both cell types. Macrophages were found to be more efficient at antigen uptake as they had phagocytosed 3- to 14-times as much AgCPs than did BMDCs.

Regarding particle size, maximum antigen uptake by macrophages was observed with 1 μm AgCPs (Figure 14b). Increasing particle size to 3 μm reduced antigen uptake by macrophages. Antigen uptake by BMDCs was independent of particle size up to 20 $\mu\text{g/ml}$ (Figure 14d). However, at 30 $\mu\text{g/ml}$ concentration, BMDCs performed similarly to macrophages in that maximum antigen uptake was observed with 1 μm AgCPs.

3.3.3. Macrophage activation

AgCPs outperformed soluble antigen in enhancing upregulation of antigen presenting machinery, co-stimulatory and activation markers on macrophages. Specifically, up to 2-fold increases in MHC I and CD80 expressions, up to a 3-fold increase in CD86 expression, and up to

a 10-fold increase in CD80 expression were observed following APC exposure to AgCPs compared to soluble antigens (Figure 15). Increases in MHC II and CD54 were also observed albeit to a lesser degree (data not shown). Upregulation of all markers was dependent on AgCP size with 1 μm AgCPs producing maximum responses.

In addition to higher activation status, CBA analyses revealed that macrophages co-incubated with AgCPs released higher amounts of pro-inflammatory cytokines (Figure 16). IL-6 and MCP-1 secretions were more than doubled with 1 μm AgCPs compared to soluble antigen while TNF- α production increased by more than 70-fold. MIP-1 α release was also modestly, but significantly increased with AgCP co-incubation. IL-1 β was not secreted by macrophages exposed to soluble antigen but secreted at high levels with AgCPs co-incubation. Similar to macrophage surface marker expression, cytokine release was dependent on AgCP size. IL-1 β , MCP-1 and IL-6 secretions were maximum with 1 μm AgCPs while TNF- α and MIP-1 α responses were highest with 3 μm AgCPs.

3.3.4. BMDC activation

Similar to the above studies with macrophages, AgCPs were more effective than soluble antigen at enhancing upregulation of antigen presenting molecules, co-stimulatory molecules and activation markers on BMDCs. Specifically, CD40 was increased by up to 5-fold, MHC I and CD54 expressions were increased by up to 2-fold on BMDCs treated with AgCPs compared to soluble antigens (Figure 17). To a lower degree, upregulation of MHC II and CD86 was also observed (data not shown). The dependence of BMDC surface marker expression on AgCP size showed a different pattern than was observed for macrophages. Maximum responses for CD40,

CD80 and CD54 expressions were elicited by 300 nm AgCPs, whereas a slightly higher expression of MHC I was produced by 1 μ m AgCPs.

CBA analysis revealed that BMDCs co-incubated with AgCPs release greater levels of pro-inflammatory cytokines (Figure 18). Secretions of IL-1 β , IL-6, MCP-1, MIP-1 α and TNF- α were increased from 5- to more than 45-fold when BMDCs were co-incubated with AgCPs rather than soluble antigen. For IL-1 β and MCP-1, cytokine release was driven by the presence of chitosan since CPs alone account for most, if not all, of the response. Particle size significantly affected cytokine release for 4 of the 5 cytokines measured. Maximum MIP-1 α release was achieved with 300nm AgCPs, maximum IL-6 and TNF- α release with 1 μ m AgCPs while MCP-1 release was maximized with 3 μ m AgCPs.

3.3.5. Antigen presentation by BMDCs

To investigate the effect of encapsulation on antigen presentation, OVA was encapsulated in chitosan particles (OvaCPs) and co-incubated with BMDCs isolated from naïve C57BL/6J mouse femer. The pulsed BMDCs were then co-cultured with CD4⁺ and CD8⁺ T-cells isolated from the spleens of transgenic OT-II and OT-I mice respectively, to investigate whether BMDCs pulsed with OvaCPs were capable of priming naive antigen-specific T-cells *in vitro*. BMDCs pulsed with OvaCPs induced significantly higher levels of proliferation in CD4⁺ OT-II cells compared to BMDCs pulsed with OVA antigen alone (Figure 19a). Furthermore, CD4⁺ proliferation increased significantly with the size of OvaCPs. BMDCs pulsed with 1 μ m and 3 μ m OvaCPs also induced significantly higher proliferative responses in CD8⁺ OT-I cells compared to BMDCs pulsed with OVA₂₅₇₋₂₆₄ peptide alone (Figure 19b). Once again, larger particles resulted in greater proliferation.

3.4. Discussion

The synthesis of chitosan nano- and microparticles to deliver drugs as well as polypeptides has been reported previously [40, 116, 131, 153]. However, formulation conditions, starting materials and resulting particle sizes vary considerably in the literature. Because uptake of particles by APCs was found to be dependent on particle size [149, 150], it was important to reproducibly synthesize AgCPs of discrete sizes to explore their effects on APC function. Consequently, we developed a set of parameters, which when manipulated, could reproducibly control chitosan particle size. SEM images and DLS data confirmed the formation of AgCPs that were unimodal and well dispersed in aqueous medium. Zeta potential measurements demonstrated that encapsulation of FITC-BSA significantly reduced the cationic surface charge of similarly sized particles from +36.8 mV to +16.8 mV. This was expected given that the pI of BSA is 4.7 and thus BSA carries an overall negative charge at neutral pH. These data are similar to those of Gordon et al., who reported a reduction from +28.8 mV to +18.3 mV when ovalbumin was adsorbed to the surfaces of chitosan nanoparticles [131]. The fact that AgCPs retained a positive surface charge in our study likely facilitated uptake by APCs. Previous research has shown that cationic particles interact with negatively charged cell membranes thus encouraging endocytosis [149, 161].

Antigen encapsulation efficiency increased slightly with particle size as anticipated. The high encapsulation efficiencies were consistent with values observed by others [114, 158]. It is likely that the negative charge of BSA facilitated a high encapsulation rate by encouraging interaction with polycationic chitosan. The effect of polypeptide charge on encapsulation efficiency is the subject of ongoing research.

Uptake studies demonstrated that particle size, concentration, and incubation time influenced AgCP uptake by APCs (Figure 14). Maximum uptake of AgCPs by both macrophages and dendritic cells was achieved by 24 h to 48 h of co-incubation. The decrease in antigen uptake after 48 h may be explained by breakdown of antigen and a subsequent loss of fluorescence signal from FITC-BSA.

For macrophages, AgCP uptake increased with particle size from 300 nm to 1 μm . However, a further increase to 3 μm , reduced antigen uptake. These data were in agreement with previous studies which demonstrated that macrophage uptake reached a maximum with 1 μm polystyrene particles with a similar positive surface charge [149, 162]. For BMDCs, antigen uptake was independent of AgCP size until the highest concentration whereupon 1 μm particles were preferentially internalized. While it is not surprising that higher concentrations of AgCPs resulted in higher levels of antigen uptake, it is noteworthy that the efficiency of uptake was found to decrease with increasing AgCP concentration. For instance, at 1 $\mu\text{g/ml}$ AgCPs, nearly all of the antigen could be detected in macrophages after 24 hours. However, at 30 $\mu\text{g/ml}$, only about 25-50% of antigen could be detected. These data indicate that uptake becomes saturated at higher antigen concentrations.

As seen in Figures 15 and 17, AgCPs outperformed soluble antigen and unloaded CPs in inducing the upregulation of antigen presenting molecules MHC I, MHC II as well as activation and co-stimulatory markers CD40, CD80, and CD86. These markers in particular were chosen as their upregulation is important for APC function during T-cell priming [163, 164]. The finding that unloaded CPs caused modest increases in surface marker expression demonstrated that chitosan itself may have modest immunostimulatory properties or that uptake of particles caused

a phenotypic change. Additional studies in our lab are focused on defining the immunomodulatory contributions of chitosan *in vitro* and *in vivo*.

Surface marker upregulation was more obvious with the macrophage cell line than with BMDCs which likely contained multiple cell types at different stages of differentiation. Nevertheless, these experiments demonstrated that delivery of encapsulated antigen provided an additive or synergistic effect compared to either soluble antigens or unloaded CPs alone. Similar to the uptake studies, macrophages responded most strongly to 1 μm AgCPs, while BMDCs responded to all sizes more or less the same.

The enhanced activation status of APCs exposed to AgCPs was confirmed in cytokine release studies. In both macrophages and BMDCs, AgCPs induced robust increases in production of all pro-inflammatory cytokines tested: IL-1 β , IL-6, TNF- α , MCP-1 and MIP-1 α . These cytokines were selected based on their potential to induce inflammatory response subsequently initiating antigen-specific immune responses. IL-1 β helps stimulate helper T cells; IL-6 is a B cell differentiation factor and a T cell activator; TNF- α induces T cell proliferation; MCP-1 induces chemotaxis of APCs; and MIP-1 α is a granulocyte activator/chemokine and induces the synthesis of other pro-inflammatory cytokines. Macrophages, not surprisingly, released greater levels of monocyte/macrophage specific cytokines MCP-1 and MIP-1. BMDCs on the other hand, produced much higher levels of IL-1 β and IL-6. In general, our results are consistent with other studies showing that particulate antigens enhance inflammatory responses by APCs [94, 165].

Up to this point, our results had indicated that AgCPs outperformed soluble antigen in all measures of APC activation. However, these findings would be futile if encapsulated antigens were not appropriately processed and presented. To this end, the ability of BMDCs pulsed with

OvaCPs to stimulate OVA-specific T cells was assessed. In accordance with our surface marker and cytokine release studies, we found that BMDCs pulsed with OvaCPs induced significantly higher OVA-specific CD4⁺ T-cell proliferation than BMDCs pulsed with soluble OVA protein. Unlike the activation studies, the CD4⁺ T-cell proliferative response, and hence, BMDC antigen presenting function increased with increasing AgCP size. It is possible that the higher concentration of antigen per 3µm particles outweighed any advantages of other AgCP sizes in cytokine release or activation status.

Similarly, BMDCs pulsed with OvaCPs induced higher OVA-specific CD8⁺ T-cell proliferation than BMDCs pulsed with OVA₂₅₇₋₂₆₄ peptide. It should be noted that, while BMDCs pulsed with peptide alone were effective at stimulating OVA-specific CD8⁺ T-cells *in vitro*, peptides are rapidly degraded and highly inefficient without an delivery system *in vivo*. Our planned studies will assess vaccine responses to AgCPs *in vivo*.

It is also worth noting that full length OVA protein was encapsulated in chitosan particles for both CD4⁺ and CD8⁺ stimulation studies. Therefore, our findings indicate that encapsulated OVA antigens were presented via both MHC I and II pathways. In fact, encapsulation of antigens by chitosan particles may facilitate endosomal escape and cross presentation [166].

3.5. Conclusion:

In this specific aim, we demonstrated that chitosan particles are capable of efficiently delivering encapsulated antigens and enhancing the activation status of both macrophages and dendritic cells. In all measures of APC activation and presentation, AgCPs outperformed soluble antigen. The ability of BMDC's pulsed with AgCP to present both MHC I and MHC II epitopes is particularly encouraging. Potential modifications of chitosan or incorporation of additional

immune response modifiers underscore the versatility of this technology to enhance or control vaccine responses. Our results indicate that AgCPs are a promising vaccine delivery platform deserving of continued exploration. Specific aim 3 will evaluate the *in vivo* immune response to chitosan particle-based antigen delivery systems.

4. SPECIFIC AIM 3: Assess *In Vivo* Immunological Activity of Chitosan Particulate Antigen Delivery System

4.1. Rationale

The studies performed in Specific Aim 2 determined the ability of the proposed systems to activate APCs and enhance antigen presentation *in vitro*. However, this is only the first step in assessing system efficacy. In this aim, chitosan particles are evaluated for their ability to induce antigen specific vaccine response *in vivo*. Specifically, humoral and cell-mediate immune response to the antigen are assessed.

4.2. Methodology

4.2.1. Reagents

Chitosan (viscosity 20-200, 200-600, and 600-1200 cPs degree of deacetylation 90%) was purchased from Primex (Siglufjordur, Iceland) and purified via filtration in hydrochloric acid and precipitation in sodium hydroxide. Pluronic F-68, acetic acid, sodium sulfate (Na₂SO₄), L-glutamine, HEPES buffer, trypsin-EDTA, and ovalbumin (OVA) were purchased from Sigma (St. Louis, MO). Concanavalin A (Con A) was purchased from Life Technologies (Green Island, NY). Cell culture medium components including, fetal bovine serum (FBS), antibiotics, Dulbecco's Modified Eagle Medium (DMEM), RPMI-1640, Alum adjuvant Imject-Alum, and tetramethylbenzidine (TMB) substrate solution medium were purchased from Thermo Scientific (Rockford, IL). Goat anti-mouse IgG, IgG1, and IgG2a antibodies were purchased from Southern Biotech (Birmingham, AL).

4.2.2. Mice

Female C57BL/6J mice were purchased from The Jackson Laboratory (Bar Harbor, ME). Mice were housed in a pathogen-free animal facility and used at 8 to 10 weeks of age. All experimental procedures were approved by the Institutional Animal Care and Use Committee at the University of Arkansas and animal care was in compliance with The Guide for Care and Use of Laboratory Animals (National Research Council).

4.2.3. Preparation of OVA loaded chitosan particles

Chitosan particles different sizes (300 nm, 1 μ m, and 3 μ m) encapsulating model antigen OVA (OvaCPs) were prepared via precipitation-coacervation as described previously in Specific Aim 1. Briefly, chitosan along with OVA was dissolved in 2% acetic acid solution. OvaCPs were formed by adding 50mM salt solution drop wise to the chitosan solution using an infusion pump (Pump 11 EliteTM, Harvard Apparatus, Holliston, MA). Nonionic stabilizer Pluronic F-68 was added and particles were allowed to stabilize for 2 hours under constant stirring and intermittent sonication using a sonicator (S4000, Misonix, Farmingdale, NY). OvaCPs were collected after centrifugation at 25,000 xg for 10min at 4°C and freeze dried (FreeZoneTM 2.5, Labconco, Kansas city, MO) before further use. Particles of various sizes were obtained by varying the formulation parameters as seen in Table 2.

4.2.4. Preparation of OVA loaded PLGA nanoparticles

PLGA nanoparticles encapsulating OVA antigen were prepared using a double emulsion solvent evaporation method. Briefly, 3% PLGA solution was prepared by dissolving 90mg of

PLGA (50/50) in 3ml of dichloromethane (DCM). OVA (2 mg) was dissolved in 200 μ l deionized water, and this antigen solution was added to PLGA solution. The solution was then sonicated for 30 seconds at 50W using a sonicator (S4000, Misonix, Farmingdale, NY) to obtain the primary w/o emulsion. The emulsion solution was added drop wise into a 2% w/v PVA solution, and the mixture was then sonicated for 2 minutes at 50W power to obtain a w/o/w emulsion. After stirring overnight to allow solvent evaporation, PLGA nanoparticles were collected through centrifugation, washed several times with DI water to remove residual PVA. OVA loaded PLGA particles were then resuspended in deionized water and freeze dried (FreeZone™ 2.5, Labconco, Kansas City, MO) before further use.

4.2.5. Characterization of OVA loaded PLGA nanoparticles

The size and size distribution of the nanoparticles were also determined by a Dynamic Light Scattering method (Zetasizer Nano ZS90™, Malvern, Westborough, MA). OVA loading efficiency was calculated indirectly. The amount of drug left in the supernatant after removing the drug-loaded particles was determined using BCA protein assay. This amount was subtracted from the initial concentration of drug to get the percentage of loading efficiency (Equation 3).

$$\text{Percentage loading efficiency} = \frac{(\text{Original conc} - \text{Supernatant conc})}{\text{Original conc}} \times 100 \quad (3)$$

4.2.6. Immunization

Six groups of five 12 week old adult female C57BL/6J mice were immunized with OVA delivered in 6 different formulations including 300 nm, 1 μ m, or 3 μ m OvaCPs, or OVA

encapsulating PLGA nanoparticles with an effective antigen dose of 50 µg/mice. Vaccination was done via sub-cutaneous injections. Separate cohorts of mice injected with OVA antigen mixed with alum adjuvant served as controls. Each group was immunized twice within 2-weeks. Four days after the final immunization, blood and spleens were collected aseptically.

4.2.7. OVA-specific antibody response

Four days after booster injection, blood from immunized mice was collected via mandibular bleeding. Whole blood was allowed to clot for 1 hour at room temperature and centrifuged at 2000g for 15 min for sera collection. Indirect enzyme-linked immunosorbent assay (ELISA) was used for detection of anti-OVA-antibodies in the sera of immunized animals. Briefly, 96 well plates were coated with 2 µg/ml OVA in 1 X PBS solution overnight at 4°C. OVA coated wells were blocked with 5% BSA in PBS for 1 hour, and washed with PBS containing 1% BSA. Serum samples from immunized mice were then added to plate and incubated for 1 h at 37°C. Wells incubated with mouse anti OVA IgG was used as positive control while wells incubated with PBS acted as negative control. The washed plates were incubated with horseradish peroxidase-conjugated anti-mouse immunoglobulin (IgG) or anti-mouse IgG1 or anti-mouse IgG2b. The plates were developed with TMB substrate solution and enzyme neutralized with 3M HCl. The absorbance at 490 nm was read on a spectrophotometer (Synergy 2™, BioTek, Winooski, VT).

4.2.8. Lymphocyte proliferation assay

Spleens obtained from immunized mice were crushed and passed through a 70 µm cell strainer (BD Falcon, Bedford, MA). Red blood cells were lysed by using ACK lysis buffer and

then resuspended in cell culture medium before further use. Irradiated splenocytes isolated from naïve C57BL/6J mice (2.5×10^5 cells/well) were cultured in RPMI-1640 supplemented with 10% FBS and pulsed with OVA in triplicate. The pulsed splenocytes acting as APCs were then co-incubated with CD4⁺ T-cells (5×10^5 cells/well) isolated from immunized mice. After a 5 day incubation, CD4⁺ T-cell proliferation in response to antigen stimulation was assessed by using the CellTiter 96 kit (Promega, Madison, WI) according to the manufacturer's instruction. Irradiated splenocytes without any OVA or CD4⁺ T-cells alone were used as negative controls. Irradiated splenocytes with CD4⁺ T-cells incubated for 72 hours with 1 µg/ml Con A were used as a positive control.

4.3. Results

4.3.1. Effect of delivery system on OVA-specific antibody response

Antigen specific serum antibody assay was used to determine the ability of OvaCPs to induce humoral response in immunized mice. Levels of anti-OVA antibodies in the sera collected from immunized mice was determined using indirect ELISA. As seen in figure 21 and 22, both AgCPs and PLGA nanoparticles produced higher anti-OVA IgG and IgG1 antibodies compared to both soluble OVA and alum-OVA. Compared to alum, immunization with OvaCPs resulted higher serum antibodies with alum resulting in OD of 0.54 compared to 3.07 observed with 1 µm OvaCPs. Also, OvaCPs influenced the humoral response against antigens with smaller particles producing higher OVA specific IgG titers.

4.3.2. Effect of delivery system on OVA-specific CD4⁺ proliferation

Lymphocyte proliferation assay was performed to determine the ability of OvaCPs to induce a proliferative T cell responses. As seen in figure 22, significantly higher CD4⁺ T- cell proliferation was observed with OvaCPs with three times higher cell proliferation observed with OvaCPs compared to OVA delivered in PLGA and alum formulation. Immunization with PLGA nanoparticles resulted in CD4⁺ to alum but lower than AgCPs of all sizes. However, no difference was observed between 300 nm, 1 μm, and 3 μm AgCPs. Also, similar proliferation was observed when comparing the Con A stimulated CD4⁺ T cells from all the groups indicating comparable number of healthy CD4⁺ T cells that have ability to respond to a proliferation signal.

4.4. Discussion

Subunit antigens are rapidly degraded by proteases upon injection and generate neither the antigen persistence nor immunostimulation required for the generation of robust antigen-specific immunity. As a result, a great deal of effort has been spent in evaluating delivery systems that are capable of protecting subunit antigens and providing the appropriate stimulus to generate antigen-specific immunity [167, 168]. In this specific aim, we have shown that encapsulation of antigen in chitosan particles increases antigen specific immune response *in vivo*. Others have investigated chitosan particle-based antigen delivery systems and showed that antigen adsorbed onto the surface of chitosan particles was preserved and can elicit an immune response [131]. However, absorption onto the particle surface is not ideal for polypeptide antigen delivery as it exposes the antigens proteolytic enzymes causing rapid degradation.

We found that encapsulation of antigens in particulate delivery systems, either chitosan or PLGA particles, enhances the OVA-specific humoral response compared to the soluble OVA or standard alum-adjuvanted OVA groups. This is consistent with other studies where encapsulation of subunit antigens in particulate delivery systems have been shown to improve antigen specific IgG production [169-171]. OvaCPs with mean sizes of 300 nm and 1 μ m elicited similar humoral responses as OVA-encapsulated PLGA nanoparticles. However, when the size of OvaCPs was increased to 3 μ m, OVA-specific antibody production decreased. These data are consistent with published data showing that particle size affected humoral response with 2-70 μ m particles eliciting significantly lower humoral immune response than submicron particles [172, 173]. Nevertheless, data from the antibody response indicated that chitosan and PLGA encapsulation produced similar antibody responses which were both markedly higher than the alum formulation.

In contrast, lymphocyte proliferation assay demonstrated that OvaCPs were superior to PLGA-OVA. PLGA-OVA elicited a response similar to that of alum which is consistent with other studies where PLGA elicited strong cell mediated immune response to encapsulated antigens similar to that of incomplete Freund's adjuvant (IFA) [171, 174]. Unlike the antibody response, antigen specific CD4⁺ proliferation was not affected by AgCP size.

Additional studies are needed to understand the nature of the adaptive immune response generated by OvaCPs. The finding that OvaCPs and PLGA were similar in antibody response but superior in CD4⁺ proliferation indicated that chitosan encapsulation may facilitate a stronger Th1 response. Analyses of cytokines produced by *in vitro* stimulated CD4⁺ will better help define the adaptive immune responses elicited by AgCPs.

4.5. Conclusion:

In this specific aim, we demonstrated that chitosan particles are capable of efficiently delivering encapsulated antigens and enhancing adaptive immunity. In all measures of OvaCPs outperformed soluble antigen and standard alum adjuvants. Compared to PLGA nanoparticles, OvaCPs elicited much stronger CD4⁺ T-cell proliferation. Also, particle size influenced the serum antibody secretion while showing minimal effect on CD4⁺ T cell proliferation. As such, our results indicate that AgCPs are a promising vaccine delivery system that can aid in producing a robust adaptive immune response towards encapsulated polypeptide antigens.

5. CONCLUSIONS AND FUTURE DIRECTIONS

Particle-based vaccine delivery systems are under exploration to enhance antigen-specific immunity against safe but poorly immunogenic subunit antigens. Chitosan is a promising biomaterial for antigen encapsulation and delivery due to its ability form nano- and microparticles in mild aqueous conditions thus preserving the antigenicity of loaded proteins. For the first time, we have shown that chitosan particles properties including particle size, protein loading efficiencies, and release parameters can be controlled by adjusting precipitation coacervation parameters. As a result, we were able to study the effect of chitosan particle size on antigen presenting function and in vivo efficacy. In vitro studies showed that AgCPs are efficiently taken up by APCs which in turn become activated to present antigens via both MHC I and MHC II pathways. Also, in vivo studies proved that AgCPs can elicit antigen-specific immune responses and can do so more effectively than alum or PLGA nanoparticles. In short, we have established chitosan particles as a promising, versatile antigen delivery system that can be used to deliver subunit antigens for a wide variety of applications.

Looking ahead, there are a number of directions one can take to improve the efficacy of AgCPs or further characterize chitosan-based antigen encapsulation. Regarding the former, chitosan particles provide a tremendous opportunity for improving or modulating an adaptive response through co-delivery of immunostimulatory compounds, such as poly I:C a TLR-3 agonist, and imiquimod, a TLR-7 agonist. The agonists would interact directly with APCs including B-cells, macrophages, and dendritic cells through TLRs resulting in stronger APC activation. APCs activated with TLR in the presence of antigen have the potential to generate antigen specific immune responses.

Furthermore, chitosan particles can be loaded with tumor associated antigens and used for vaccination against tumors. For example, chitosan particles can be loaded with tyrosinase related protein 2 (TRP-2) which is overexpressed in melanoma cells for vaccination against melanoma. Similarly, chitosan particles containing luteinizing hormone-releasing hormone (LHRH) can be used for vaccination against breast, ovarian, and prostate cancer. Vaccination using particulate antigens has several advantages over traditional cancer treatments involving surgery, radiation, and chemotherapy. Most importantly, cancer vaccines have the potential to generate tumor-specific immunity which protects cancer patients from recurrence. In general, cancer vaccination is safer with fewer side effects

Chitosan particles may also encapsulate immunostimulatory cytokines such as GM-CSF, IL-2, and IL-12 which have already demonstrated antitumor activity. Cytokines can be co-delivered along with subunit antigens to enhance antigen specific immune responses. Another strategy would be to inject chitosan particles encapsulating cytokines directly into solid tumors and use a patient's own tumor cells as the source of antigen. This allows for the development of personalized medicine that can be used to induce a tumor specific response in any patient irrespective of tumor phenotype.

Also, our studies have shown that the particles were taken up by APCs resulting in APC activation and presentation of antigen with both MHC I and MHC II epitopes. However, mechanisms involved in endosomal escape of antigen resulting in cross presentation of the MHC I epitope were not understood. Chitosan may act as proton sponge that can burst lysosomes resulting in antigen release into the cytosol. In the future, we can track intracellular trafficking via confocal microscopy. Lysosomes can be labeled with pH sensitive dyes to co-localize AgCPs. Antigens escaping lysosome will result in a diffuse fluorescence showing antigen release

into the cytosol. Chitosan particles can be compared to PLGA particles which have no known ability to escape lysosomes.

In addition, we have shown that chitosan particle properties can be controlled systematically by varying formulation factors. However, we did not explore the effect of interdependency between formulation factors on particle properties. As such, in the future, comprehensive factorial analyses can be performed with factors including chitosan degree of deacetylation, protein isoelectric point, solution volume, etc., that would take into account factor interdependency. Full factorial analysis can be used to develop factorial equation (see equation 3) that can be used to determine parameters for formulation factors to obtain particles of required properties. This equation can then be used to prepare chitosan particles of various sizes, protein loading efficiencies, and release.

$$\text{Particle parameters} = A - B(X) - C(Y) + D(Z) - E(XY) - F(XZ) - G(YZ) + XYZ \quad (3)$$

Where X, Y, and Z represents formulation factor parameters; A, B, C, D, E, F, and G are constants derived from factorial analysis.

The ability to scale up particle production is important for commercialization of chitosan particle based antigen/protein delivery systems. We hypothesize that the concentration and addition rate of precipitant salts can be adjusted to scale. For instance, to prepare 300 nm particle using a 10 ml reaction setup, 1 ml of 1 M salt solution was added to chitosan solution at the rate of 8 ml/min resulting in 100 mM final precipitant salt concentration in 7.5 sec. We hypothesize that the time needed for the precipitant salt concentration to reach 100 mM is the critical factor in controlling particle size. Using this hypothesis, 300 nm particles can be obtained from 1L system by adding 10 ml of 10 M salt solution can be added at the rate of 1.3 ml/sec. Another approach

would be to add 100 ml of 1 M salt solution at the rate of 13 ml/sec to obtain 300 nm particles. As such, particles with similar properties might be obtained either by increasing initial precipitant salt concentration or salt addition rate or both in proportion to reaction volume. It will be interesting to see if the variation in precipitant salt concentration and addition rate influence particle size.

Stability and storage of the particle is also important for commercialization. Protein release studies showed that particles stored in non-ionic medium like deionized water retain most of the encapsulated protein even after 2 weeks of incubation. However, further studies are required to determine optimal storage conditions with minimal effect on the stability of chitosan-protein complexes. As such, protein release studies can be used to determine the stability of chitosan particles over long periods of time when stored in non-ionic medium. Also, further studies can be done to assess the limits of other storage methods including freeze drying in maintaining chitosan particle stability and protein bioactivity. Briefly, chitosan particles stored for various period of time up to 12 months can be tested for encapsulation efficiency. Also, in vitro bioactivity studies can be performed to determine the effect of storage conditions on physiological function of the encapsulated proteins.

Our studies have shown that protein release properties of the particles depend on the binding strength of proteins with strongly binding OVA being released from particles at much slower rates compared to relatively weakly binding but similar sized BSA. As such, further studies are required to understand the effect of chitosan and protein charge densities on particle protein release. Chitosan molecular charge density can be controlled by varying the degree of deacetylation or through functionalization of chitosan. Similarly, protein anionic charge density can be modified through point mutations replacing positively charged amino acids like arginine

or histidine or lysine with negatively charged amino acids including aspartic acid or glutamic acid. A limiting factor in this strategy is that mutation of protein may affect the antigenicity and even activity of protein. Ultimately, chitosan or protein molecules may be programmed to facilitate slower or faster release of protein therapeutics.

Protein release studies showed that the type of precipitant salt used influences the rate of protein release. Particles prepared using salts with high hydrating strength releasing protein at higher rate compared to particles prepared using salts with lower hydrating strength. The mechanism of action is not clear given that protein release experiments were all performed in PBS. It is possible that small quantities of precipitant salts might persist within particle complexes thus influencing the interaction between chitosan and protein. The presence of precipitant salts within the particles can be tested using mass spectrometry. Another potential reason for the variation in protein release might be that precipitant salts influence the porosity of particles during particle formation and therefore the subsequent protein release. Further studies may explore the effect of precipitant salt on porosity by measuring porosity of resultant particles using scanning electron microscopy (SEM) and volumetric analysis to measure the change in volume of hydrated particles compared to dry samples.

Non-ionic pluronic was used as a surfactant for preparation of chitosan particles given pluronic's inability to interact with chitosan particles ionotropically. However, small quantities of pluronic might be trapped within the particle complex and influence particle properties. We do not suspect that the amount of pluronic present in the particles is detrimental to cells as no cell death was observed in our in vitro studies. Nevertheless it is useful to quantify the amount of pluronic present. A colorimetric assay involving the interaction of pluronic with cobalt

thiocyanate can be used to quantify pluronic by measuring the absorbance of the complex at 328 nm. Also, the effect of pluronic contamination on chitosan particle properties can be determined.

In summary, we have established that chitosan particle properties can be controlled by varying formulation parameters. However, further work is required to standardize chitosan particle preparation protocols for commercial use. Also, we have shown that chitosan particles are capable of inducing antigen specific immune response towards encapsulate antigens. However, we have only scratched the surface of this promising platform with further studies required to realize the true potential of chitosan particles as vaccine and immunotherapy delivery systems.

Table 1. Effect of formulation factors on particle size, polydispersity index (PDI) and protein loading efficiency; *Data are presented as mean \pm standard deviation for three independent experiments. ** No particle formation. ^a Viscosity range of chitosan was indicated by manufacturer as obtained at a concentration of 1 mg/ml (w/v) in 1% acetic acid

Factor	Run	Mean Size* (nm)	PDI	Loading Efficiency*
Precipitant salt	Na ₂ SO ₄	427 \pm 7.6	0.113	54.0 \pm 2.6
	(NH ₄) ₂ SO ₄	551.9 \pm 3.5	0.135	62.5 \pm 6.1
	MgSO ₄	445 \pm 7.7	0.124	47.5 \pm 2
	Na ₃ C ₆ H ₅ O ₇	490 \pm 18.3	0.154	83.7 \pm 3.5
	Na ₃ PO ₄	1621 \pm 188	0.667	14.6 \pm 1.7
	NaCl	-**	-	-
Chitosan Viscosity ^a (molecular weight)	<20 cPs	418 \pm 16.2	0.104	50.3 \pm 2.3
	20-200 cPs	424 \pm 7.7	0.160	56.5 \pm 3.4
	200-600 cPs	605 \pm 13.3	0.190	56.5 \pm 2.6
	600-1200 cPs	728 \pm 15	0.212	53.5 \pm 4.3
	1200-2000 cPs	854 \pm 26.2	0.385	58.5 \pm 4.2
Chitosan Concentration	0.5 mg/ml	334 \pm 27.5	0.093	58.5 \pm 3.4
	1 mg/ml	418 \pm 3.5	0.113	57.3 \pm 2.5
	2 mg/ml	521 \pm 2.8	0.259	59.9 \pm 6.8
	3 mg/ml	587 \pm 10.6	0.182	73.6 \pm 2.2
	5 mg/ml	656 \pm 13.6	0.277	92 \pm 0.8
Sonication power	0 W	922 \pm 79.2	0.657	92.3 \pm 1.8
	10 W	438 \pm 3.9	0.182	88.3 \pm 5.3
	20 W	418 \pm 9.6	0.156	74.2 \pm 6.3
	40 W	421 \pm 4.1	0.098	56.5 \pm 2.6
Precipitant addition rate	0.2 ml/min	774 \pm 33.2	0.580	71.9 \pm 7
	1 ml/min	574 \pm 9.1	0.351	67.3 \pm 3.2
	3 ml/min	495 \pm 3.6	0.250	65.3 \pm 3.6
	5 ml/min	444 \pm 5.6	0.210	62 \pm 2.8
	8 ml/min	424 \pm 2.1	0.121	58.1 \pm 2.2
Protein	Insulin	411 \pm 19.3	0.195	98.3 \pm 0.5
	Ova	423 \pm 3.6	0.178	96.5 \pm 1.1
	BSA	424 \pm 7.7	0.160	58.1 \pm 2.5
	Con A	410 \pm 5.5	0.113	53.5 \pm 3.6

Table 2: Experimental design for protein release studies: Effect of particle size. Data are presented as mean \pm standard deviation for three independent experiments.

Particle group	Chitosan conc	Precipitant salt	Protein	Salt addition rate	Mean Size (nm)	Protein loading efficiency (%)
300nm	0.5 mg/ml	Na ₂ SO ₄	FITC-BSA	8 ml/min	318.2 \pm 11	58.1 \pm 3.7
1 μ m	3 mg/ml	Na ₂ SO ₄	FITC-BSA	1 ml/min	1133 \pm 54.1	83.5 \pm 8.3
3 μ m	5 mg/ml	Na ₂ SO ₄	FITC-BSA	0.2 ml/min	2871 \pm 216	96.6 \pm 0.6

Table 3: Experimental design for protein release studies: Effect of precipitant salt composition. Data are presented as mean \pm standard deviation for three independent experiments.

Particle group	Chitosan conc	Precipitant salt	Protein	Salt addition rate	Mean Size (nm)	Protein loading efficiency (%)
Na ₂ SO ₄	1 mg/ml	Na ₂ SO ₄	FITC-BSA	8 ml/min	448 \pm 12	56.4 \pm 6.3
(NH ₄) ₂ SO ₄	1 mg/ml	(NH ₄) ₂ SO ₄	FITC-BSA	8 ml/min	561 \pm 3.4	62 \pm 5.3
MgSO ₄	1 mg/ml	MgSO ₄	FITC-BSA	8 ml/min	462 \pm 6.3	54.3 \pm 3.4
Na ₃ C ₆ H ₅ O ₇	1 mg/ml	Na ₃ C ₆ H ₅ O ₇	FITC-BSA	8 ml/min	478 \pm 64.3	86 \pm 2.1
Na ₃ PO ₄	1 mg/ml	Na ₃ PO ₄	FITC-BSA	8 ml/min	1423 \pm 156	14.3 \pm 6.6

Table 4: Experimental design for protein release studies: Effect of protein molecular weight. Data are presented as mean \pm standard deviation for three independent experiments.

Particle group	Chitosan conc	Precipitant salt	Protein	Salt addition rate	Mean Size (nm)	Protein loading efficiency (%)
FITC-Insulin	1 mg/ml	Na ₂ SO ₄	FITC-Insulin	8 ml/min	421 \pm 10.1	99.2 \pm 0.12
FITC-OVA	1 mg/ml	Na ₂ SO ₄	FITC-OVA	8 ml/min	429 \pm 3.6	98 \pm 0.4
FITC-BSA	1 mg/ml	Na ₂ SO ₄	FITC-BSA	8 ml/min	448 \pm 22.4	56.4 \pm 3.2
FITC-Con A	1 mg/ml	Na ₂ SO ₄	FITC-Con A	8 ml/min	452 \pm 5	53.4 \pm 1.8

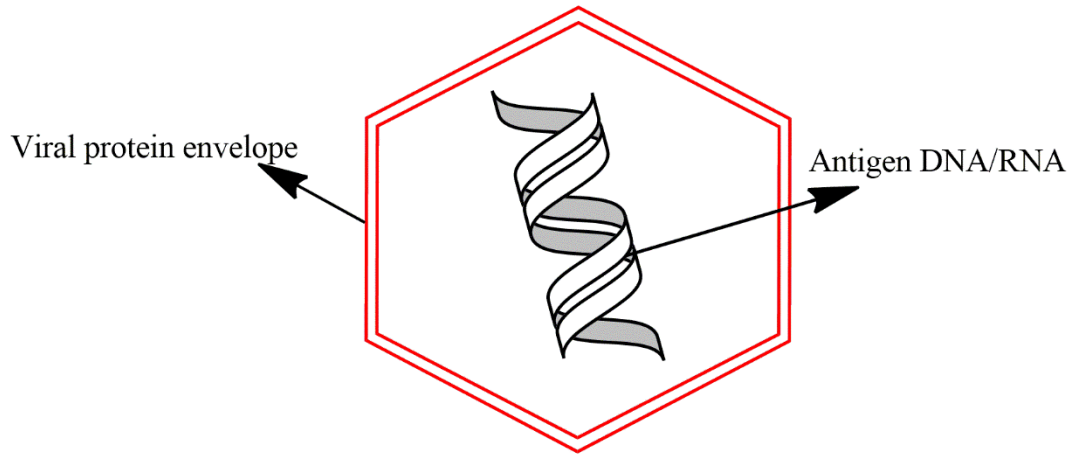


Figure. 1. Schematic representation of viral vector particle constituting carrier viral protein envelope and antigen genetic material.

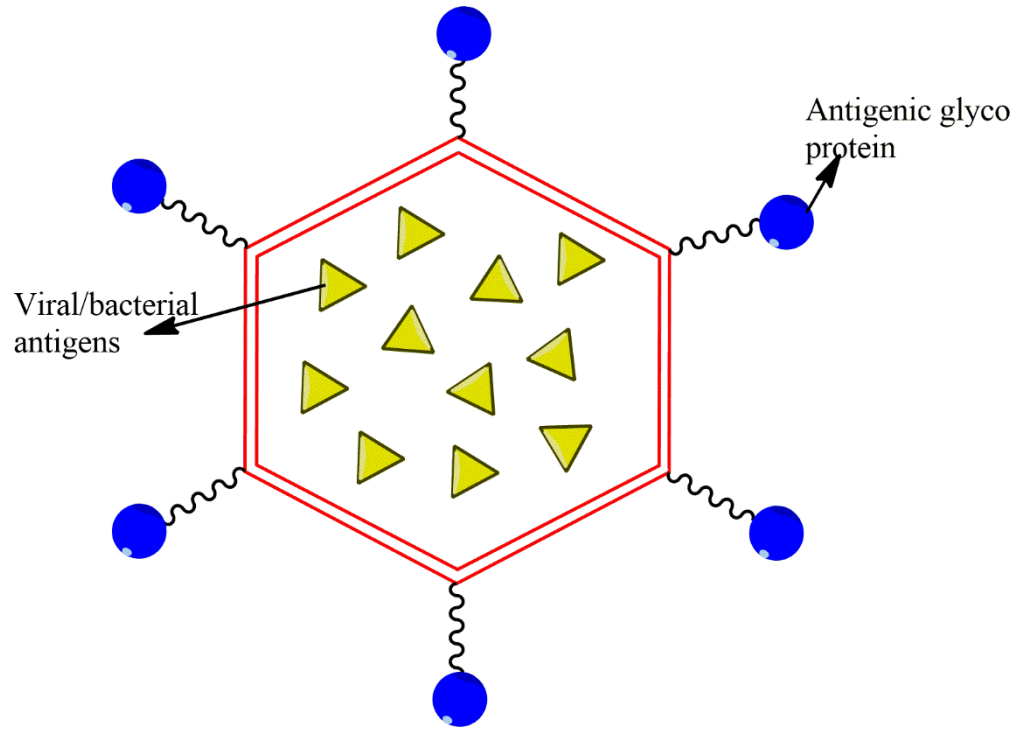


Figure. 2. Schematic representation of virus like particle delivery system.

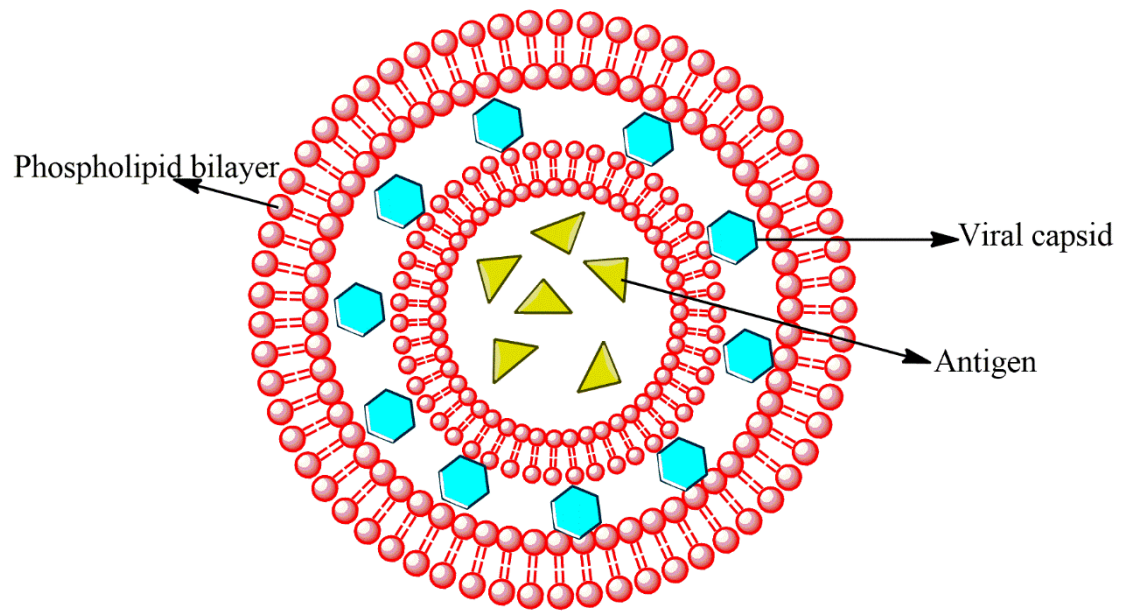


Figure. 3. Schematic representation of multi-layered liposomal particle encompassing both antigen and viral capsids acting as immunopotentiators.

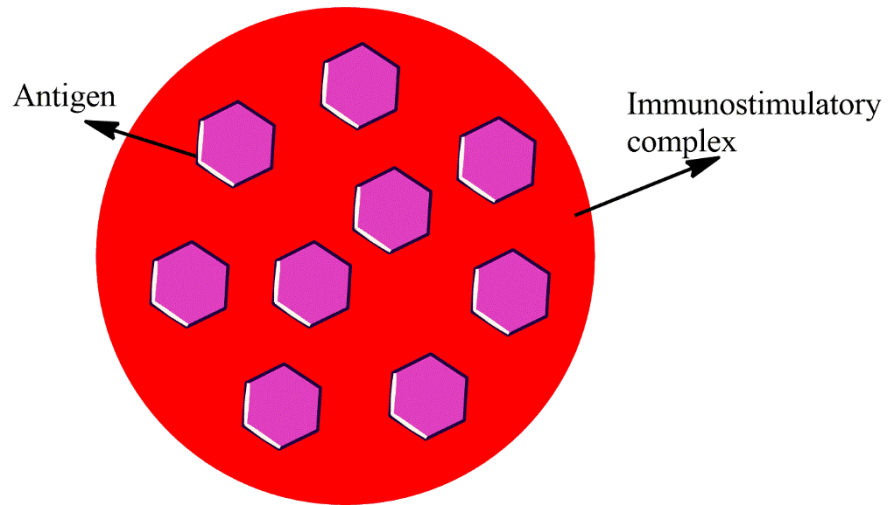


Figure. 4. Schematic representation of ISCOM with hydrophobic antigen loaded into the phospholipid/cholesterol cage.

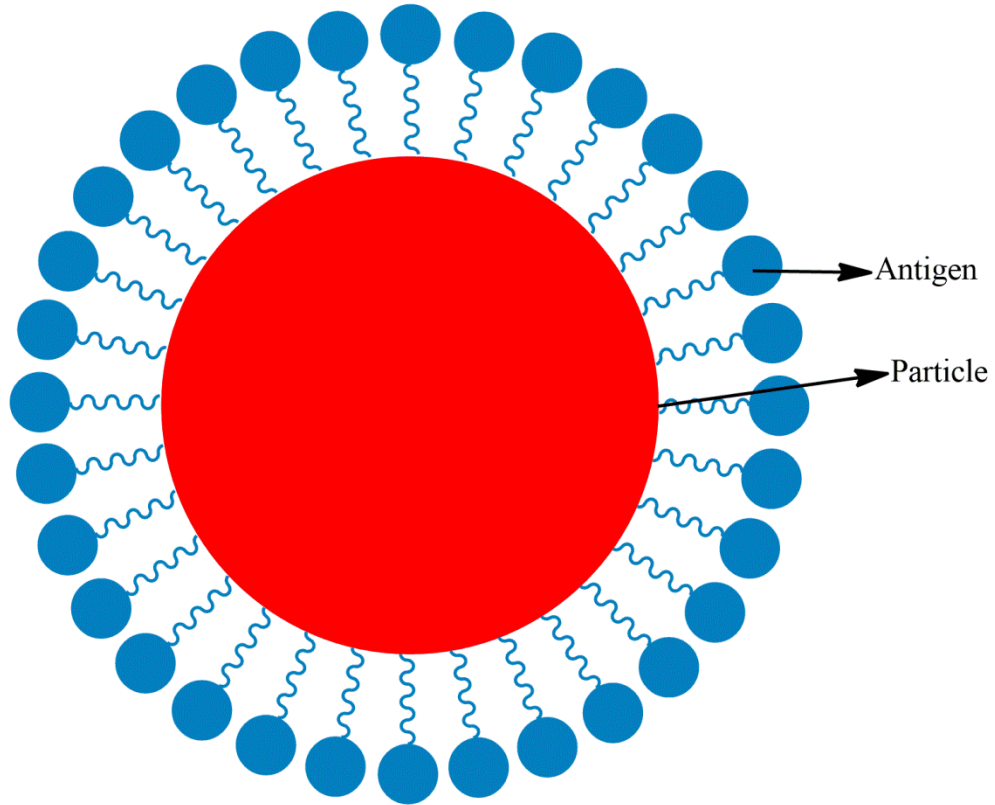


Figure. 5. Schematic representation of non-degradable nano/micoparticle vaccine delivery system; Particle can be designed to carry antigens while particle itself acts as an adjuvant or have adjuvant conjugated along with antigen.

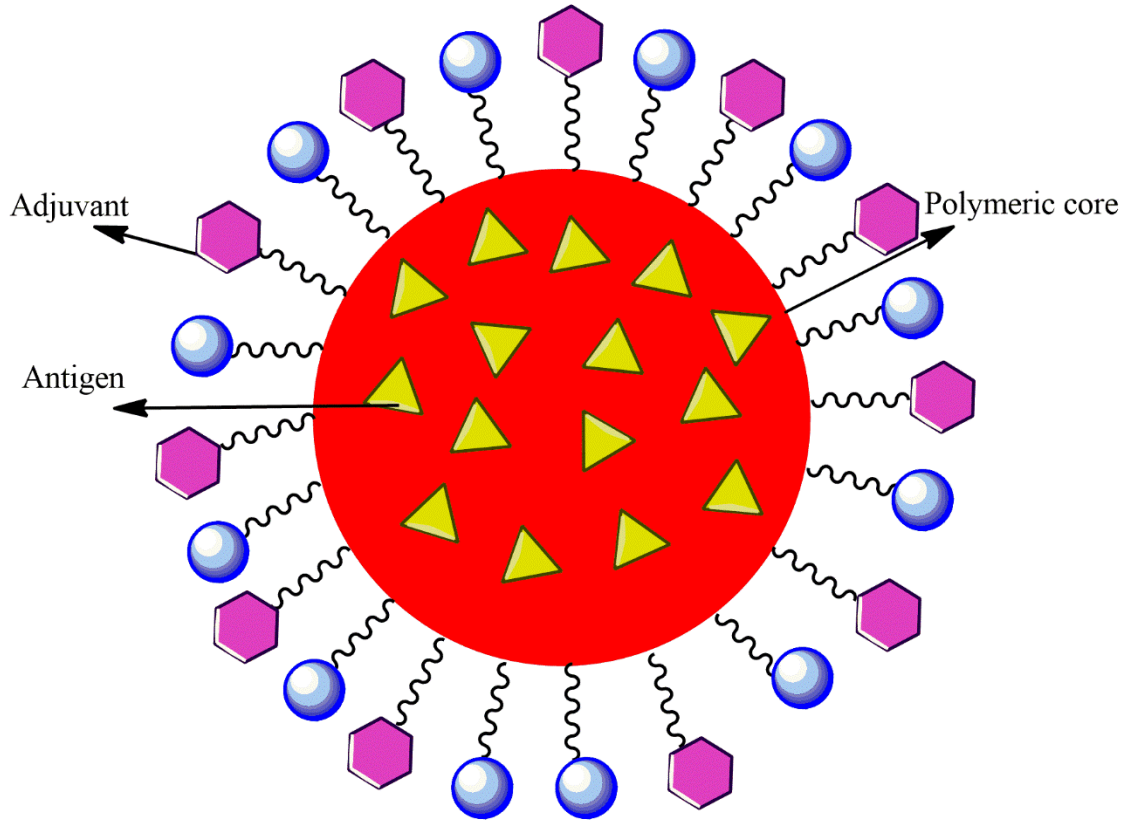


Figure 6. Schematic representation of degradable polymeric particle; Particle can be designed to carry antigens while particle itself acts as an adjuvant or have adjuvant conjugated along with antigen.

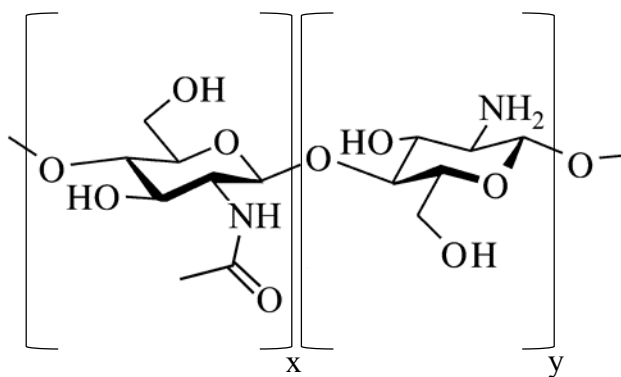


Figure. 7. Chemical structure of chitosan. Chitosan is an unbranched copolymer of N-acetylglucosamine (x) and glucosamine (y) units linked by $\beta(1-4)$ glycosidic bonds where the ratio of y to x is greater than 1.5.

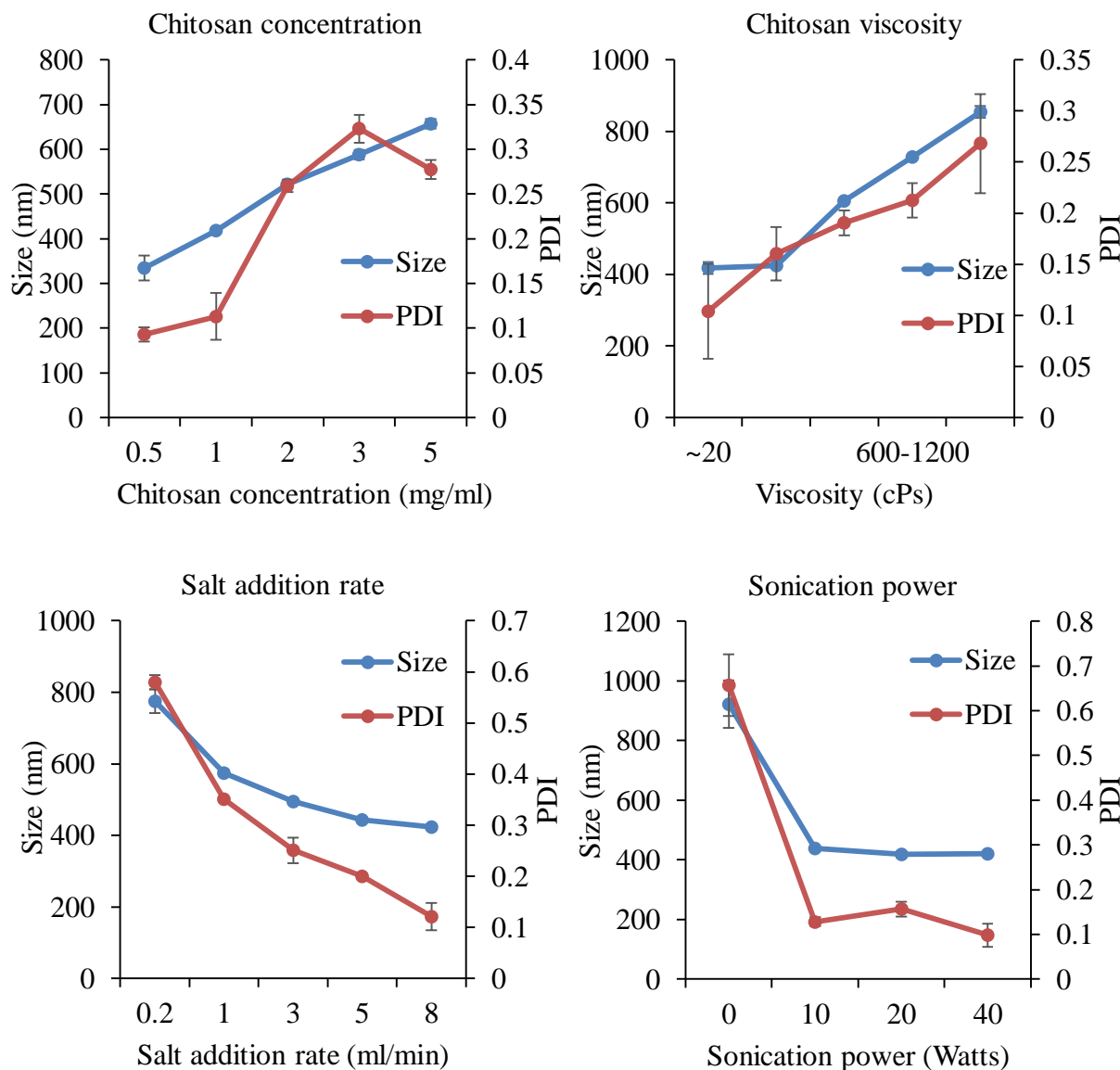


Figure 8. Effect of precipitation-coacervation parameters on chitosan-FITC-BSA particle size and PDI. Parameters including: chitosan concentration, molecular weight/viscosity, precipitant salt addition rate, and sonication power were varied following the experimental design described in Table 1. Resultant particle size and PDI of the resultant particles were determined by DLS. Data are presented as mean \pm standard deviation of three independent experiments.

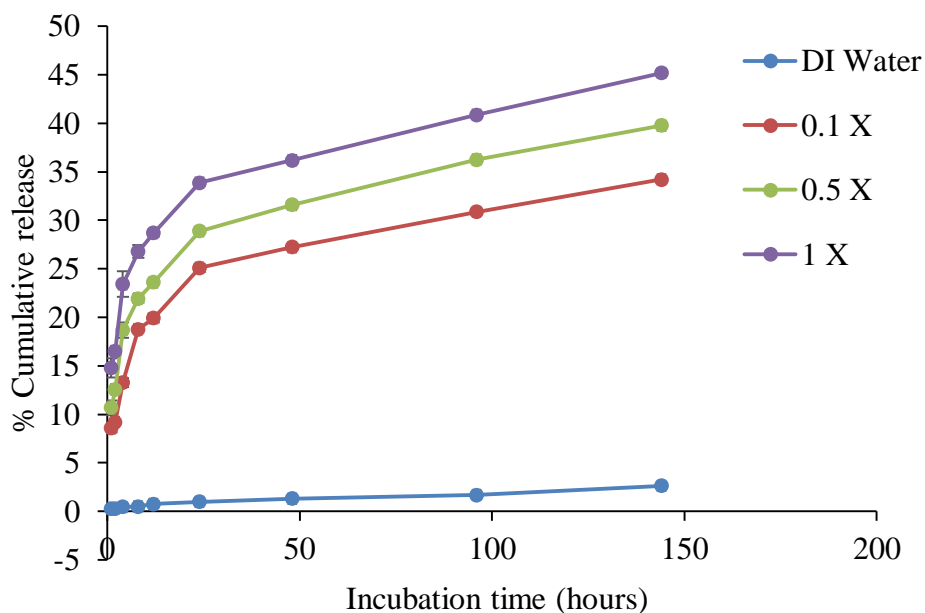


Figure. 9. Effect of salinity of release medium on protein release; Particles prepared using precipitant salt Na_2SO_4 encapsulating model protein FITC-BSA are incubated with 0.1X, 0.5X, 1 X PBS. Particles incubated in deionized water (DI water) served as negative control. Samples were collected at each time point and protein release was quantified by measuring fluorescence via fluorescence spectroscopy. Cumulative protein release was calculated by adding the protein released at each individual time point.

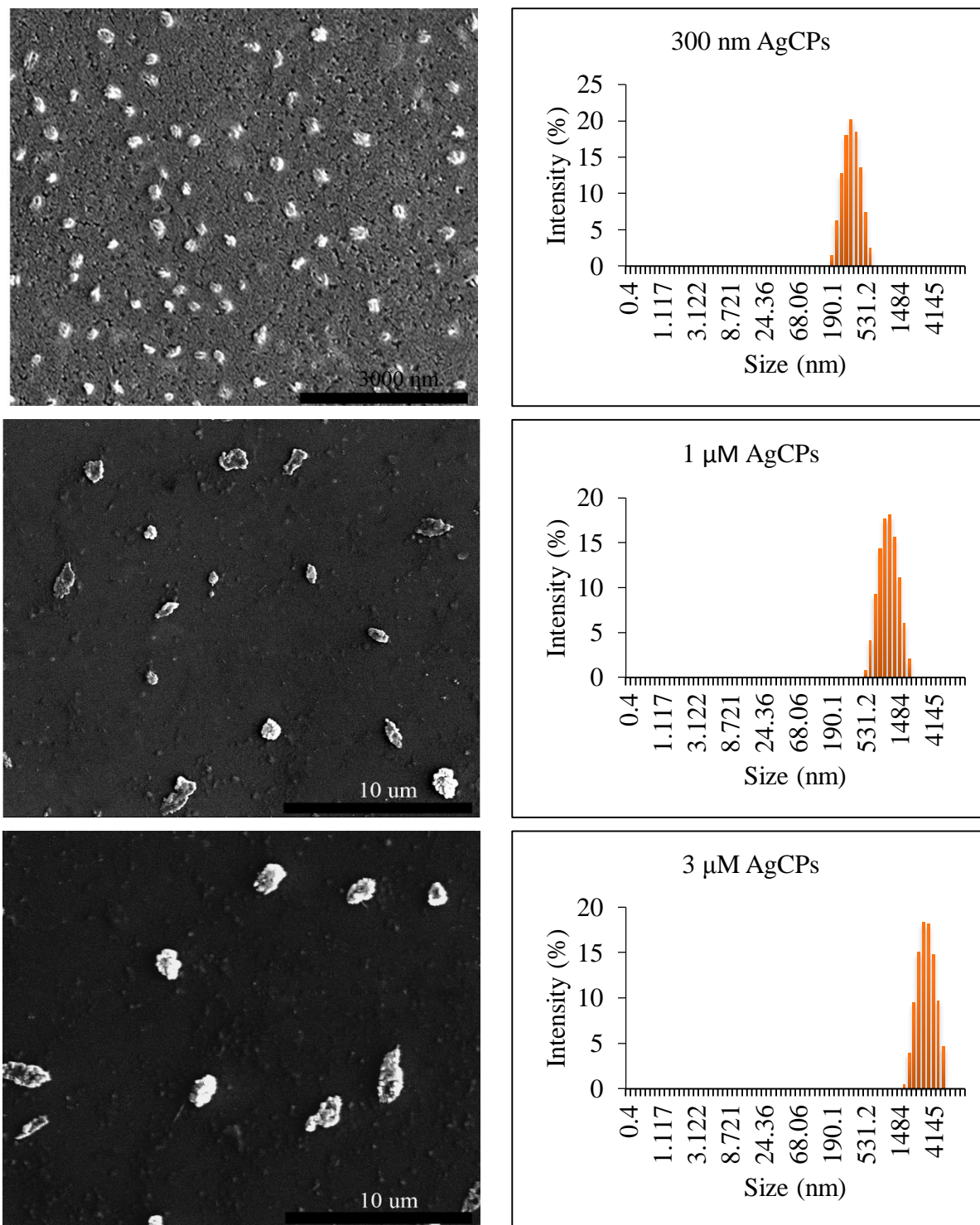


Figure. 10. Morphology and size distribution of AgCPs. Representative SEM images and DLS data show that 300 nm AgCPs, 1 μM AgCPs, and 3 μM AgCPs, are unimodally distributed and spherical to elliptical with porous non-uniform structures.

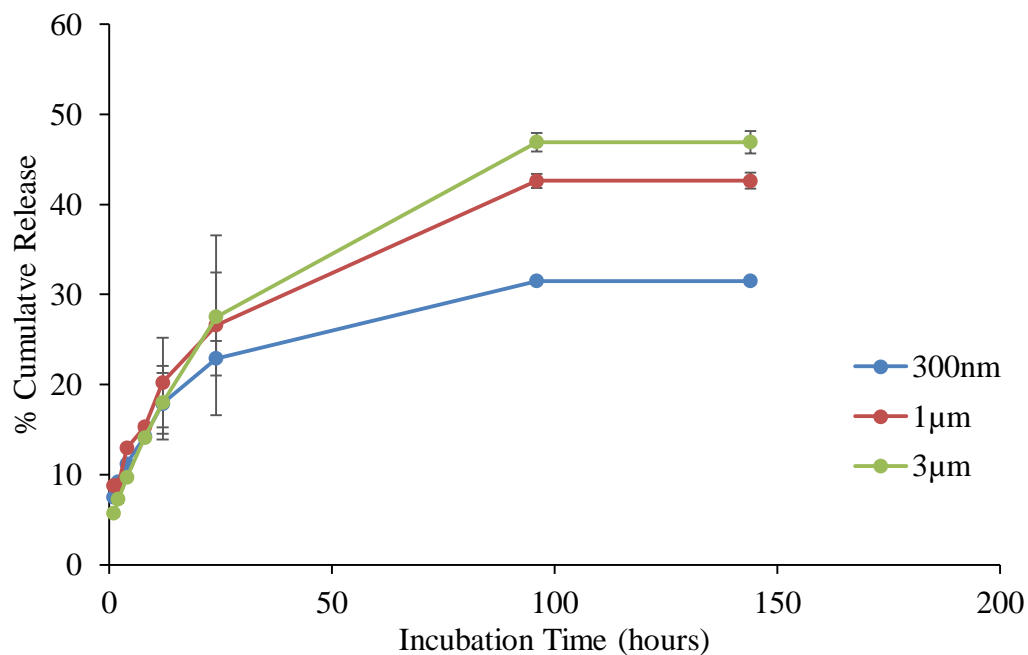


Figure. 11. Effect of chitosan particle size on protein release; 300nm, 1 µm, and 3 µm CPs encapsulating model protein FITC-BSA were incubated with PBS. Samples were collected at each time point and protein release was quantified by measuring fluorescence via fluorescence spectroscopy. Cumulative protein release was calculated by adding the protein release at each individual time point.

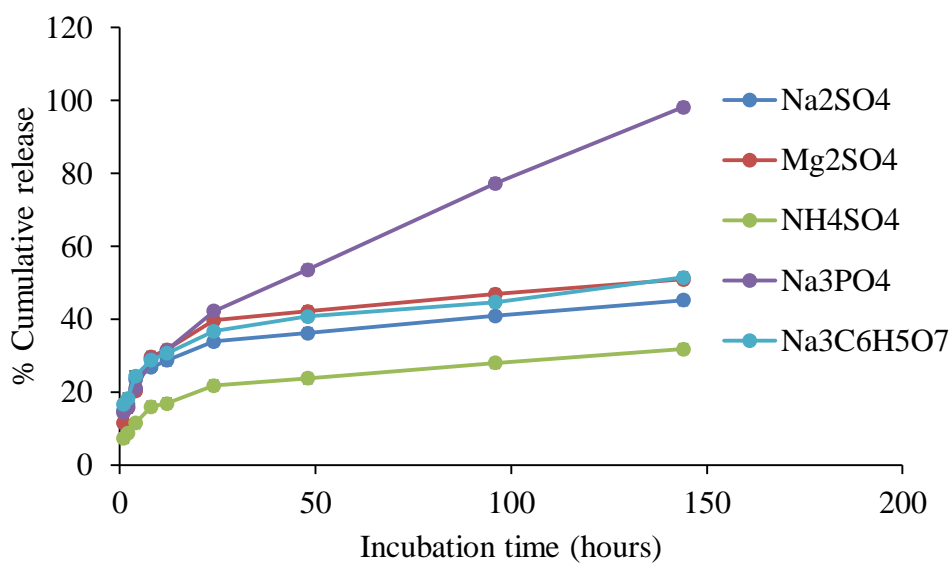


Figure. 12. Effect of ionic strength of precipitating salt on protein release; Particles prepared using hofmeister series ionic precipitant salts Na₂SO₄, (NH₄)₂SO₄, MgSO₄, Na₃C₆H₅O₇, and Na₃PO₄ encapsulating model protein FITC-BSA were incubated with PBS. Samples were collected at each time point and protein release was quantified by measuring fluorescence via fluorescence spectroscopy. Cumulative protein release was calculated by adding the protein release at each individual time point.

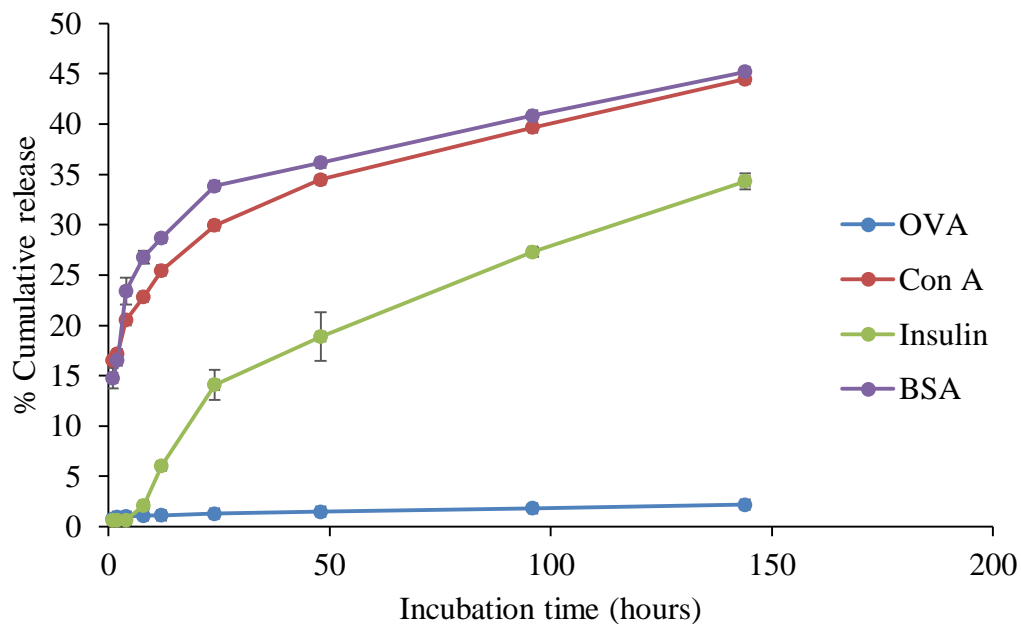


Figure.13. Effect of encapsulated protein size on protein release by particles; Particles encapsulating model proteins FITC-Insulin, FITC-OVA, FITC-BSA, and FITC-Con A were incubated with PBS. Samples were collected at each time point and protein release was quantified by measuring fluorescence via fluorescence spectroscopy. Cumulative protein release was calculated by adding the protein release at each individual time point.

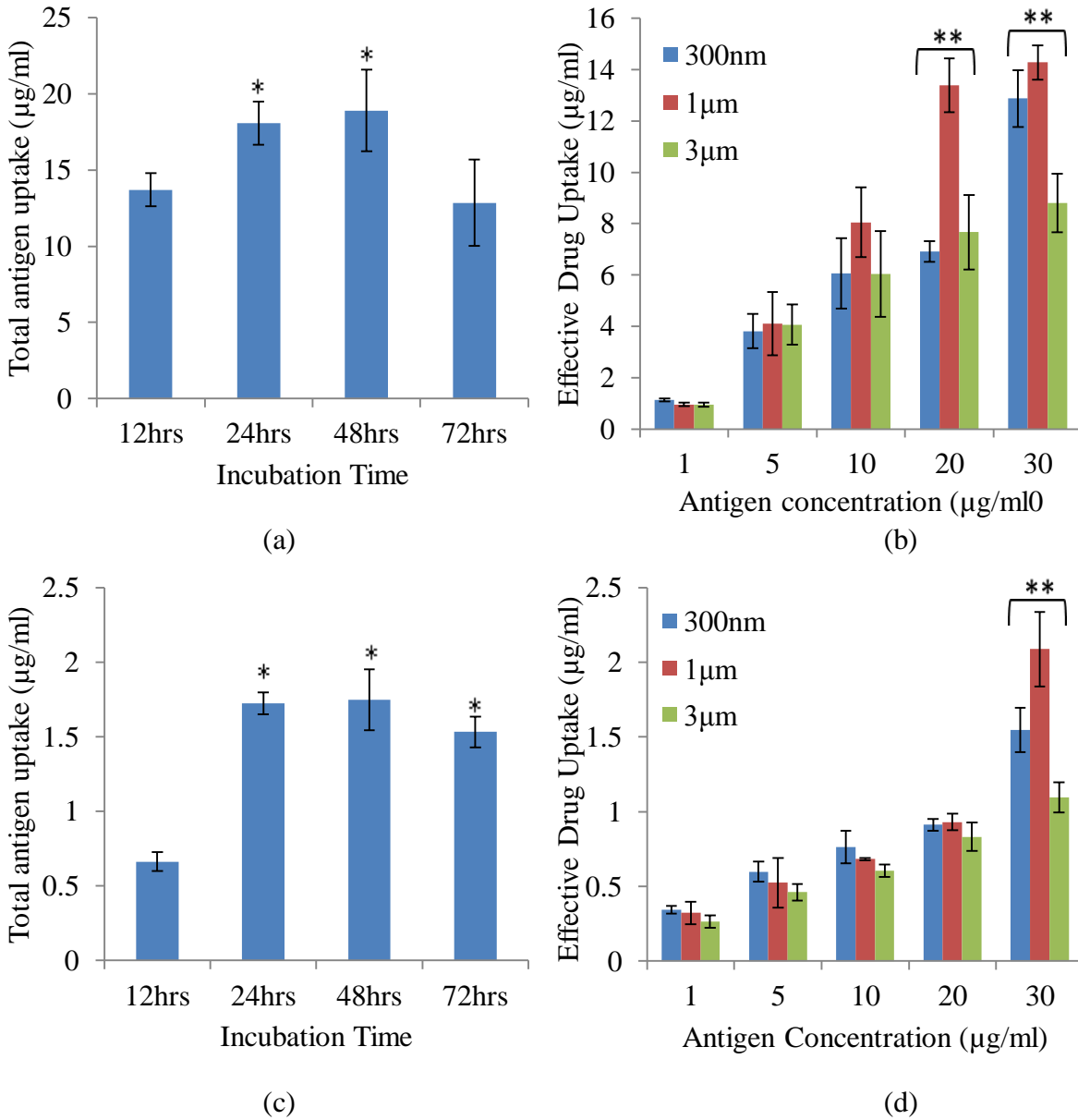


Figure 14. Effect of size, concentration, and incubation time on uptake of AgCPs by APCs. (a) RAW 264.7 macrophages or (c) BMDCs were co-incubated with 1µm AgCPs at an effective antigen/FITC-BSA concentration of 30 µg/ml for 12, 24, or 48 h. (b) RAW 264.7 macrophages or (d) BMDCs were co-incubated with 300nm, 1µm, or 3µm AgCPs at effective antigen concentrations of 1, 5, 10, 20, or 30 µg/ml for 24 h. After each co-incubation, cells were rinsed three times with PBS and lysed with 1% triton solution. The amount of FITC-BSA released was quantified via fluorescence spectroscopy. Data are presented as mean ± standard deviation from three independent experiments. * $p \leq 0.05$ vs. 12 h incubation; ** $p \leq 0.05$ comparing AgCP sizes for a particular antigen concentration.

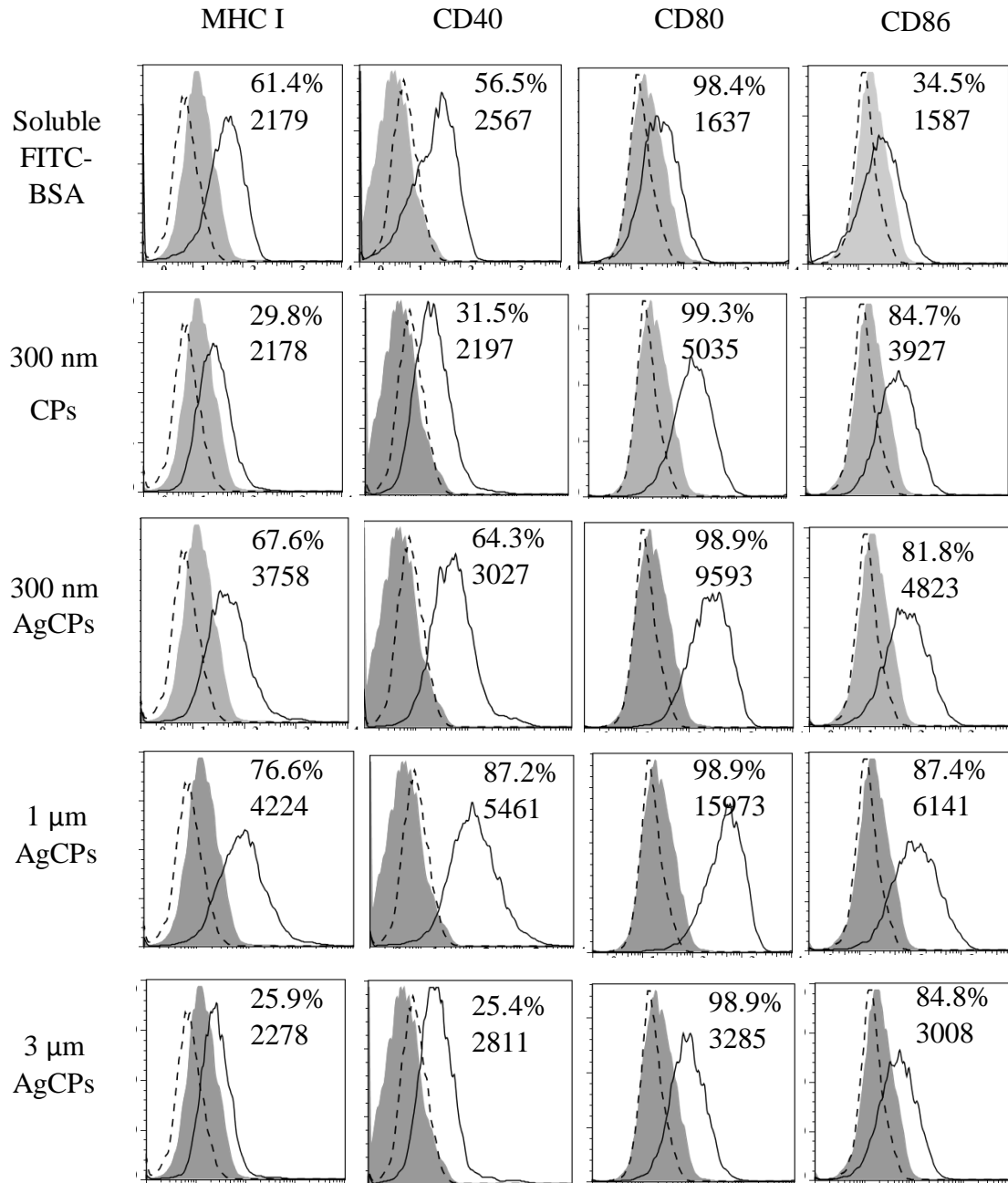


Figure. 15. Surface marker expression by RAW 264.7 macrophages following exposure to soluble antigen, CPs without antigen or AgCPs. Macrophages were co-incubated with soluble or particulate antigens at a final antigen concentration of 30 $\mu\text{g}/\text{ml}$. After 24 h, cells were rinsed three times, harvested, blocked with purified anti-mouse CD16/CD32 and stained with fluorescence-labeled antibodies to MHC molecules and activation markers (solid lines). Filled histograms represent cells treated with medium alone. Dotted line histograms are treated cells stained with appropriate isotype controls. All histograms are from one representative experiment of three independent experiments producing similar results. Panel numbers indicate the mean percentages of positive cells (top number) and mean fluorescence intensities (bottom number) of respective samples.

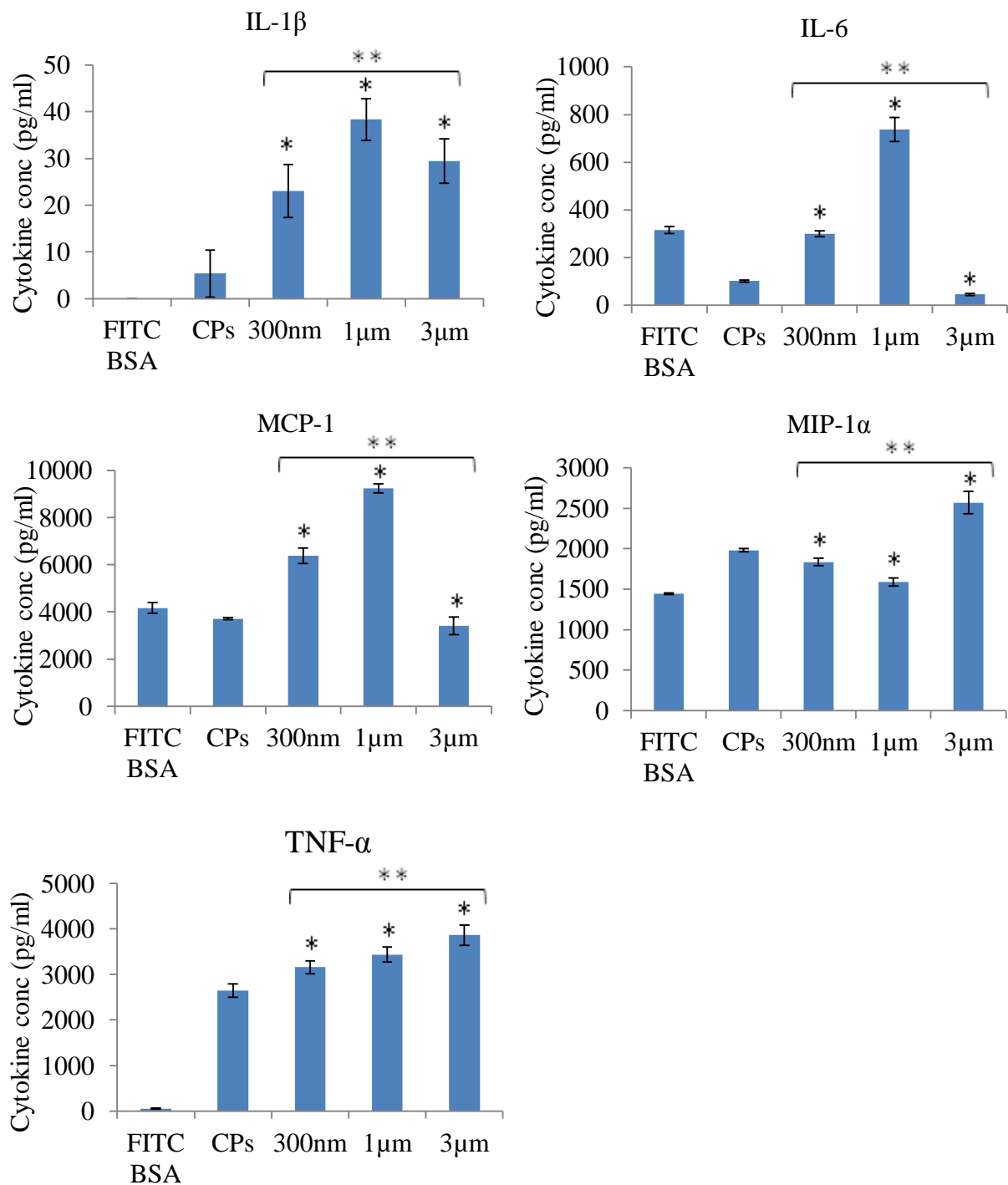


Figure 16. Cytokine release by RAW 264.7 macrophages. Cells were co-incubated with soluble or particulate antigens at a final antigen concentration of 30 μ g/ml. After 24 h, supernatants of all groups were collected and analyzed for cytokine production using a customized CBA flex set. Data are presented as mean \pm standard deviation from three independent experiments. * $p \leq 0.05$ vs. soluble antigen (FITC-BSA); ** $p \leq 0.05$ vs. other sizes of AgCPs.

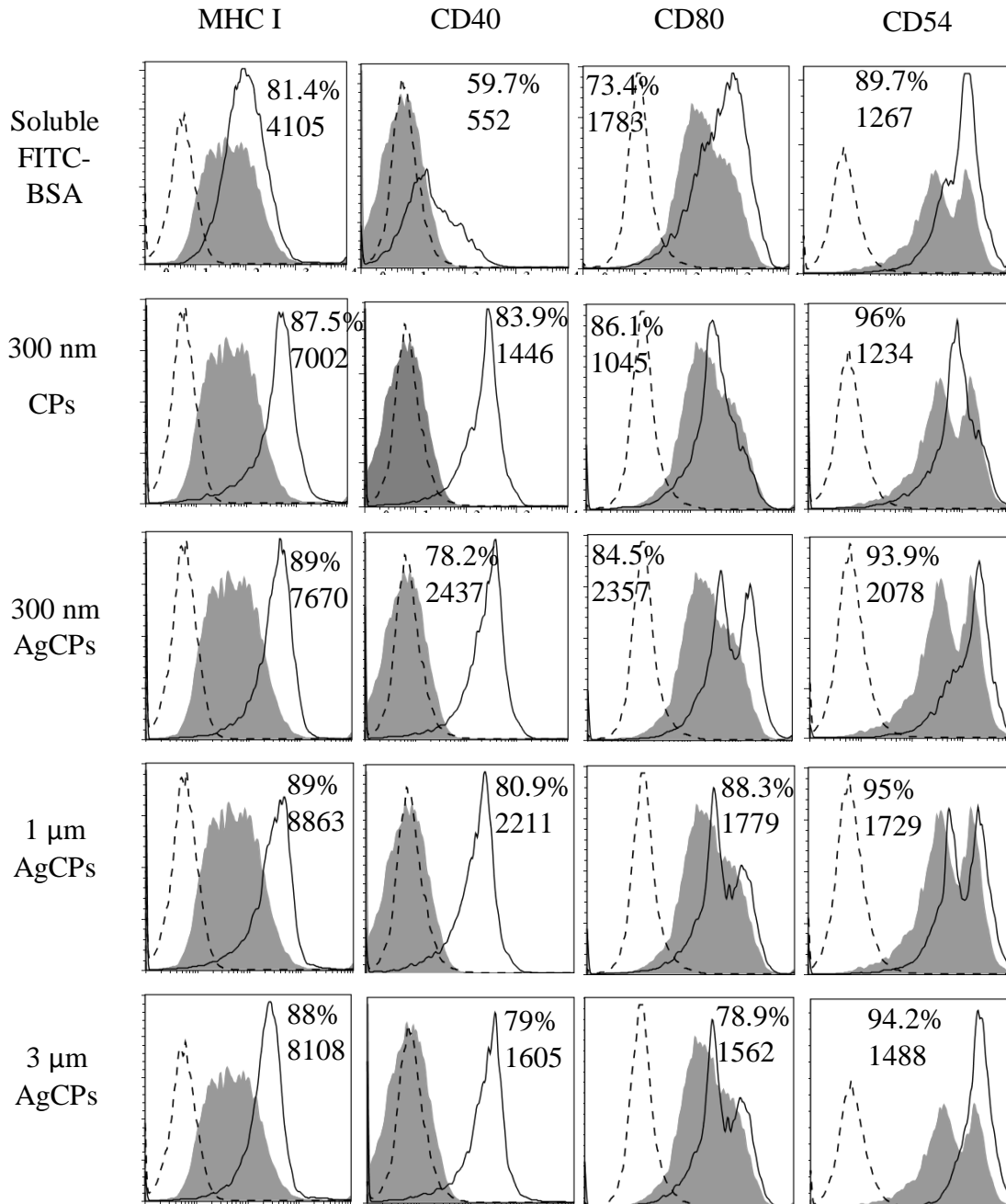


Figure. 17. Surface marker expression by BMDCs following exposure to soluble antigen, CPs without antigen or AgCPs. Macrophages were co-incubated with soluble or particulate antigens at a final antigen concentration of 30 $\mu\text{g}/\text{ml}$. After 24 h, cells were rinsed three times, blocked with purified anti-mouse CD16/CD32 and stained with fluorescence-labeled antibodies to MHC molecules and activation markers (solid lines). Filled histograms represent cells treated with medium alone. Dotted line histograms are treated cells stained with appropriate isotype controls. All histograms are from one representative experiment of three independent experiments producing similar results. Panel numbers indicate the mean percentages of positive cells (top number) and mean fluorescence intensities (bottom number) of respective samples.

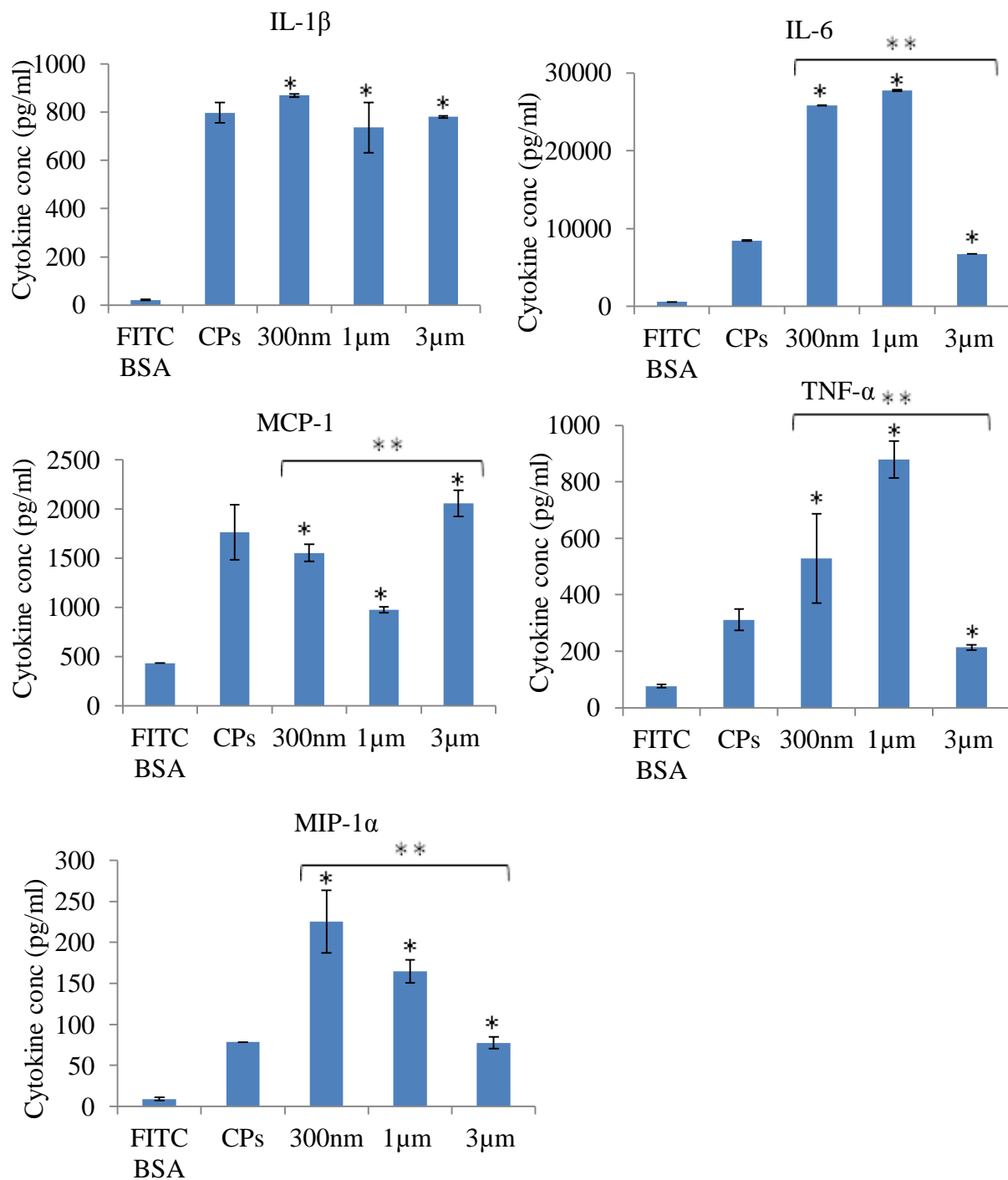
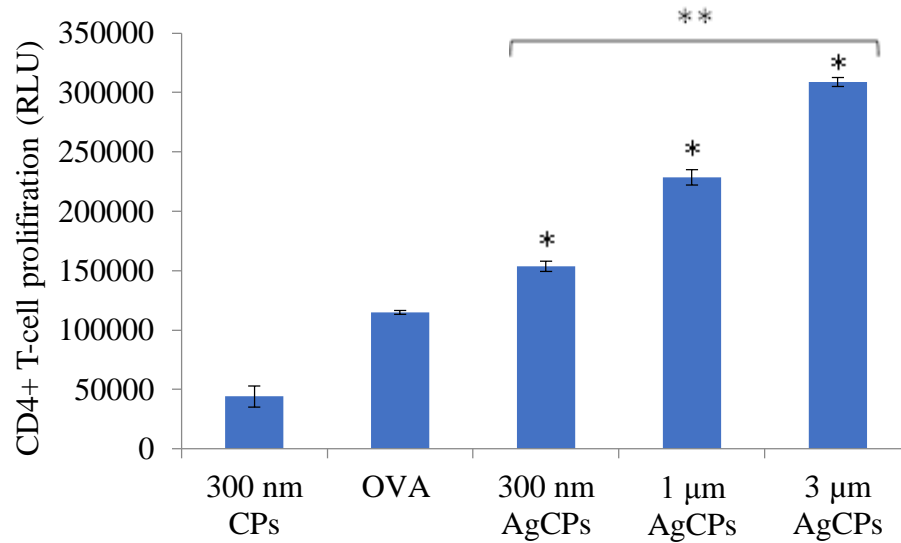
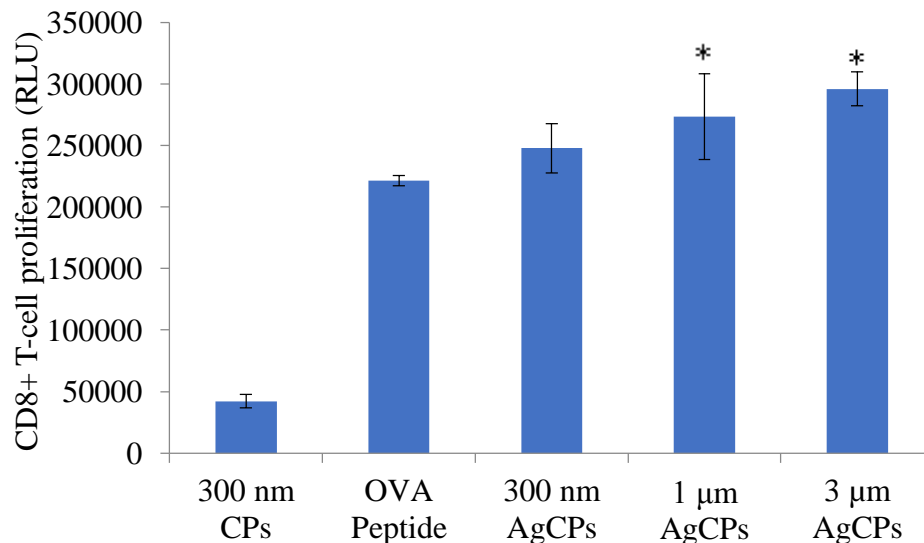


Figure. 18. Cytokine release by BMDCs. Cells were co-incubated with soluble or particulate antigens at a final antigen concentration of 30 μ g/ml. After 24 h, supernatants of all groups were collected and analyzed for cytokine production using a customized CBA flex set. Data are presented as mean \pm standard deviation from three independent experiments. * $p \leq 0.05$ vs. soluble antigen (FITC-BSA); ** $p \leq 0.05$ vs. other sizes of AgCPs.



(a)



(b)

Figure. 19. Proliferation of (a) OVA-specific CD4⁺ T-cells, and (b) OVA-specific CD8⁺ T-cells in response to presentation of antigen by BMDCs. BMDCs were pulsed with CPs, AgCPs, soluble full length OVA or the MHC I-restricted OVA₂₅₇₋₂₆₄ peptide for 24 h and then co-incubated with CD4⁺ or CD8⁺ T-cells from OT-II or OT-I mice, respectively. After 72 h, T cell proliferation was determined via a non-radioactive proliferation assay (CellTiter Glo; Promega, Madison, WI). Data are presented as mean relative light unit (RLU) ± standard deviation from one of two independent experiments with similar results. *p ≤ 0.05 vs. OVA or OVA peptide; **p ≤ 0.05 vs other AgCP sizes.

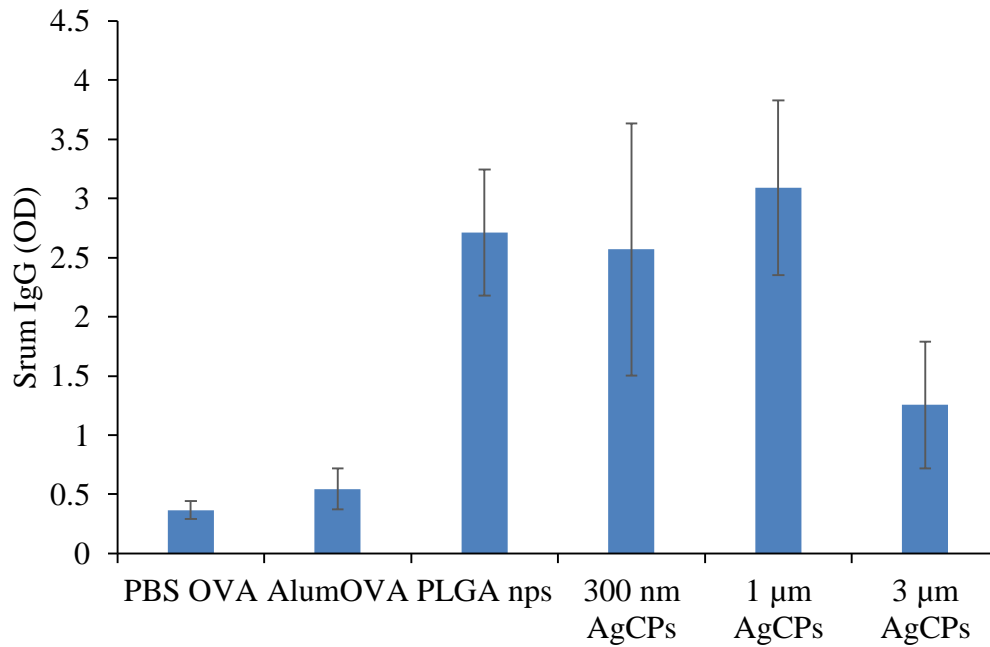


Figure. 20. Serum anti-OVA IgG antibodies. Adult C57BL/6J mice were immunized two weeks apart with one of six vaccines: OVA alone, OVA formulated with alum, PLGA-OVA, 300 nm, 1 μm, and 3 μm OvaCPs. Sera were collected five days after booster injection and analyzed using ELISA. Mouse anti-OVA antibodies were used as positive controls with PBS acting as negative control. The data represent the mean ± standard deviation of two independent immunization experiments (n = 10, 5 mice per vaccine x 2).

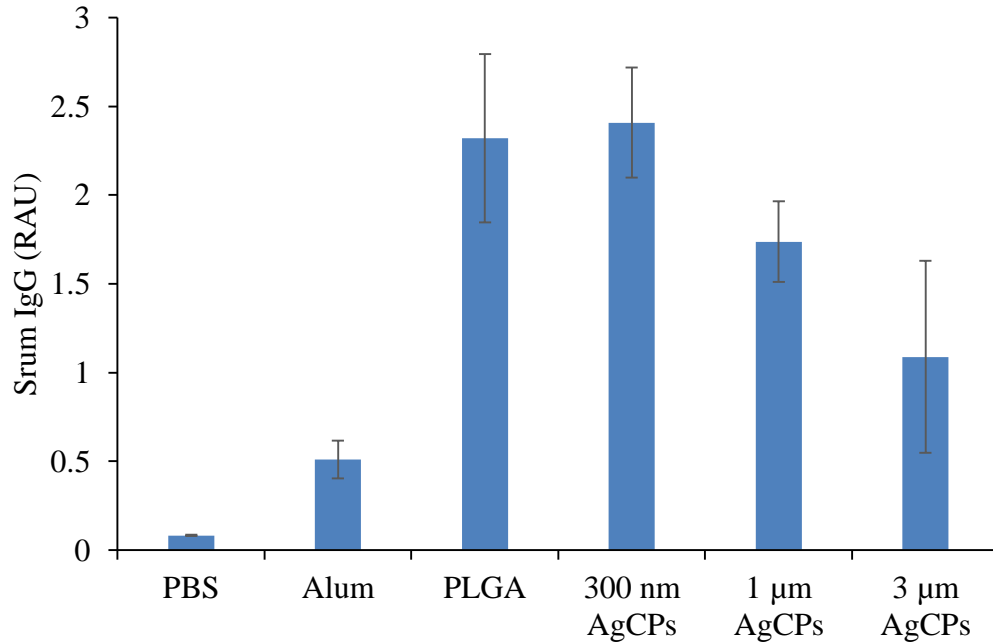
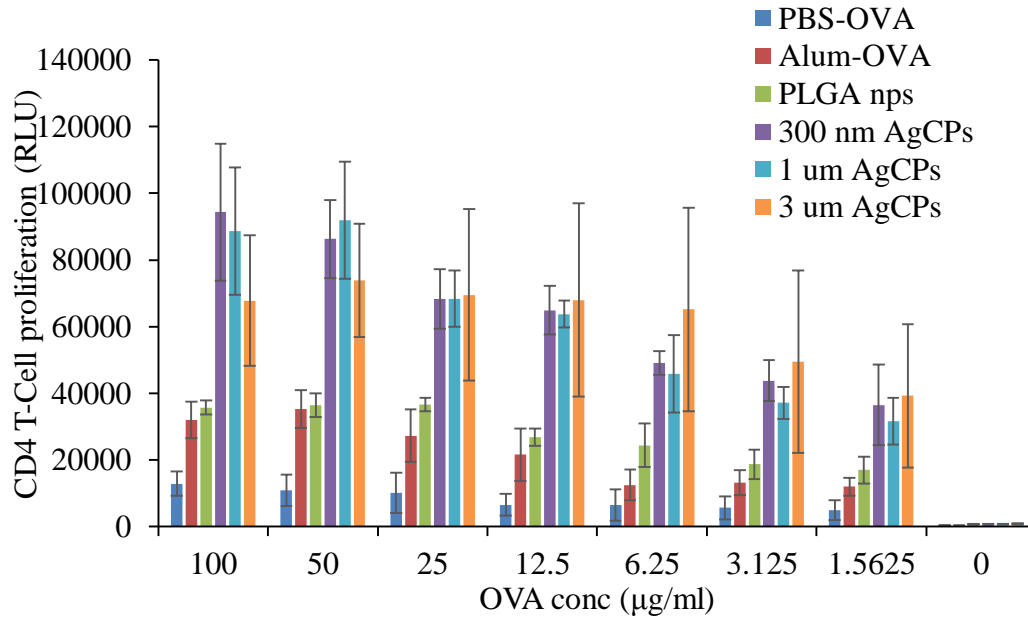
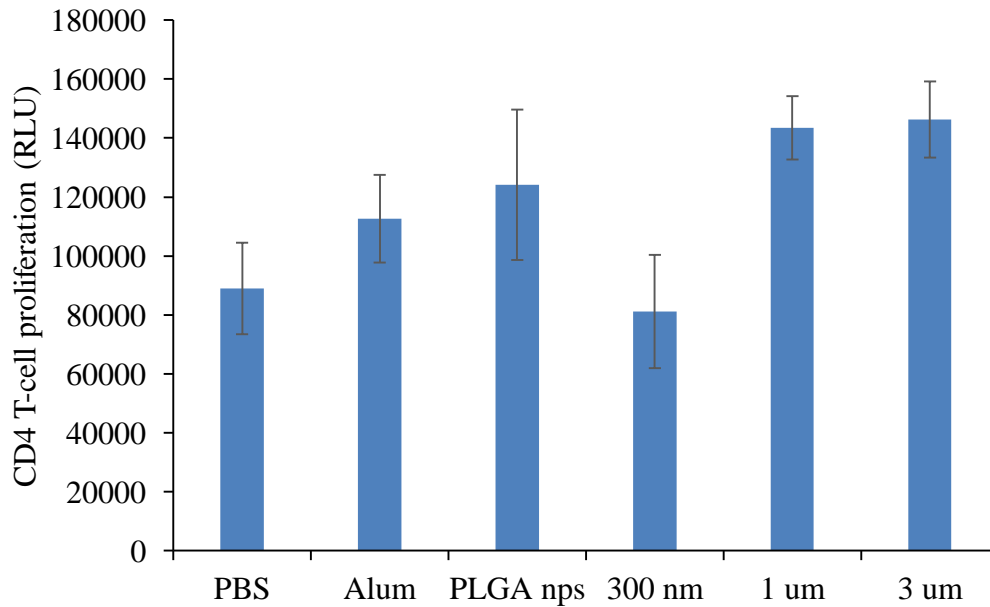


Figure. 21. Serum anti-OVA IgG1 antibodies. Adult C57BL/6J Mice were immunized two weeks apart with one of six vaccines: OVA alone, OVA formulated with alum, PLGA-OVA, 300 nm, 1 μm, and 3 μm OvaCPs. Sera were collected five days after booster injection and analyzed using ELISA. Mouse anti-OVA antibodies were used as positive controls with PBS acting as negative control. The data represent the mean ± standard deviation of two independent immunization experiments (n = 10, 5 mice per vaccine x 2).



(a)



(b)

Figure. 22. (a) Proliferation of CD4⁺ T-cells isolated from immunized mice. Adult C57BL/6J Mice were immunized two weeks apart with one of six vaccines: OVA alone, OVA formulated with alum, PLGA-OVA, 300 nm, 1 µm, and 3 µm OvaCPs. Five days post-booster injection. CD4⁺ T-cells from individual mice were isolated from immunized mice spleens and co-cultured with irradiated splenocytes isolated from naïve mice pulsed with OVA. (b) Cells stimulated with Con A served as the positive controls. The data represent the mean ± standard deviation of two independent immunization experiments (n = 10, 5 mice per vaccine x 2).

6. REFERENCES

- [1] Schijns VE. Immunological concepts of vaccine adjuvant activity. *Current opinion in immunology*. 2000;12:456-63.
- [2] Detmer A, Glenting J. Live bacterial vaccines--a review and identification of potential hazards. *Microb Cell Fact*. 2006;5:23.
- [3] Dietrich G, Collioud A, Rothen SA. *Developing and Manufacturing Attenuated Live Bacterial Vaccines*. 2008.
- [4] Mortimer EA, Jr. Immunization against infectious disease. *Science*. 1978;200:902-7.
- [5] O'Hagan DT, Valiante NM. Recent advances in the discovery and delivery of vaccine adjuvants. *Nature reviews*. 2003;2:727-35.
- [6] Singh M, O'Hagan D. Advances in vaccine adjuvants. *Nature biotechnology*. 1999;17:1075-81.
- [7] Peltola H, Kilpi T, Anttila M. Rapid disappearance of *Haemophilus influenzae* type b meningitis after routine childhood immunisation with conjugate vaccines. *The Lancet*. 1992;340:592-4.
- [8] Ribeiro GS, Reis JN, Cordeiro SM, Lima JB, Gouveia EL, Petersen M, et al. Prevention of *Haemophilus influenzae* type b (Hib) meningitis and emergence of serotype replacement with type a strains after introduction of Hib immunization in Brazil. *J Infect Dis*. 2003;187:109-16.
- [9] Huygen K, Content J, Denis O, Montgomery DL, Yawman AM, Deck RR, et al. Immunogenicity and protective efficacy of a tuberculosis DNA vaccine. *Nature medicine*. 1996;2:893-8.
- [10] Shinoda K, Xin KQ, Jounai N, Kojima Y, Tamura Y, Okada E, et al. Polygene DNA vaccine induces a high level of protective effect against HIV-vaccinia virus challenge in mice. *Vaccine*. 2004;22:3676-90.
- [11] Morein B, Villacres-Eriksson M, Sjolander A, Bengtsson KL. Novel adjuvants and vaccine delivery systems. *Vet Immunol Immunopathol*. 1996;54:373-84.

- [12] Perrie Y, Mohammed AR, Kirby DJ, McNeil SE, Bramwell VW. Vaccine adjuvant systems: enhancing the efficacy of sub-unit protein antigens. *Int J Pharm.* 2008;364:272-80.
- [13] Gallichan WS, Rosenthal KL. Long-lived cytotoxic T lymphocyte memory in mucosal tissues after mucosal but not systemic immunization. *The Journal of experimental medicine.* 1996;184:1879-90.
- [14] O'Hagan DT, Rappuoli R. Novel approaches to vaccine delivery. *Pharm Res.* 2004;21:1519-30.
- [15] O'Hagan DT, Singh M. Microparticles as vaccine adjuvants and delivery systems. *Expert review of vaccines.* 2003;2:269-83.
- [16] Janeway CA, Jr., Medzhitov R. Innate immune recognition. *Annu Rev Immunol.* 2002;20:197-216.
- [17] Gupta RK. Aluminum compounds as vaccine adjuvants. *Advanced drug delivery reviews.* 1998;32:155-72.
- [18] Singh M, Ugozzoli M, Kazzaz J, Chesko J, Soenawan E, Mannucci D, et al. A preliminary evaluation of alternative adjuvants to alum using a range of established and new generation vaccine antigens. *Vaccine.* 2006;24:1680-6.
- [19] Powell M, Newman M, Ulrich JT, Myers K. Monophosphoryl Lipid A as an Adjuvant. *Vaccine Design: Springer US;* 1995. p. 495-524.
- [20] Ulrich JT, Myers KR. Monophosphoryl lipid A as an adjuvant. Past experiences and new directions. *Pharm Biotechnol.* 1995;6:495-524.
- [21] Gustafson GL, Rhodes MJ. Bacterial cell wall products as adjuvants: early interferon gamma as a marker for adjuvants that enhance protective immunity. *Res Immunol.* 1992;143:483-8; discussion 573-4.
- [22] Reed SG, Bertholet S, Coler RN, Friede M. New horizons in adjuvants for vaccine development. *Trends Immunol.* 2009;30:23-32.
- [23] De Gregorio E, Tritto E, Rappuoli R. Alum adjuvanticity: unraveling a century old mystery. *European journal of immunology.* 2008;38:2068-71.

[24] Sabel MS, Sondak VK. Pros and cons of adjuvant interferon in the treatment of melanoma. *The oncologist*. 2003;8:451-8.

[25] Giannini SL, Hanon E, Moris P, Van Mechelen M, Morel S, Dessy F, et al. Enhanced humoral and memory B cellular immunity using HPV16/18 L1 VLP vaccine formulated with the MPL/aluminium salt combination (AS04) compared to aluminium salt only. *Vaccine*. 2006;24:5937-49.

[26] Klinman DM, Barnhart KM, Conover J. CpG motifs as immune adjuvants. *Vaccine*. 1999;17:19-25.

[27] Krieg AM, Yi AK, Matson S, Waldschmidt TJ, Bishop GA, Teasdale R, et al. CpG motifs in bacterial DNA trigger direct B-cell activation. *Nature*. 1995;374:546-9.

[28] Klinman DM, Yamshchikov G, Ishigatsubo Y. Contribution of CpG motifs to the immunogenicity of DNA vaccines. *J Immunol*. 1997;158:3635-9.

[29] Roman M, Martin-Orozco E, Goodman JS, Nguyen MD, Sato Y, Ronaghy A, et al. Immunostimulatory DNA sequences function as T helper-1-promoting adjuvants. *Nature medicine*. 1997;3:849-54.

[30] Weiner GJ, Liu H-M, Wooldridge JE, Dahle CE, Krieg AM. Immunostimulatory oligodeoxynucleotides containing the CpG motif are effective as immune adjuvants in tumor antigen immunization. *Proceedings of the National Academy of Sciences*. 1997;94:10833-7.

[31] Kensil CR. Saponins as vaccine adjuvants. *Crit Rev Ther Drug Carrier Syst*. 1996;13:1-55.

[32] Moore A, McCarthy L, Mills KH. The adjuvant combination monophosphoryl lipid A and QS21 switches T cell responses induced with a soluble recombinant HIV protein from Th2 to Th1. *Vaccine*. 1999;17:2517-27.

[33] Kensil CR, Wu JY, Anderson CA, Wheeler DA, Amsden J. QS-21 and QS-7: purified saponin adjuvants. *Dev Biol Stand*. 1998;92:41-7.

[34] Rajput ZI, Hu SH, Xiao CW, Arijo AG. Adjuvant effects of saponins on animal immune responses. *J Zhejiang Univ Sci B*. 2007;8:153-61.

- [35] Deng K, Adams MM, Damani P, Livingston PO, Ragupathi G, Gin DY. Synthesis of QS-21-xylose: establishment of the immunopotentiating activity of synthetic QS-21 adjuvant with a melanoma vaccine. *Angew Chem Int Ed Engl*. 2008;47:6395-8.
- [36] Evans TG, McElrath MJ, Matthews T, Montefiori D, Weinhold K, Wolff M, et al. QS-21 promotes an adjuvant effect allowing for reduced antigen dose during HIV-1 envelope subunit immunization in humans. *Vaccine*. 2001;19:2080-91.
- [37] Lin R, Tarr PE, Jones TC. Present status of the use of cytokines as adjuvants with vaccines to protect against infectious diseases. *Clin Infect Dis*. 1995;21:1439-49.
- [38] Bradney CP, Sempowski GD, Liao HX, Haynes BF, Staats HF. Cytokines as adjuvants for the induction of anti-human immunodeficiency virus peptide immunoglobulin G (IgG) and IgA antibodies in serum and mucosal secretions after nasal immunization. *J Virol*. 2002;76:517-24.
- [39] Boyaka PN, McGhee JR. Cytokines as adjuvants for the induction of mucosal immunity. *Advanced drug delivery reviews*. 2001;51:71-9.
- [40] Ozbas-Turan S, Akbuga J, Aral C. Controlled release of interleukin-2 from chitosan microspheres. *J Pharm Sci*. 2002;91:1245-51.
- [41] Zaharoff DA, Rogers CJ, Hance KW, Schlom J, Greiner JW. Chitosan solution enhances the immunoadjuvant properties of GM-CSF. *Vaccine*. 2007;25:8673-86.
- [42] Randolph GJ, Inaba K, Robbiani DF, Steinman RM, Muller WA. Differentiation of phagocytic monocytes into lymph node dendritic cells in vivo. *Immunity*. 1999;11:753-61.
- [43] Kanke M, Sniecinski I, DeLuca PP. Interaction of microspheres with blood constituents: I. Uptake of polystyrene spheres by monocytes and granulocytes and effect on immune responsiveness of lymphocytes. *J Parenter Sci Technol*. 1983;37:210-7.
- [44] Tabata Y, Ikada Y. Macrophage phagocytosis of biodegradable microspheres composed of L-lactic acid/glycolic acid homo- and copolymers. *Journal of biomedical materials research*. 1988;22:837-58.
- [45] Thiele L, Merkle HP, Walter E. Phagocytosis and phagosomal fate of surface-modified microparticles in dendritic cells and macrophages. *Pharmaceutical research*. 2003;20:221-8.

- [46] Bachmann MF, Rohrer UH, Kundig TM, Burki K, Hengartner H, Zinkernagel RM. The influence of antigen organization on B cell responsiveness. *Science (New York, NY)*. 1993;262:1448-51.
- [47] Bachmann MF, Zinkernagel RM. Neutralizing antiviral B cell responses. *Annual review of immunology*. 1997;15:235-70.
- [48] Storni T, Ruedl C, Renner WA, Bachmann MF. Innate immunity together with duration of antigen persistence regulate effector T cell induction. *J Immunol*. 2003;171:795-801.
- [49] Garland SM, Hernandez-Avila M, Wheeler CM, Perez G, Harper DM, Leodolter S, et al. Quadrivalent vaccine against human papillomavirus to prevent anogenital diseases. *The New England journal of medicine*. 2007;356:1928-43.
- [50] Harper DM, Franco EL, Wheeler C, Ferris DG, Jenkins D, Schuind A, et al. Efficacy of a bivalent L1 virus-like particle vaccine in prevention of infection with human papillomavirus types 16 and 18 in young women: a randomised controlled trial. *Lancet*. 2004;364:1757-65.
- [51] Kreuter J. Nanoparticles and microparticles for drug and vaccine delivery. *Journal of anatomy*. 1996;189 (Pt 3):503-5.
- [52] Draper SJ, Heeney JL. Viruses as vaccine vectors for infectious diseases and cancer. *Nat Rev Microbiol*.8:62-73.
- [53] Limbach KJ, Richie TL. Viral vectors in malaria vaccine development. *Parasite Immunol*. 2009;31:501-19.
- [54] Choi Y, Chang J. Viral vectors for vaccine applications. *Clin Exp Vaccine Res*.2:97-105.
- [55] Peek LJ, Middaugh CR, Berkland C. Nanotechnology in vaccine delivery. *Advanced drug delivery reviews*. 2008;60:915-28.
- [56] Grgacic EV, Anderson DA. Virus-like particles: passport to immune recognition. *Methods (San Diego, Calif)*. 2006;40:60-5.
- [57] Madalinski K, Sylvan SP, Hellstrom U, Mikolajewicz J, Zembrzuska-Sadkowska E, Piontek E. Antibody responses to preS components after immunization of children with low doses of BioHepB. *Vaccine*. 2001;20:92-7.

[58] Harper DM, Franco EL, Wheeler CM, Moscicki AB, Romanowski B, Roteli-Martins CM, et al. Sustained efficacy up to 4.5 years of a bivalent L1 virus-like particle vaccine against human papillomavirus types 16 and 18: follow-up from a randomised control trial. *Lancet*. 2006;367:1247-55.

[59] Nardin EH, Oliveira GA, Calvo-Calle JM, Wetzel K, Maier C, Birkett AJ, et al. Phase I testing of a malaria vaccine composed of hepatitis B virus core particles expressing *Plasmodium falciparum* circumsporozoite epitopes. *Infection and immunity*. 2004;72:6519-27.

[60] Heurtault B, Frisch B, Pons F. Liposomes as delivery systems for nasal vaccination: strategies and outcomes. *Expert Opin Drug Deliv*.7:829-44.

[61] Gregory AE, Titball R, Williamson D. Vaccine delivery using nanoparticles. *Front Cell Infect Microbiol*.3:13.

[62] Henriksen-Lacey M, Korsholm KS, Andersen P, Perrie Y, Christensen D. Liposomal vaccine delivery systems. *Expert Opin Drug Deliv*.8:505-19.

[63] Alving CR. Liposomes as carriers of antigens and adjuvants. *Journal of immunological methods*. 1991;140:1-13.

[64] Alving CR, Banerji B, Shiba T, Kotani S, Clements JD, Richards RL. Liposomes as vehicles for vaccines. *Prog Clin Biol Res*. 1980;47:339-55.

[65] Guan HH, Budzynski W, Koganty RR, Krantz MJ, Reddish MA, Rogers JA, et al. Liposomal formulations of synthetic MUC1 peptides: effects of encapsulation versus surface display of peptides on immune responses. *Bioconjugate chemistry*. 1998;9:451-8.

[66] Palmer M, Parker J, Modi S, Butts C, Smylie M, Meikle A, et al. Phase I study of the BLP25 (MUC1 peptide) liposomal vaccine for active specific immunotherapy in stage IIIB/IV non-small-cell lung cancer. *Clin Lung Cancer*. 2001;3:49-57; discussion 8.

[67] Mohammed AR, Bramwell VW, Coombes AG, Perrie Y. Lyophilisation and sterilisation of liposomal vaccines to produce stable and sterile products. *Methods (San Diego, Calif)*. 2006;40:30-8.

[68] Drane D, Pearse MJ, Schijns VEJC, O'Hagan DT. 12 - The ISCOMATRIX™ adjuvant. *Immunopotentiators in Modern Vaccines*. London: Academic Press; 2006. p. 191-215.

[69] Barr IG, Mitchell GF. ISCOMs (immunostimulating complexes): the first decade. *Immunol Cell Biol.* 1996;74:8-25.

[70] Rimmelzwaan GF, Nieuwkoop N, Brandenburg A, Sutter G, Beyer WE, Maher D, et al. A randomized, double blind study in young healthy adults comparing cell mediated and humoral immune responses induced by influenza ISCOM vaccines and conventional vaccines. *Vaccine.* 2000;19:1180-7.

[71] Ennis FA, Cruz J, Jameson J, Klein M, Burt D, Thippawong J. Augmentation of human influenza A virus-specific cytotoxic T lymphocyte memory by influenza vaccine and adjuvanted carriers (ISCOMS). *Virology.* 1999;259:256-61.

[72] Pearse MJ, Drane D. ISCOMATRIX adjuvant for antigen delivery. *Adv Drug Deliv Rev.* 2005;57:465-74.

[73] Lenarczyk A, Le TT, Drane D, Malliaros J, Pearse M, Hamilton R, et al. ISCOM based vaccines for cancer immunotherapy. *Vaccine.* 2004;22:963-74.

[74] Cox JC, Sjolander A, Barr IG. ISCOMs and other saponin based adjuvants. *Advanced drug delivery reviews.* 1998;32:247-71.

[75] De Souza Reboucas J, Esparza I, Ferrer M, Sanz ML, Irache JM, Gamazo C. Nanoparticulate adjuvants and delivery systems for allergen immunotherapy. *J Biomed Biotechnol.* 2012:474605.

[76] Kalkanidis M, Pietersz GA, Xiang SD, Mottram PL, Crimeen-Irwin B, Ardipradja K, et al. Methods for nano-particle based vaccine formulation and evaluation of their immunogenicity. *Methods (San Diego, Calif.)* 2006;40:20-9.

[77] Mahvi DM, Shi FS, Yang NS, Weber S, Hank J, Albertini M, et al. Immunization by particle-mediated transfer of the granulocyte-macrophage colony-stimulating factor gene into autologous tumor cells in melanoma or sarcoma patients: report of a phase I/IB study. *Hum Gene Ther.* 2002;13:1711-21.

[78] Fuller DH, Loudon P, Schmaljohn C. Preclinical and clinical progress of particle-mediated DNA vaccines for infectious diseases. *Methods (San Diego, Calif.)* 2006;40:86-97.

- [79] Pusic K, Aguilar Z, McLoughlin J, Kobuch S, Xu H, Tsang M, et al. Iron oxide nanoparticles as a clinically acceptable delivery platform for a recombinant blood-stage human malaria vaccine. *FASEB J*.27:1153-66.
- [80] Fifis T, Gamvrellis A, Crimeen-Irwin B, Pietersz GA, Li J, Mottram PL, et al. Size-dependent immunogenicity: therapeutic and protective properties of nano-vaccines against tumors. *J Immunol*. 2004;173:3148-54.
- [81] Vidard L, Kovacsovics-Bankowski M, Kraeft SK, Chen LB, Benacerraf B, Rock KL. Analysis of MHC class II presentation of particulate antigens of B lymphocytes. *J Immunol*. 1996;156:2809-18.
- [82] Kwon YJ, Standley SM, Goh SL, Frechet JM. Enhanced antigen presentation and immunostimulation of dendritic cells using acid-degradable cationic nanoparticles. *J Control Release*. 2005;105:199-212.
- [83] Gamvrellis A, Leong D, Hanley JC, Xiang SD, Mottram P, Plebanski M. Vaccines that facilitate antigen entry into dendritic cells. *Immunol Cell Biol*. 2004;82:506-16.
- [84] Mahapatro A, Singh DK. Biodegradable nanoparticles are excellent vehicle for site directed in-vivo delivery of drugs and vaccines. *J Nanobiotechnology*.9:55.
- [85] Xiang SD, Scholzen A, Minigo G, David C, Apostolopoulos V, Mottram PL, et al. Pathogen recognition and development of particulate vaccines: does size matter? *Methods (San Diego, Calif)*. 2006;40:1-9.
- [86] AKAGI, #160, Takami, BABA, Masanori, AKASHI, et al. Biodegradable Nanoparticles as Vaccine Adjuvants and Delivery Systems: Regulation of Immune Responses by Nanoparticle-Based Vaccine. Heidelberg, ALLEMAGNE: Springer.
- [87] Bramwell VW, Perrie Y. Particulate delivery systems for vaccines: what can we expect? *The Journal of pharmacy and pharmacology*. 2006;58:717-28.
- [88] Panyam J, Labhasetwar V. Biodegradable nanoparticles for drug and gene delivery to cells and tissue. *Advanced drug delivery reviews*. 2003;55:329-47.

- [89] Wendorf J, Singh M, Chesko J, Kazzaz J, Soewanan E, Ugozzoli M, et al. A practical approach to the use of nanoparticles for vaccine delivery. *Journal of pharmaceutical sciences*. 2006;95:2738-50.
- [90] Spiers ID, Eyles JE, Baillie LW, Williamson ED, Alpar HO. Biodegradable microparticles with different release profiles: effect on the immune response after a single administration via intranasal and intramuscular routes. *The Journal of pharmacy and pharmacology*. 2000;52:1195-201.
- [91] Combadiere B, Mahe B. Particle-based vaccines for transcutaneous vaccination. *Comp Immunol Microbiol Infect Dis*. 2008;31:293-315.
- [92] Fredriksen BN, Grip J. PLGA/PLA micro- and nanoparticle formulations serve as antigen depots and induce elevated humoral responses after immunization of Atlantic salmon (*Salmo salar* L.). *Vaccine*.30:656-67.
- [93] Raghuvanshi RJ, Mistra A, Talwar GP, Levy RJ, Labhasetwar V. Enhanced immune response with a combination of alum and biodegradable nanoparticles containing tetanus toxoid. *J Microencapsul*. 2001;18:723-32.
- [94] Elamanchili P, Diwan M, Cao M, Samuel J. Characterization of poly(D,L-lactic-co-glycolic acid) based nanoparticulate system for enhanced delivery of antigens to dendritic cells. *Vaccine*. 2004;22:2406-12.
- [95] Florindo HF, Pandit S, Lacerda L, Goncalves LM, Alpar HO, Almeida AJ. The enhancement of the immune response against *S. equi* antigens through the intranasal administration of poly-epsilon-caprolactone-based nanoparticles. *Biomaterials*. 2009;30:879-91.
- [96] Broos S, Lundberg K, Akagi T, Kadowaki K, Akashi M, Greiff L, et al. Immunomodulatory nanoparticles as adjuvants and allergen-delivery system to human dendritic cells: Implications for specific immunotherapy. *Vaccine*.28:5075-85.
- [97] Murillo M, Gamazo C, Irache JM, Goni MM. Polyester microparticles as a vaccine delivery system for brucellosis: influence of the polymer on release, phagocytosis and toxicity. *Journal of drug targeting*. 2002;10:211-9.
- [98] Soppimath KS, Aminabhavi TM, Kulkarni AR, Rudzinski WE. Biodegradable polymeric nanoparticles as drug delivery devices. *J Control Release*. 2001;70:1-20.

- [99] Agnihotri SA, Mallikarjuna NN, Aminabhavi TM. Recent advances on chitosan-based micro- and nanoparticles in drug delivery. *J Control Release*. 2004;100:5-28.
- [100] Felt O, Buri P, Gurny R. Chitosan: a unique polysaccharide for drug delivery. *Drug development and industrial pharmacy*. 1998;24:979-93.
- [101] Kas HS. Chitosan: properties, preparations and application to microparticulate systems. *J Microencapsul*. 1997;14:689-711.
- [102] Sinha VR, Singla AK, Wadhawan S, Kaushik R, Kumria R, Bansal K, et al. Chitosan microspheres as a potential carrier for drugs. *Int J Pharm*. 2004;274:1-33.
- [103] Chandy T, Sharma CP. Chitosan--as a biomaterial. *Biomater Artif Cells Artif Organs*. 1990;18:1-24.
- [104] Chandy T, Sharma CP. Chitosan matrix for oral sustained delivery of ampicillin. *Biomaterials*. 1993;14:939-44.
- [105] Mao HQ, Roy K, Troung-Le VL, Janes KA, Lin KY, Wang Y, et al. Chitosan-DNA nanoparticles as gene carriers: synthesis, characterization and transfection efficiency. *J Control Release*. 2001;70:399-421.
- [106] Janes KA, Fresneau MP, Marazuela A, Fabra A, Alonso MJA. Chitosan nanoparticles as delivery systems for doxorubicin. *Journal of Controlled Release*. 2001;73:255-67.
- [107] Pittler MH, Ernst E. Dietary supplements for body-weight reduction: a systematic review. *The American journal of clinical nutrition*. 2004;79:529-36.
- [108] Wedmore I, McManus JG, Pusateri AE, Holcomb JB. A special report on the chitosan-based hemostatic dressing: experience in current combat operations. *The Journal of trauma*. 2006;60:655-8.
- [109] Amidi M, Mastrobattista E, Jiskoot W, Hennink WE. Chitosan-based delivery systems for protein therapeutics and antigens. *Advanced drug delivery reviews*. 62:59-82.
- [110] Artursson P, Lindmark T, Davis SS, Illum L. Effect of chitosan on the permeability of monolayers of intestinal epithelial cells (Caco-2). *Pharmaceutical research*. 1994;11:1358-61.

- [111] Schipper NG, Olsson S, Hoogstraate JA, deBoer AG, Varum KM, Artursson P. Chitosans as absorption enhancers for poorly absorbable drugs 2: mechanism of absorption enhancement. *Pharmaceutical research*. 1997;14:923-9.
- [112] Di Colo G, Burgalassi S, Zambito Y, Monti D, Chetoni P. Effects of different N-trimethyl chitosans on in vitro/in vivo ofloxacin transcorneal permeation. *Journal of pharmaceutical sciences*. 2004;93:2851-62.
- [113] Fernandez-Urrusuno R, Calvo P, Remunan-Lopez C, Vila-Jato JL, Alonso MJ. Enhancement of nasal absorption of insulin using chitosan nanoparticles. *Pharmaceutical research*. 1999;16:1576-81.
- [114] Pan Y, Li YJ, Zhao HY, Zheng JM, Xu H, Wei G, et al. Bioadhesive polysaccharide in protein delivery system: chitosan nanoparticles improve the intestinal absorption of insulin in vivo. *Int J Pharm*. 2002;249:139-47.
- [115] Gan Q, Wang T. Chitosan nanoparticle as protein delivery carrier--systematic examination of fabrication conditions for efficient loading and release. *Colloids and surfaces*. 2007;59:24-34.
- [116] Nagamoto T, Hattori Y, Takayama K, Maitani Y. Novel chitosan particles and chitosan-coated emulsions inducing immune response via intranasal vaccine delivery. *Pharmaceutical research*. 2004;21:671-4.
- [117] Zaharoff DA, Rogers CJ, Hance KW, Schlom J, Greiner JW. Chitosan solution enhances both humoral and cell-mediated immune responses to subcutaneous vaccination. *Vaccine*. 2007;25:2085-94.
- [118] Seferian PG, Martinez ML. Immune stimulating activity of two new chitosan containing adjuvant formulations. *Vaccine*. 2000;19:661-8.
- [119] Xu Y, Du Y. Effect of molecular structure of chitosan on protein delivery properties of chitosan nanoparticles. *Int J Pharm*. 2003;250:215-26.
- [120] van der Lubben IM, Verhoef JC, van Aelst AC, Borchard G, Junginger HE. Chitosan microparticles for oral vaccination: preparation, characterization and preliminary in vivo uptake studies in murine Peyer's patches. *Biomaterials*. 2001;22:687-94.

- [121] Bugamelli F, Raggi MA, Orienti I, Zecchi V. Controlled insulin release from chitosan microparticles. *Arch Pharm (Weinheim)*. 1998;331:133-8.
- [122] Ko JA, Park HJ, Hwang SJ, Park JB, Lee JS. Preparation and characterization of chitosan microparticles intended for controlled drug delivery. *Int J Pharm*. 2002;249:165-74.
- [123] Huang Y, Yeh M, Chiang C. Formulation factors in preparing BTM-chitosan microspheres by spray drying method. *Int J Pharm*. 2002;242:239-42.
- [124] Zaharoff DA, Hoffman BS, Hooper HB, Benjamin CJ, Jr., Khurana KK, Hance KW, et al. Intravesical immunotherapy of superficial bladder cancer with chitosan/interleukin-12. *Cancer research*. 2009;69:6192-9.
- [125] Chandy T, Sharma CP. Chitosan as a biomaterial. *Biomater Artif Cells Artif Organs*. 1990;18:1-24.
- [126] Gan Q, Wang T. Chitosan nanoparticle as protein delivery carrier—Systematic examination of fabrication conditions for efficient loading and release. *Colloids and Surfaces B: Biointerfaces*. 2007;59:24-34.
- [127] Koppolu B, Zaharoff DA. The effect of antigen encapsulation in chitosan particles on uptake, activation and presentation by antigen presenting cells. *Biomaterials*. 34:2359-69.
- [128] Lim ST, Martin GP, Berry DJ, Brown MB. Preparation and evaluation of the in vitro drug release properties and mucoadhesion of novel microspheres of hyaluronic acid and chitosan. *J Control Release*. 2000;66:281-92.
- [129] Siepmann J, Faisant N, Akiki J, Richard J, Benoit JP. Effect of the size of biodegradable microparticles on drug release: experiment and theory. *J Control Release*. 2004;96:123-34.
- [130] Berthold A, Cremer K, Kreuter J. Preparation and characterization of chitosan microspheres as drug carrier for prednisolone sodium phosphate as model for anti-inflammatory drugs. *J Control Release*. 1996;39:17-25.
- [131] Gordon S, Saupe A, McBurney W, Rades T, Hook S. Comparison of chitosan nanoparticles and chitosan hydrogels for vaccine delivery. *J Pharm Pharmacol*. 2008;60:1591-600.

- [132] Terbojevich M, Cosani A, Muzzarelli RAA. Molecular parameters of chitosans depolymerized with the aid of papain. *Carbohydrate Polymers*. 1996;29:63-8.
- [133] Hu B, Pan C, Sun Y, Hou Z, Ye H, Zeng X. Optimization of fabrication parameters to produce chitosan-tripolyphosphate nanoparticles for delivery of tea catechins. *Journal of agricultural and food chemistry*. 2008;56:7451-8.
- [134] Gan Q, Wang T, Cochrane C, McCarron P. Modulation of surface charge, particle size and morphological properties of chitosan-TPP nanoparticles intended for gene delivery. *Colloids and surfaces*. 2005;44:65-73.
- [135] Kobiasi MA, Chua BY, Tonkin D, Jackson DC, Mainwaring DE. Control of size dispersity of chitosan biopolymer microparticles and nanoparticles to influence vaccine trafficking and cell uptake. *Journal of Biomedical Materials Research Part A*.100A:1859-67.
- [136] Tang ES, Huang M, Lim LY. Ultrasonication of chitosan and chitosan nanoparticles. *Int J Pharm*. 2003;265:103-14.
- [137] Genta I, Perugini P, Pavanetto F. Different molecular weight chitosan microspheres: influence on drug loading and drug release. *Drug development and industrial pharmacy*. 1998;24:779-84.
- [138] Cacace MG, Landau EM, Ramsden JJ. The Hofmeister series: salt and solvent effects on interfacial phenomena. *Q Rev Biophys*. 1997;30:241-77.
- [139] Record MT, Jr., Guinn E, Pegram L, Capp M. Introductory lecture: interpreting and predicting Hofmeister salt ion and solute effects on biopolymer and model processes using the solute partitioning model. *Faraday discussions*.160:9-44; discussion 103-20.
- [140] Tokumitsu H, Ichikawa H, Fukumori Y. Chitosan-gadopentetic acid complex nanoparticles for gadolinium neutron-capture therapy of cancer: preparation by novel emulsion-droplet coalescence technique and characterization. *Pharm Res*. 1999;16:1830-5.
- [141] Chang KLB, Lin J. Swelling behavior and the release of protein from chitosan pectin composite particles. *Carbohydrate Polymers*. 2000;43:163-9.
- [142] O'Hagan DT, Singh M, Ulmer JB. Microparticle-based technologies for vaccines. *Methods*. 2006;40:10-9.

- [143] O'Hagan DT, Valiante NM. Recent advances in the discovery and delivery of vaccine adjuvants. *Nature Reviews Drug Discovery*. 2003;2:727-35.
- [144] Clark TG, Cassidy-Hanley D. Recombinant subunit vaccines: potentials and constraints. *Dev Biol (Basel)*. 2005;121:153-63.
- [145] Schlom J, Gulley JL, Arlen PM. Paradigm shifts in cancer vaccine therapy. *Exp Biol Med (Maywood)*. 2008;233:522-34.
- [146] Schlom J, Gulley JL, Arlen PM. Role of vaccine therapy in cancer: biology and practice. *Curr Oncol*. 2007;14:238-45.
- [147] Qu B, Rosenberg RN, Li L, Boyer PJ, Johnston SA. Gene vaccination to bias the immune response to amyloid-beta peptide as therapy for Alzheimer disease. *Arch Neurol*. 2004;61:1859-64.
- [148] O'Hagan DT, Rappuoli R. Novel approaches to vaccine delivery. *Pharm Res*. 2004;21:1519-30.
- [149] He C, Hu Y, Yin L, Tang C, Yin C. Effects of particle size and surface charge on cellular uptake and biodistribution of polymeric nanoparticles. *Biomaterials*. 2010;31:3657-66.
- [150] Thiele L, Rothen-Rutishauser B, Jilek S, Wunderli-Allenspach H, Merkle HP, Walter E. Evaluation of particle uptake in human blood monocyte-derived cells in vitro. Does phagocytosis activity of dendritic cells measure up with macrophages? *J Control Release*. 2001;76:59-71.
- [151] Scheicher C, Mehlig M, Dienes HP, Reske K. Uptake of bead-adsorbed versus soluble antigen by bone marrow derived dendritic cells triggers their activation and increases their antigen presentation capacity. *Adv Exp Med Biol*. 1995;378:253-5.
- [152] Scheicher C, Mehlig M, Dienes HP, Reske K. Uptake of microparticle-adsorbed protein antigen by bone marrow-derived dendritic cells results in up-regulation of interleukin-1 alpha and interleukin-12 p40/p35 and triggers prolonged, efficient antigen presentation. *Eur J Immunol*. 1995;25:1566-72.
- [153] Singh M, Chakrapani A, O'Hagan D. Nanoparticles and microparticles as vaccine-delivery systems. *Expert Rev Vaccines*. 2007;6:797-808.

- [154] Zaharoff DA, Hance KW, Rogers CJ, Schlom J, Greiner JW. Intratumoral immunotherapy of established solid tumors with chitosan/IL-12. *J Immunother*. 2010;33:697-705.
- [155] Arca HC, Gunbeyaz M, Senel S. Chitosan-based systems for the delivery of vaccine antigens. *Expert Rev Vaccines*. 2009;8:937-53.
- [156] Bernkop-Schnurch A. Chitosan and its derivatives: potential excipients for peroral peptide delivery systems. *Int J Pharm*. 2000;194:1-13.
- [157] van der Lubben IM, Verhoef JC, Borchard G, Junginger HE. Chitosan and its derivatives in mucosal drug and vaccine delivery. *Eur J Pharm Sci*. 2001;14:201-7.
- [158] Berthold A, Cremer K, Kreuter J. Preparation and characterization of chitosan microspheres as drug carrier for prednisolone sodium phosphate as model for antiinflammatory drugs. *Journal of Controlled Release*. 1996;39:17-25.
- [159] van der Lubben IM, Verhoef JC, Borchard G, Junginger HE. Chitosan for mucosal vaccination. *Adv Drug Deliv Rev*. 2001;52:139-44.
- [160] Inaba K, Swiggard WJ, Steinman RM, Romani N, Schuler G, Brinster C. Isolation of dendritic cells. *Curr Protoc Immunol*. 2009;Chapter 3:Unit 3 7.
- [161] Harush-Frenkel O, Rozentur E, Benita S, Altschuler Y. Surface charge of nanoparticles determines their endocytic and transcytotic pathway in polarized MDCK cells. *Biomacromolecules*. 2008;9:435-43.
- [162] Shanbhag AS, Jacobs JJ, Black J, Galante JO, Glant TT. Macrophage/particle interactions: effect of size, composition and surface area. *J Biomed Mater Res*. 1994;28:81-90.
- [163] Banchereau J, Briere F, Caux C, Davoust J, Lebecque S, Liu YJ, et al. Immunobiology of dendritic cells. *Annu Rev Immunol*. 2000;18:767-811.
- [164] Banchereau J, Steinman RM. Dendritic cells and the control of immunity. *Nature*. 1998;392:245-52.
- [165] Sharp FA, Ruane D, Claass B, Creagh E, Harris J, Malyala P, et al. Uptake of particulate vaccine adjuvants by dendritic cells activates the NALP3 inflammasome. *Proc Natl Acad Sci U S A*. 2009;106:870-5.

[166] Chang KL, Higuchi Y, Kawakami S, Yamashita F, Hashida M. Efficient gene transfection by histidine-modified chitosan through enhancement of endosomal escape. *Bioconjug Chem.* 2010;21:1087-95.

[167] des Rieux A, Fievez V, Garinot M, Schneider YJ, Preat V. Nanoparticles as potential oral delivery systems of proteins and vaccines: a mechanistic approach. *J Control Release.* 2006;116:1-27.

[168] Tamber H, Johansen P, Merkle HP, Gander B. Formulation aspects of biodegradable polymeric microspheres for antigen delivery. *Advanced drug delivery reviews.* 2005;57:357-76.

[169] Shephard MJ, Todd D, Adair BM, Po AL, Mackie DP, Scott EM. Immunogenicity of bovine parainfluenza type 3 virus proteins encapsulated in nanoparticle vaccines, following intranasal administration to mice. *Res Vet Sci.* 2003;74:187-90.

[170] Zheng X, Huang Y, Zheng C, Dong S, Liang W. Alginate-chitosan-PLGA composite microspheres enabling single-shot hepatitis B vaccination. *AAPS J.*12:519-24.

[171] O'Hagan DT, Rahman D, McGee JP, Jeffery H, Davies MC, Williams P, et al. Biodegradable microparticles as controlled release antigen delivery systems. *Immunology.* 1991;73:239-42.

[172] Katare YK, Muthukumaran T, Panda AK. Influence of particle size, antigen load, dose and additional adjuvant on the immune response from antigen loaded PLA microparticles. *International journal of pharmaceutics.* 2005;301:149-60.

[173] Ott G, Barchfeld GL, Van Nest G. Enhancement of humoral response against human influenza vaccine with the simple submicron oil/water emulsion adjuvant MF59. *Vaccine.* 1995;13:1557-62.

[174] Hamdy S, Molavi O, Ma Z, Haddadi A, Alshamsan A, Gobti Z, et al. Co-delivery of cancer-associated antigen and Toll-like receptor 4 ligand in PLGA nanoparticles induces potent CD8⁺ T cell-mediated anti-tumor immunity. *Vaccine.* 2008;26:5046-57.